AD-A036 695 TEXAS UNIV AT AUSTIN DEFENSE RESEARCH LAB F/G 12/1
EFFECTS OF SEVERAL TYPES OF DAMPING ON THE DYNAMICAL BEHAVIOR O--ETC(U)
JAN 67 J F BYERS NOBSR-93125
UNCLASSIFIED DRL-A-272 NL

1 OF 2
ADA036695

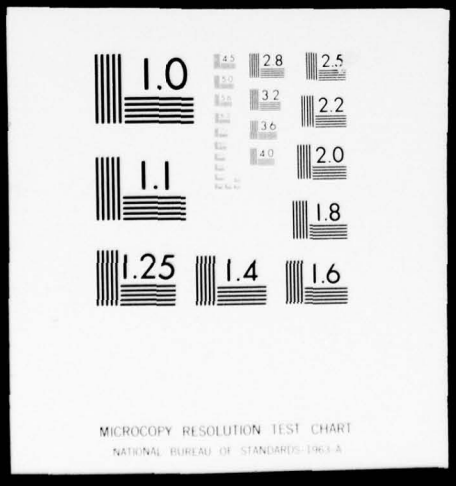

DEFENSE RESEARCH LABORATORY

THE UNIVERSITY OF TEXAS

AUSTIN, TEXAS 78712

MOST Project -4

DRL-A-272

EFFECTS OF SEVERAL TYPES OF DAMPING ON THE DYNAMICAL BEHAVIOR OF HARMONICALLY FORCED SINGLE-DEGREE-OF-FREEDOM SYSTEMS

by

Jimmy F. Byers

2 January 1967

Copy No. 2

153 p.

FD 103

SF0010318

DRL Acoustical Report No. 272

A technical report prepared under Contract NObsr-93125,
Project Serial No. SF0010318, Task 8048

DEFENSE RESEARCH LABORATORY
THE UNIVERSITY OF TEXAS
AUSTIN, TEXAS 78712

107500

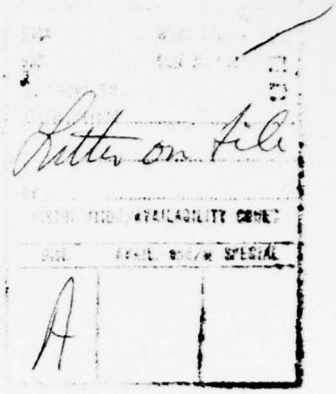

ABSTRACT

In general, the investigation of practical dynamical systems is more heuristic than rigorous; consequently, most literature attempts to provide a conceptual key to the general treatment of the response by correlation with linear theory. Practically none of this literature sets forth any new ideas of basic methods of attack. The usual attack is by extending present classical methods rather than by inventing new basic approaches. The major limitation found in the existing work is the lack of comprehensive understanding of the basic parameters of simple nonlinear oscillators.

This thesis presents an accurate solution of several types of damping on the dynamical behavior of harmonically forced single-degree-of-freedom systems. The study is based on the fundamental parameters of the system. The fundamental response is described with reference to the equivalent damping energy, the Ritz method, and dimensional analysis. Dimensional analysis is used to develop a method for predicting the general response diagram characteristics. The high accuracy of the solutions permitted the collection of some very important design data. The results are presented in both graphical and tabular form and may be useful to those engaged in calibration, design, and data analysis of work requiring an accurate solution. Also, the linearized methods give results sufficiently accurate for many engineering applications. The prediction of response characteristics by dimensional analysis should be of interest.

The time-histories of displacement, velocity, and acceleration are presented along with the response diagrams of displacement, velocity, acceleration, phase angle, and energy curves by both the linear and accurate solutions.

TABLE OF CONTENTS

LIST OF FIGURES

LIST OF FIGURES (Continued)

LIST OF FIGURES (Continued)

LIST OF FIGURES (Continued)

LIST OF TABLES

NOMENCLATURE

The following nomenclature is used in this thesis:

A	Frontal drag area, ft^2
C	General damping coefficient β_1, units vary
C_c	Viscous critical damping coefficient, dimensionless
C_x	General damping or drag coefficient, units vary
D	General constant, units vary
d	Dimensionless frequency ratio, ω/ω_n
E	Total damping energy per cycle, in.-lb
F	Amplitude of harmonic forcing function, lb
F_D	Fluid-dynamic drag force, lb
g	Acceleration of gravity, $in./sec^2$
k	Spring constant, lb/in.
L	Length, in.
M	Total system mass, $lb\text{-}sec^2/in.$
S	Unit stress, $lb/in.^2$
T	Steady-state period, sec
T_t	Time, sec
t	Instantaneous value of time, sec
W	Weight of mass, lb
X	Peak amplitude of steady-state displacement, in.
X_1	Magnitude of steady-state displacement for Coulomb damping, in.
X_2	Magnitude of steady-state displacement for viscous damping, in.

NOMENCLATURE (Continued)

X_3	Magnitude of steady-state displacement for velocity-squared damping, in.
X_4	Magnitude of steady-state displacement for displacement-squared damping, in.
x	Instantaneous value of the displacement, in.
$\dot{x}$	Instantaneous derivative of displacement with respect to time, in./sec
$\ddot{x}$	Instantaneous second derivative of displacement with respect to time, in./sec^2
β_1	Coulomb damping coefficient, lb
β_2	Viscous damping coefficient, lb-sec/in.
β_3	Velocity-squared damping coefficient, lb-sec^2/in.^{2}
β_4	Displacement-squared damping coefficient, lb/in.^{2}
γ	Coefficient for Ritz solution, $C/(2\ M\omega_n)$, dimensionless
ζ	Viscous critical damping ratio, β_2/C_c, dimensionless
θ	Phase angle, radians
ρ	Fluid mass density, slug/ft^3
σ	General variable for any angle, radians
ω	Circular frequency of forcing function, radians/second
ω_n	Natural circular frequency, radians/second .

INTRODUCTION

This thesis is an analytical and numerical investigation of the effects of several different types of damping on a harmonically-forced single-degree-of-freedom system. At present there exists no basic comparison technique or analytic procedure for the accurate plotting of the response of a damped physical system. The main objective is the establishment of the physically correct expression for the damping ratio so that the effects of the damping function can be accurately described and compared with other functions. The customary critical damping ratio does not describe cases other than the viscous case. This thesis presents the correct ratios for four basic damping functions and an approach for determining the expression for a general damping function.

The effects of damping on the general dynamical response of a physical system is important for both qualitative and quantitative investigations.

Qualitative studies are important because of their wide application to distributed systems. In general, they are treated by applying assumptions that will simplify the problem analytically. The conceptual key to the general idealization of distributed systems is the understanding and intuitive knowledge of the problem. Once the problem is well defined physically, available mathematical tools may be applied. Almost without exception all vibration problems are treated analytically as lumped-parameter systems.

The analytic procedures describe the system in terms of linear theory. This description generally takes the form of successive linear approximations. The correct assumption for the solution almost never is obvious. For example, in the dynamic calibration of shock and vibration pickups, measured outputs are sometimes differentiated to determine velocity, acceleration, and/or jerk

of a sinusoidal motion applied to a system. The assumption is that there exist no higher harmonics in the motion. The basic difficulty with this differentiating process is that a high-frequency component can have an arbitrarily small amplitude in the original wave form and an arbitrarily large amplitude in the differentiated wave form, if the frequency of the component is high. The component frequencies may be either amplitude, phase, and/or frequency distorted. The effect of differentiating an assumed linear motion to obtain the solution would be questionable. Also, these steady-state solutions are obtained only if the physical parameters change in a specified way.

Almost all of the analytical and experimental work has very little basis for comparing the effects of damping with other systems. This work usually is limited to a study of amplitude, velocity, acceleration, or phase angle instead of a simultaneous evaluation of all the parameters. This is particularly true for nonlinear response. Indeed, some authors neglect the effects of damping or give only a cursory description of its effect on the system.

In order to make a complete qualitative and quantitative analysis of the problem, every pertinent physical property should be described in detail. The general and specific variations of these properties must be accurately described.

The small amount of experimental data available is for specific environmental conditions and is taken with methods and equipment that are not well defined. Also, it is difficult to determine the effect of inherent equipment characteristics. For example, an accelerometer-cable combination can completely filter harmonic components. The usual methods lead to an analysis of the maximum values of the response; therefore, full insight into

the problem is not obtained. A detailed analysis of the motion should include a study of the time-histories of the response. In order to accomplish this it is necessary to have an extremely accurate solution to the problem.

Since most of the basic theory of operation of physical systems rests on the assumption that the linear theory with constant coefficient describes them, it is logical to evaluate the problem in this manner.

The most logical attack to the problem would be to obtain the exact steady-state and transient solution. The most practical approach would be to do this for the most common types of damping, i.e., Coulomb, viscous, velocity-squared, and displacement-squared, that are encountered in practical applications. Since a multiple degree of freedom system would introduce other unknowns, a sinusoidally forced single-degree of freedom system will be considered. This will provide the information necessary for an accurate evaluation of the effects of damping on system response.

The object of this thesis, therefore, is to (1) obtain an accurate solution to the four basic damping cases, (2) compare the results with the basic theory, (3) investigate the general and specific effects of damping, (4) reach conclusions concerning these effects, (5) obtain accurate design data, and (6) provide an adequate base for future research of combined damping cases.

CHAPTER I

STATEMENT AND FORMULATION OF THE THEORETICAL PROBLEM

The dissipation of energy of some type and degree occurs in all physical systems. The effect on mechanical systems is regarded generally as being undesirable except for vibration control or shock isolation problems. The desirable effects of damping have been used to good advantage in some limited instrument design areas. For example, the mechanical movement of graphic recorders may be damped in such a manner as to preserve the phase shift characteristics over a wide frequency range. It seems possible that other desirable characteristics of the dissipation forces could be utilized if their characteristics were known.

In order to fully utilize the optimum response characteristics of a dynamical system it is necessary to know such steady-state properties as (a) resonant bandwidth, (b) damping ratio, (c) damped natural frequency, (d) phase angle, (e) phase angle shift, (f) harmonic content of the motion, (g) the maximum displacement, velocity, acceleration, and (h) the waveform of the response.

Practically all mechanical apparatus are subjected to acceleration loading. The evaluation of the transient response to this loading is almost entirely experimental. The effects of shock are determined by subjecting the equipment to a known impact condition and observing the failure by visual inspection or photographic techniques. This procedure obviously is undesirable since it would be better to be able to predict the effects in the initial design stage. The basic difficulty is evaluating the effects of rate of loading on the test piece and the test instrumentation. The evaluation of the rate of loading for various types of damping functions should include

analysis of the third derivative with respect to time (jerk). A study of these data could provide sufficient information to design suitable test instrumentation.

In shock isolation problems it is desirable to compare the response characteristics of a damped system to determine the peak amplitude, velocity, and acceleration versus time of occurrence. The simultaneous evaluation of transient energy would be required to choose the optimum system. Since the wave forms of displacement and velocity vary with the type and degree of damping, the energy will vary considerably.

The establishment of a suitable system of equations that will allow a qualitative and a quantitative study of these effects requires careful consideration.

The qualitative aspect of the problem requires the establishment of parameters that can be applied to a physical problem. Sound judgment as to how far an idealization may be carried without affecting the response must be established. However, actual design and practical applications require a complete and accurate knowledge of the general response of the system, which is obtainable only through quantitative analysis. The above statements indicate a rather broad attack on the problem; however, practical limitations restrict the number of equations considered. Therefore, these investigations are limited to those damping forces which are basic to design practice. These damping forces are Coulomb, velocity, velocity-squared, and displacement-squared damping.

A wide range of problems can be represented analytically with constant mass and constant spring properties. This is particularly true in instrument design since springs with hysteresis errors of no more than 0.02 per cent[*15] accuracy are readily available. Therefore, constant mass and spring characteristics can be considered without loss of generality.

---

*Superscript numbers refer to the References, p. 141.

Almost none of the forcing functions are sinusoidal; however, many are periodic. The effect of the forcing function on a general study of dissipation effects is not significant, since any function can be completely described by amplitude, period, and wave form. Therefore, a sinusoidal function will be considered.

The system to be studied is represented schematically in Fig. 1. It consists of a mass M, a linear spring of rate k, a harmonic forcing function $F \sin(\omega t)$, and a generalized damper represented by $Cf(x,\dot{x})$. Equating the sum of the non-inertial forces in the direction of motion on the mass to mass times acceleration and rearranging yields

$$M\ddot{x} + Cf(x,\dot{x}) + kx = F \sin(\omega t) . \qquad (1)$$

In Eq. (1) kx is the spring force on the mass, $Cf(x,\dot{x})$ is the damping force, $M\ddot{x}$ is the inertia force, and $F \sin(\omega t)$ is the forcing function. The instantaneous displacement and time are x and t, respectively. The forcing function amplitude is F and ω is the circular frequency of the forcing function.

Excluding the cases of no damping and viscous damping, there exists no exact analytic method of solving the above equation that will give both steady-state and transient solutions. The solutions that are available apply only to special cases and then the linear approximations are to "first order" accuracy.

Equation (1) approximates many real systems; therefore, the evaluation of the effects of basic damping functions should reveal useful design information. Also, a wide variety of problems are predominantly affected by one of the basic forms of damping. For example, the fluid-dynamic drag on a fully-submerged body is predominantly velocity-squared.

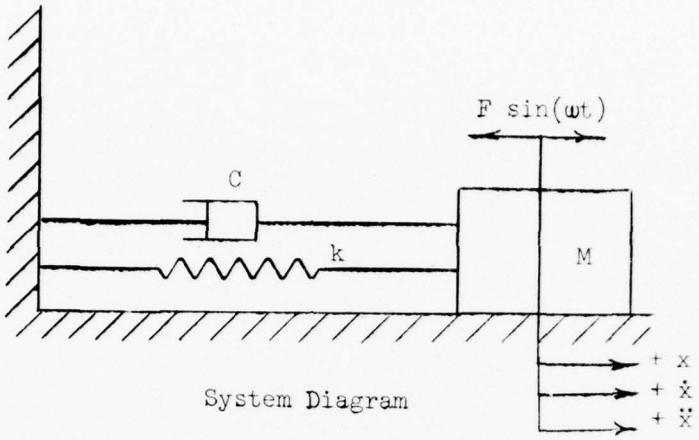

System Diagram

$$M\ddot{x} + \beta_1 \frac{\dot{x}}{|\dot{x}|} + kx = F \sin \omega t$$

$$M\ddot{x} + \beta_2 \dot{x} + kx = F \sin \omega t$$

$$M\ddot{x} + \beta_3 \dot{x} |\dot{x}| + kx = F \sin \omega t$$

$$M\ddot{x} + \beta_4 x^2 \frac{\dot{x}}{|\dot{x}|} + kx = F \sin \omega t$$

Equations of Motion

FIGURE 1

SYSTEM DIAGRAM WITH EQUATIONS

Velocity-squared damping is most predominant in practical applications of fluid dynamics. The magnitude of the damping force is $C_x \rho A \frac{\dot{x}^2}{2}$.

For a particular problem all of the variables are well defined except C_x. The value of C_x can be obtained by testing in a wind or water tunnel or by reference to previous work. Hoerner[6] has published a book that gives the values of C_x for many configurations encountered in practice. The combination of these coefficients with the solution to Eq. (1) will permit an accurate description of the motion of systems affected by this damping force. Also, fluid flow in pipes[7] has been represented by a constant times $\dot{x}^{1.8}$. The fundamental study of a Helmholtz resonator[11] is closely represented by Eq. (1) except for the radiation losses at the end of the neck.

Coulomb friction is a constant force and independent of velocity or displacement. The direction of the force opposes the relative motion across the damper. For periodic motion the relative velocity is zero twice during each cycle; in practice the coefficient of friction is a function of the materials at the interface. The static and dynamic coefficients differ by a factor of 2 to 5, and an effective value of the coefficient is customarily used. The coefficient of rolling friction for preloaded ball and roller bearings is fairly constant. In general, shafts sliding through sleeve bearings and structural joints may be approximated with an effective damping coefficient.

The displacement-squared function[13,4] has been used to represent the total damping caused by structural joints and internal material damping. It is represented by the specific damping energy which is the area within the stress-strain hysteresis loop of the material. Therefore the specific damping energy is a function of the stress level and is independent of the

shape, stress distribution, and volume of the material. The expression for the specific damping energy is $C\ S^n$, where the constant n = 2.0 to 3.0 for the usual stress levels encountered in both ferrous and nonferrous materials. A rather comprehensive list of the values of n are given on page 36-35 of Ref. 4. Although the above equation is rather general, it is impossible to represent a general hysteresis loop.[14]

CHAPTER II

LINEARIZED ANALYTIC INVESTIGATIONS

A. Survey of Methods

For a general damping function, Eq. (1) is nonintegrable and experimental and analytical methods of solving the equations must be considered. The use of an analog computer is not desirable because of the inherent inaccuracy, particularly when nonlinear elements are used; therefore analytic procedures are considered.

Several analytic procedures of solving the equation customarily are considered: separation of variables, representation of the solution by a power series, methods of generating functions, method of successive approximations, and representation of the solution by finite integrals. In general, the separation of variables is not possible and the solution by Laplace transforms apply only to linear differential equations over a small interval of a region. The other procedures are generally effected by assuming a homogeneous and a particular solution. The homogeneous solution is the solution of a freely vibrating system and the particular solution is included to represent the forcing of the system. As a result of these assumptions the solutions are interpreted as a superposition of the linear assumptions. Thus the result has real sense only for linear systems. The response for light or no damping is explained as the superposition of sub or super harmonics. The response for the damped case is distorted by phase and amplitude variations which these linear assumptions do not describe.

Since the existing methods are based on linear concepts, Minorsky[8], Stoker[12], and others have suggested that completely new concepts might be developed to treat the nonlinear problems. No specific suggestions are made; however, Stoker proposed the method of matching the response with a driving force.

The general nonlinear response consists of harmonics of all orders and an excitation force with a corresponding frequency might excite and sustain one of the harmonics. Therefore a plausible physical explanation for the effects of damping should be independent of linear assumptions.

There exists no general analytic method for obtaining an exact solution of Eq. (1). Approximate solutions of a known mathematical form may be assumed. Generally, these solutions present formidable mathematical difficulties if other than first order approximations are assumed. The major difficulty is determining the basic form and the required number of terms to include in the estimate. The methods vary somewhat, but the procedure is to assume the solution consists of linear independent functions, i.e.,

$$x(t) = x_o(t) + D_1\, x_1(t) + D_2\, x_2(t) + \ldots + D_n\, x_n(t)\ , \qquad (2)$$

where the D_i are considered as constants or functions of the independent variable, depending upon the mathematical procedure. In general, $x_o(t)$ is the basic form of the solution and is the term that contains the initial conditions for the entire solution. This solution is substituted into the differential equation and evaluated by various methods.

With the perturbation method[12], the solution is approximated by a function of the independent variable whose coefficients are in powers of a small parameter, μ, of the nonlinear term

$$x(t) = x_o(t) + \mu\, x_1(t) + \mu^2\, x_2(t) + \ldots\ . \qquad (3)$$

This assumed solution is substituted into the differential equation, and coefficients of like powers of the small parameter, μ, are equated to zero. As the coefficients are determined they are substituted into Eq. (3) to form the solution. The term $x_o(t)$ is called the generating solution and represents the exact solution of the differential equation when $\mu \to 0$. The initial condition

$$x(t_o) = x_o(t_o) \tag{4}$$

is used to evaluate the arbitrary constants that occur when the solutions are formed at each step.

The frequency of the oscillation is usually expanded in a power series

$$\omega = \omega_o + \mu\omega_1 + \mu^2\omega_2 + \dots , \tag{5}$$

with the initial conditions

$$\omega(t_o) = \omega_o(t_o) \tag{6}$$

applied in the same manner as the steady-state amplitude expression above. This provides a technique for eliminating secular terms which have the amplitude growing indefinitely with time. Since the accuracy of the method depends on the number of correction terms used and the magnitude of the nonlinearity, this procedure would not provide an accurate base for comparing the effects of the damping functions. Also, the perturbation method is less useful where changes in amplitude and phase occur. This is precisely the major effect of damping on the response.

The method of variation of parameters[2,10] provides a better technique for describing the changes in amplitude and phase. This procedure provides for the constants of the assumed solution to be functions of the

independent variable. The technique is customarily illustrated with the following solution:

$$x = X(t) \sin(\omega t + \varphi(t)). \tag{7}$$

The derivative of Eq. (7) is

$$\begin{aligned}\dot{x} &= \dot{X}(t) \sin(\omega t + \varphi(t)) + X(t) \cos(\omega t + \varphi(t)) [\omega + \dot{\varphi}(t)] \\ &= \dot{X}(t) \sin(\omega t + \varphi(t)) + X(t)\, \omega \cos(\omega t + \varphi(t)) \\ &\qquad + X(t)\, \dot{\varphi}(t) \cos(\omega t + \varphi(t)).\end{aligned} \tag{8}$$

This velocity expression must be changed to be compatible with the original assumed solution, thus the additional restriction

$$\dot{X}(t) \sin(\omega t + \varphi(t)) + X(t)\, \dot{\varphi}(t) \cos(\omega t + \varphi(t)) = 0. \tag{9}$$

The acceleration becomes

$$\begin{aligned}\ddot{x} &= \frac{d}{dt} X(t)\, \omega \cos(\omega t + \varphi(t)) \\ &= \dot{X}(t)\, \omega \cos(\omega t + \varphi(t)) - X(t)\, \omega^2 \sin(\omega t + \varphi(t)) \\ &\qquad - X(t)\, \dot{\varphi}(t)\, \omega \sin(\omega t + \varphi(t)).\end{aligned} \tag{10}$$

Equations (9) and (10) are substituted into the equations of motion. The equations may be solved for $\dot{X}$ and $\dot{\varphi}$.

Because of the nonlinearity it may not be possible to solve the two equations exactly. In this case the values are customarily evaluated by the averaging procedure of Krylov and Bogoliubov,[1]

$$\dot{X}_{avg} = \frac{-\mu}{2\pi\omega} \int_0^{2\pi} F(x,\dot{x},t) \cos\varphi \, d\varphi \tag{11}$$

$$\dot{\varphi}_{avg} = \frac{\mu}{2\pi X\omega} \int_0^{2\pi} F(x,\dot{x},t) \sin\varphi \, d\varphi. \tag{12}$$

The amplitude, X, and phase, φ, are treated as constants when determining the average value.

Several methods of evaluating the residual error (the arithmetic difference of the approximate solution from the exact solution)* of an assumed function are available. The most important methods are the virtual work, Ritz, Harmonic Balance, and Galeriken methods.[10] The approximate solution is substituted into the differential equation and the resulting error is defined as a function of the independent variable. Since the residual is not a direct indication of the difference between the assumed and exact solution, the evaluation of this error has been treated by various means.

The virtual work and Ritz methods[10] require the average energy to be zero over the interval in question by specifying the instantaneous virtual work to be zero. When the virtual work expression is derived from Lagrange's equation,

$$\int_{t_1}^{t_2} \epsilon(\tilde{x},t) \; \Sigma \frac{\partial \tilde{x}}{\partial D} \; \delta D \; dt = 0 \; , \tag{13}$$

where $\tilde{x}$ is the assumed solution, δ is the first variation of $\tilde{x}$ with respect to D. The expression for the integral to be minimized contains a term that specifies the manner in which the parameters of the approximate solution are to be determined. The practical value of knowing the manner of determining the coefficients has not been demonstrated.

In (2) the D_i are coefficients and the X_i are orthogonal over the [illegible] of integration.

[illegible] solution, as determined by the Ritz procedure, is obtained by estimating functions that can be minimized by the integral

$$J = \int \epsilon(t) \; \varphi_i(t) dt = 0. \tag{14}$$

*See page 92.

In Eq. (2) the $X_i(t)$ are orthogonal functions over the integration interval. The D_i are minimized by requiring $\frac{\partial J}{\partial D_i} = 0$. This gives n algebraic equations.

The principle of harmonic balance[2,10] requires the approximate solution to be adjusted to satisfy all terms of the fundamental frequency. This procedure can be used for the same class of problems as the variation of parameters. The periodic solution must be expressed as a Fourier series, i.e., the solution is a periodic function in time.

In Eq. (2) the $X_i(t)$ are orthogonal circular functions and the D_i are functions of time. The residual is formed by substituting the solution into the integrals of the Ritz procedure

$$\int_o^{2\pi} \epsilon(t) \cos \omega t d(\omega t) = 0 \tag{15}$$

$$\int_o^{2\pi} \epsilon(t) \cos n\omega t d(\omega t) = 0. \tag{16}$$

The Galeriken method[10] is the same as the Ritz method, except that the residual is minimized by the principle of least squares. This criterion is more appealing mathematically; however, the number of algebraic equations obtained is twice the number obtained by the Ritz method, less one. The residual is given by

$$J = \int_{t_1}^{t_2} \epsilon^2(t)\, d(t). \tag{17}$$

The major difficulty of assuming a functional form for the displacement and substituting its derivatives in the differential equation is the error in the wave forms. No mathematical procedure has been found that will adequately describe the solution. For cases of "small" damping, excellent results have been obtained for the displacement. It should be

noted that the same difficulties exist for distributed systems. The application of Tschebyscheff polynominals to the equation of motion of a fundamental system yield practical results for a lightly damped infinite medium only.[12]

At any rate, the above methods yield analytical expressions that are relatively good for displacements, fair for velocities, and perhaps no good at all for accelerations. Accuracy in the derivatives can be obtained only by an accurate description of the displacement. The mathematical difficulties of deriving accurate expressions becomes impractical for known displacement wave forms. Since the nonlinear problems present unknown conditions, the most expedient method for evaluating the general characteristics of a system is the procedure that would yield results of equal accuracy for all damping cases.

Basically, the numerical procedures consist of stepwise integration of the equation by estimating the value of the dependent variables at each step. These values are substituted into the differential equation to determine the accuracy of the calculations. The methods of choosing the values of the variables to substitute into the equation range from choosing the values from a random table to more efficient methods for analytically estimating the solution. The most efficient methods are based on Taylor's[4] development about a point; therefore, the accuracy is a function of the order of the development and the step size. The Runge-Kutta[4] formulas are a direct extension of Taylor's development. The solution can be continued by the Adams-Moulton[4] method which weighs previous slopes to determine the value at the next step. The procedure is practically impossible without a digital computer; however, the accuracy is easily controlled.

The complexity and accuracy of the above procedures vary with the

nonlinearity of the problem. An estimate of the accuracy of these methods can be made by comparing the analytical solution to experimental data or to a more accurate integration procedure.

The inclusion of both sine and cosine terms is necessary to describe the solution of a damped system. It generally is reasoned that damping causes phase distortion in all nonlinear problems as it does in the viscous case. Certainly curves with large variations in wave form and period can be described mathematically with this technique. It is impossible to know which terms of the series to include in the estimate of a solution. In general, the transient solution would contain more terms than the steady-state solution, since amplitude and phase variations are greater for this condition. This makes the evaluation of the phase angle variations for the damping case even more important.

Since the Coulomb equation is not considered strictly nonlinear, it is appropriate to discuss other linear procedures. The most widely used method of treating linear systems is the equivalent energy method.[7] The equivalent energy method is based on equal energy dissipated in both linear and nonlinear dampers. The use of the equivalent damping factor in the viscous solution gives a direct evaluation of the nonharmonic character of the motion.

The author feels the reason that very little is known about effective damping on dynamical systems is the lack of knowledge of the natural response of the system. Certainly the proper evaluation of a damping function and/or coefficient could not be made if the natural response of the system is unknown. Comparison of peak amplitudes for the measurement of damping coefficients is not sufficiently accurate for exact design requirements. A detailed study of the motion wave form and phase variation over a cycle of motion should reveal some interesting design information.

B. The Equivalent Energy Method

The energy method has been used to approximate the response of single-degree-of-freedom systems subject to nonlinear damping forces. This approximation is effected by replacing the linear damping coefficient in the linear solution with an equivalent nonlinear element, which is determined by integrating the basic expression for the energy dissipated per cycle in the nonlinear damper. This equivalence is based on the assumption that for one period of steady-state motion the energy dissipated in the linear damper is the same as the energy dissipated in the nonlinear damper. The basic assumption is that the motion is described by the forcing function.

If the general expression for the nonlinear damping force is $f(x,\dot{x})$, then the expression for the energy per cycle for the solution $x = X \sin \omega t$ is the integral of the product of the damping force and the velocity, $\dot{x} = X\,\omega \cos \omega t$, over a cycle,

$$E = \int_{\text{cycle}} f(x,\dot{x})\, F\left(\frac{dx}{dt}\ \frac{dt}{dx}\right) dx$$

or

$$E = \int_{\text{cycle}} f(x,\dot{x})\, \dot{x} dt \ . \tag{18}$$

The energy dissipated per cycle for any damping force $f(x,\dot{x})$ may be obtained by substituting the damping force into this equation. For the motion assumed above, the equation becomes

$$E = X\omega \int_{0}^{\frac{2\pi}{\omega}} f(x,\dot{x}) \cos \omega t dt. \tag{19}$$

The results of substituting the expressions for $f(x,\dot{x})$ into Eq. (19) are shown in Table 1.

The expressions for the amplitudes and corresponding phase angles are found by substituting the normalized damping coefficient into the viscous equations for the displacement and phase angle,[2,3]

$$X = \frac{\frac{F}{k}}{\sqrt{\left[1-\left(\frac{\omega}{\omega_n}\right)^2\right]^2 + 4\zeta^2 \frac{\omega^2}{\omega_n^2}}} \quad , \tag{20}$$

and

$$\tan \theta = \frac{2\zeta \frac{\omega}{\omega_n}}{1 - \left(\frac{\omega}{\omega_n}\right)^2} \quad . \tag{21}$$

The final expressions are shown in columns 4 and 5 of Table 1. It should be noted that the identical solutions could have been obtained with the Ritz two-term procedure.

C. Ritz Method

The Ritz Method[7] is a convenient mathematical procedure for approximating the solution to Eq. (1). It is relatively easy to include nonlinearities in any or all of the terms. The solutions for the damping cases considered are given for comparison with the Equivalent Energy Method.

A two-term approximation of the solution

$$x = X \sin(\omega t - \theta) \tag{22}$$

is assumed. The derivatives of the solution are substituted into Eq. (14). These integrals replace the appropriate terms of Eq. (1).

TABLE 1

THE RITZ TWO TERM APPROXIMATION AND THE EQUIVALENT ENERGY METHOD FOR STEADY-STATE EXPRESSIONS

TYPE OF DAMPING	DAMPING FORCE	F (X,ω)	DISPLACEMENT	PHASE ANGLE
COULOMB	$\beta_1 \frac{X\dot{X}}{\lvert\dot{X}\rvert}$	$\frac{4}{\pi X \omega_n}$	$X_1 = \frac{F/k}{\sqrt{\left[1-\left(\frac{\omega}{\omega_n}\right)^2\right]^2 + 4r^2\left(\frac{4}{\pi X \omega_n}\right)^2}}$	$\text{Tan } \theta = \frac{\frac{4\beta_1}{\pi X}}{1-\left(\frac{\omega}{\omega_n}\right)^2}$
VISCOUS	$\beta_2 \dot{X}$	$\frac{\omega}{\omega_n}$	$X_2 = \frac{F/k}{\sqrt{\left[1-\left(\frac{\omega}{\omega_n}\right)^2\right]^2 + 4r^2\left(\frac{\omega}{\omega_n}\right)^2}}$	$\text{Tan } \theta = \frac{\beta_2 \omega}{1-\left(\frac{\omega}{\omega_n}\right)^2}$
VELOCITY SQUARED	$\beta_3 \dot{X} \lvert\dot{X}\rvert$	$\frac{8}{3}\frac{\omega^2 X}{\pi \omega_n}$	$X_3 = \frac{F/k}{\sqrt{\left[1-\left(\frac{\omega}{\omega_n}\right)^2\right]^2 + 4r^2\left(\frac{8}{3}\frac{\omega^2 X}{\pi \omega_n}\right)^2}}$	$\text{Tan } \theta = \frac{\beta_3\left(\frac{8}{3}\frac{\omega^2 X}{\pi \omega_n}\right)}{1-\left(\frac{\omega}{\omega_n}\right)^2}$
DISPLACEMENT SQUARED	$\beta_4 \frac{X^2\dot{X}}{\lvert\dot{X}\rvert}$	$\frac{4}{3}\frac{X}{\pi \omega_n}$	$X_4 = \frac{F/k}{\sqrt{\left[1-\left(\frac{\omega}{\omega_n}\right)^2\right]^2 + 4r^2\left(\frac{4}{3}\frac{X}{\pi \omega_n}\right)^2}}$	$\text{Tan } \theta = \frac{2r\left(\frac{4}{3}\frac{X}{\pi \omega_n}\right)}{1-\left(\frac{\omega}{\omega_n}\right)^2}$

$$-\omega^2 X \int_0^{2\pi} \sin(\omega t-\theta) \sin \omega t d(\omega t)$$

$$+ \frac{c}{M} \int_0^{2\pi} f(x,\dot{x}) \sin \omega t d(\omega t)$$

$$+ \frac{k}{M} X \int_0^{2\pi} \sin(\omega t-\theta) \sin \omega t d(\omega t)$$

$$- \frac{F}{M} \int_0^{2\pi} \sin \omega t \sin \omega t d(\omega t) = 0.$$

Let $\sigma = \omega t-\theta$,

then

$$\omega t = \sigma + \theta,$$

and

$$d(\omega t) = d\sigma .$$

The first and third integrals are

$$2 \int_0^{\pi} \sin(\sigma) \sin(\sigma + \theta) d\sigma .$$

Using the trigonometric identity

$$\sin(\sigma + \theta) = \sin \sigma \cos \theta + \cos \sigma \sin \theta$$

$$\text{and } \tfrac{1}{2} \sin 2\sigma = \sin \sigma \cos \sigma$$

the integral becomes

$$2 \int_0^{\pi} \left[\sin^2 \sigma \cos \theta + \tfrac{1}{2} \sin 2\sigma \sin \theta \right] d\sigma .$$

Integrating and substituting integration limits

$$2 \left[\frac{\pi}{2} \cos \theta \right] = \pi \cos \theta .$$

The integral of the fourth term is π. Thus one algebraic equation in X and θ is

$$-\omega^2 X\pi \cos\theta + \frac{c}{m}\int_o^{2\pi} f(x,\dot{x}) \sin \omega t d(\omega t)$$

$$+ \frac{k}{m} X\pi \cos\theta = \frac{F}{m}\pi .$$

Using the other orthogonal integral, another equation in X and θ is obtained:

$$-\omega^2 X\pi \sin\theta + \frac{c}{m}\int_o^{2\pi} f(x,\dot{x}) \cos \omega t d\omega t$$

$$+ \frac{k}{m} X\pi \sin\theta = 0.$$

Solving the above equations for X and θ yields

$$\left[1 - \left(\frac{\omega}{\omega_n}\right)^2\right]^2 + \left(\frac{c^2}{M^2\omega_n^2}\right) F(X,\omega) = \left(\frac{F}{kX}\right)^2 \tag{23}$$

and

$$\tan\theta = \frac{\frac{c}{M\omega_n} F(X,\omega)}{1-\left(\frac{\omega}{\omega_n}\right)^2} \tag{24}$$

where

$$F(X,\omega) = \int_o^{2\pi} f(x,\dot{x}) \sin\sigma \, d\sigma \quad . \tag{25}$$

D. Presentation of Analytic Results

The result of substituting the expressions for $f(x,\dot{x})$ into Eq. (25) and integrating for $F(X,\omega)$ is shown in column 3 of Table 1. The expressions for the displacement and phase angle, as given by Eqs. (23) and (24) are shown in columns 4 and 5 of Table 1.

The general equations for the maximum steady-state displacement are given in column 2, Table 2. The equations that are obtained by

TABLE 2

ALGEBRAIC STEADY-STATE EXPRESSIONS USED IN COMPUTER PROGRAM

TYPE OF DAMPING	GENERAL EXPRESSION FOR DISPLACEMENT	COMPUTER EQUATION WITH THE VALUES OF ASSUMED CONSTANTS	MAX. FREQ. RESPONSE
COULOMB	$X_1 = \dfrac{\left[\dfrac{F^2}{k^2} - \dfrac{\beta_1^2}{M^2\omega_n^2}\dfrac{16}{\pi^2\omega_n^2}\right]^{\frac{1}{2}}}{1-\left(\dfrac{\omega}{\omega_n}\right)^2}$	$X_1 = \dfrac{\pm\left[1 - \dfrac{16\beta_1^2}{\pi^2}\right]^{\frac{1}{2}}}{1-\left(\dfrac{\omega}{\omega_n}\right)^2}$	$d_{max} = 1$
VISCOUS	$X_2 = \dfrac{F/k}{\left[\left[1-\left(\dfrac{\omega}{\omega_n}\right)^2\right]^2 + \dfrac{\beta_2^2}{M^2\omega_n^2}\dfrac{\omega^2}{\omega_n^2}\right]^{\frac{1}{2}}}$	$X_2 = \dfrac{1}{\left(\left[1-\left(\dfrac{\omega}{\omega_n}\right)^2\right]^2 + \dfrac{\beta_2^2}{M^2\omega_n^2}\dfrac{\omega^2}{\omega_n^2}\right)^{\frac{1}{2}}}$	$d_{max} = \sqrt{1-2\beta_2^2}$
VELOCITY SQUARED	$X_3 = \left(\dfrac{-\left[1-\left(\dfrac{\omega}{\omega_n}\right)^2\right]^2 \pm \left[\left[1-\left(\dfrac{\omega}{\omega_n}\right)^2\right]^4 + 4\left(\dfrac{\beta_3^2}{M^2\omega_n^2}\right)\dfrac{64\omega^4}{9\pi^2\omega_n^2}\dfrac{F^2}{k^2}\right]^{\frac{1}{2}}}{2\left[\dfrac{64\beta_3^2\omega^4}{9\pi^2k^2}\right]}\right)^{\frac{1}{2}}$	$X_3 = \left(\dfrac{-\left[1-\left(\dfrac{\omega}{\omega_n}\right)^2\right]^2 \pm \left[\left[1-\left(\dfrac{\omega}{\omega_n}\right)^2\right]^4 + 4\left(\dfrac{64\beta_3\omega^4}{9\pi^2}\right)\right]^{\frac{1}{2}}}{2\left[\dfrac{64\beta_3^2\omega^4}{9\pi^2}\right]}\right)^{\frac{1}{2}}$	(NOT OBTAINABLE)
DISPLACEMENT SQUARED	$X_4 = \left(\dfrac{-\left[1-\left(\dfrac{\omega}{\omega_n}\right)^2\right]^2 \pm \left[\left[1-\left(\dfrac{\omega}{\omega_n}\right)^2\right]^4 + 4\left(\dfrac{\beta_4^2}{M^2\omega_n^2}\right)\dfrac{16}{9\pi^2\omega_n^2}\dfrac{F^2}{k^2}\right]^{\frac{1}{2}}}{2\left[\dfrac{\beta_4^2}{M^2\omega_n^2}\dfrac{16}{9\pi^2\omega_n^2}\right]}\right)^{\frac{1}{2}}$	$X_4 = \left(\dfrac{-\left[1-\left(\dfrac{\omega}{\omega_n}\right)^2\right]^2 \pm \left[\left[1-\left(\dfrac{\omega}{\omega_n}\right)^2\right]^4 + \dfrac{64\beta_4^2}{9\pi^2}\right]^{\frac{1}{2}}}{2\left[\dfrac{16\beta_4^2}{9\pi}\right]}\right)^{\frac{1}{2}}$	$d_{max} = \frac{2}{4}$

substituting the fixed parameters of the problem (see Table 2) into the general equations are shown in column 3 of Table 2.

The position of maximum frequency response as a function of damping ratio for the damping cases can be determined by differentiating the equation of motion with respect to the frequency ratio and equating the result to zero. The value of the maximum amplitude is then determined by substituting this frequency ratio into the amplitude equation. In all cases except the velocity-squared case the separation of the variables after the differentiation can be accomplished. The results are shown in column 4 of Table 2.

The choice of damping coefficients to substitute into the algebraic expressions in Table 2 are not obvious; however, the equivalent damping energy method may be used to approximate the coefficients. The expressions for the coefficients are given in Table 3. The coefficients were determined by normalizing the energy expression and substituting the viscous coefficient into the resulting equation, the only assumption being the equality of energy for the two expressions. The normalized expressions are given in Table 3.

Many authors (such as Wieland[16]) have performed experiments by assuming the damping coefficients at the resonant frequency are sufficiently accurate to determine the response at all frequencies. Therefore, the damping equivalent coefficients are determined on this basis so that the error of this assumption can be determined. Also, the range of the coefficients may be approximated by this method, since a value for the frequency peak amplitudes cannot be determined beforehand. Although these coefficients are obviously wrong for the exact solution, they are correct for the assumed linear solution. The coefficients can be evaluated at the resonant peak.

TABLE 3

LINEARIZED EQUIVALENT VISCOUS COEFFICIENTS

TYPE OF DAMPING	LINEARIZED DAMPING TERM	EQUIVALENT COEFFICIENT NORMALIZED TO VISCOUS	DAMPING COEFFICIENT CORRESPONDING TO ASSUMED VISCOUS VALUES
COULOMB	$\beta_1 = \frac{M\omega_n^2 \pi X}{4}$	$\beta_1 = \frac{\beta_2 \omega_n \pi X}{4}$	0.007715313 0.3857656 0.7715313 1.543063
VISCOUS	$\beta_2 = \frac{\omega_n^2 M}{\omega}$	———	0.005 0.025 0.05 0.1
VELOCITY SQUARED	$\beta_3 = \frac{3}{8} \frac{\pi \omega_n^2 M}{\omega^2 X}$	$\beta_3 = \frac{3}{8} \frac{\beta_2 \pi}{\omega_n X}$	0.00002998179 0.001499089 0.002998178 0.005996357
DISPLACEMENT SQUARED	$\beta_4 = \frac{3}{4} \frac{\pi \omega_n^2 M}{X}$	$\beta_4 = \frac{3}{4} \frac{\beta_2 \omega_n \pi}{X}$	0.231449 1.15725 2.314490 4.628979

The degree of error can be estimated by solving the displacement expressions given in Table 2. The algebraic equations in Table 2 have only positive roots for the values of the dissipation coefficients considered. By definition the magnitude of the assumed solution is a real positive number. Therefore, the other roots of the equations are not considered. A computer program (see page 123) was written to solve the expressions for the steady-state displacement and phase angle equations (column 3 of Table 2) with the coefficients in Table 3. The values of the displacement and phase angle are substituted into Eq. (22), the assumed solution, which is substituted into the differential equation for the corresponding damping case (see Fig. 1, p. 7).

The steady-state displacement response diagrams are shown in Figs. 2 through 9. They are plotted as a function of the damping ratios shown. The root-mean-square (RMS) error was calculated over each cycle (150 points/cycle). A chart of the RMS error is shown in Table 4. The value of the error for the viscous case is in the order of 10^{-10}. These values were checked on the desk calculator and found to be correct. Table 4 shows that the RMS error in the solution for cases other than viscous damping range from 10^{-1} to 10^{-3} over a cycle. The variation for 200 points per cycle gave the same order of magnitude of the RMS error.

Since the incremental values indicate an insignificant change in the RMS error, a comparison of these incremental values with the exact solution would reveal little additional information to add to the peak amplitude analysis above. Also, a detailed analysis of the phase angle error is not beneficial.

TABLE 4

RMS ERROR OF THE ANALYTIC SOLUTIONS OF THE EQUATIONS OF MOTION

The RMS error of the analytic solutions of the equations of motion are given in the following pages.

The equations are presented in the same order as they appear in Fig. 1. Also, the same designation is used. The damping coefficients are indicated in the second column. The steady-state amplitude is shown in column 3. The phase angle (in radians) is given in column 4. The frequencies are shown in column 5. The RMS error is shown in the last column. The second line under each equation designation is the value of the steady-state displacement, velocity, and acceleration, respectively.

The values of the damping coefficients are:

Beta	X_1	X_2	X_3	X_4
1	0.0077153	0	0	0.2
2	0.1	0.005	0.00003	0.3086125
3	0.3857656	0.03	0.0005	0.50000
4	0.6	0.025	0.0014991	1.00000
5	0.7715313	0.04	0.0015	1.5430630
6		0.05	0.0029982	2.0000
7		0.06	0.003	3.086125
8		0.0719816	0.0043163	3.50000
9		0.08	0.005	4.44283
10		0.1	0.0059964	6.17225

EQUATION	BETA	X	THETA	OMGA	ERROR
(X1)	1	1.3497E 00	9.82E-03	10	3.3527E-03
1.3495850E 00		1.3496477E 01	1.3495850E 02		
(X1)	1	2.7571E 01	3.14E 00	20	7.7153E-03
2.7571428E 1		5.5142856E 02	1.1028571E 04		
(X1)	1	7.5097E-01	3.14E 00	30	7.7153E-03
7.5097276E-01		2.2528482E 01	6.7587549E 02		
(X1)	1	3.1796E-01	3.14E 00	40	7.7153E-03
3.1795717E-01		1.2718287E 01	5.0873147E 02		
(X1)	2	1.3387E 00	1.28E-01	10	3.5796E-02
1.3277679E 00		1.3386631E 01	1.3277679E 02		
(X1)	2	2.7347E 01	3.01E 00	20	4.3525E-02
2.7346975E 01		5.4693952E 02	1.0938790E 04		
(X1)	2	7.4486E-01	3.01E 00	30	4.6035E-02
7.4484794E-01		2.2345778E 01	6.7036314E 02		
(X1)	2	3.1537E-01	3.01E 00	40	4.3534E-02
3.1536877E-01		1.2614751E 01	5.0459003E 02		
(X1)	3	1.1756E 00	5.13E-01	10	8.0987E-02
1.0240378E 00		1.1756249E 01	1.0240378E 02		
(X1)	3	2.4016E 01	2.63E 00	20	1.6790E-01
2.4016147E 01		4.8032290E 02	9.6064588E 03		
(X1)	3	6.5414E-01	2.63E 00	30	1.8832E-01
6.5414151E-01		1.9623194E 01	5.8872736E 02		
(X1)	3	2.7696E-01	2.63E 00	40	1.6788E-01
2.7694463E-01		1.1077787E 01	4.4311141E 02		
(X1)	4	8.7091E-01	8.69E-01	10	1.1177E-01
6.6088915E-01		8.7090378E 00	6.6088915E 01		
(X1)	4	1.7791E 01	2.27E 00	20	2.6113E-01
1.7791105E 01		3.5582214E 02	7.1164421E 03		
(X1)	4	4.8459E-01	2.27E 00	30	2.9450E-01
4.8458843E-01		1.4536930E 01	4.3612959E 02		
(X1)	4	2.0517E-01	2.27E 00	40	2.6111E-01
2.0516153E-01		8.2064600E 00	3.2825845E 02		
(X1)	5	2.5250E-01	1.38E 00	10	2.4779E-01
2.4765960E-01		2.5249626E 00	2.4765960E 01		
(X1)	5	5.1581E 00	1.76E 00	20	3.3582E-01
5.1581379E 00		1.0316276E 02	2.0632552E 03		
(X1)	5	1.4049E-01	1.76E 00	30	3.5898E-01
1.4049403E-01		4.2146815E 00	1.2644463E 02		
(X1)	5	5.9484E-02	1.76E 00	40	3.3591E-01
5.9484294E-02		2.3793718E 00	9.5174870E 01		

TABLE 4 (CONTINUED)

(X2)	1	7.5097E-01	3.14E 00	30	5.5567E-10
7.5097276E-01		2.2528482E 01	6.7587549E 02		
(X2)	1	3.1796E-01	3.14E 00	40	4.2251E-10
3.1795717E-01		1.2718287E 01	5.0873147E 02		
(X2)	2	1.3496E 00	6.75E-03	10	1.1774E-10
1.3495887E 00		1.3496188E 01	1.3495887E 02		
(X2)	2	2.6580E 01	2.87E 00	20	9.2710E-09
2.6579608E 01		5.3159217E 02	1.0631843E 04		
(X2)	2	7.5093E-01	3.13E 00	30	5.4217E-10
7.5091765E-01		2.2527625E 01	6.7582589E 02		
(X2)	2	3.1795E-01	3.14E 00	40	4.3126E-10
3.1794441E-01		1.2717778E 01	5.0871105E 02		
(X2)	3	1.2510E 00	3.85E-01	10	9.0714E-11
1.1595455E 00		1.2509961E 01	1.1595455E 02		
(X2)	3	1.6636E 00	1.63E 00	20	5.1300E-10
1.6636249E 00		3.3272499E 01	6.6544996E 02		
(X2)	3	6.2219E-01	2.55E 00	30	5.1683E-10
6.2218146E-01		1.8665640E 01	5.5996332E 02		
(X2)	3	2.9707E-01	2.78E 00	40	3.8277E-10
2.9704489E-01		1.1881793E 01	4.7527182E 02		
(X2)	4	1.2788E 00	3.25E-01	10	1.0117E-10
1.2116948E 00		1.2788097E 01	1.2116948E 02		
(X2)	4	1.9948E 00	1.64E 00	20	6.3031E-10
1.9947213E 00		3.9894431E 01	7.9788854E 02		
(X2)	4	6.5433E-01	2.63E 00	30	5.0750E-10
6.5432348E-01		1.9628729E 01	5.8889113E 02		
(X2)	4	3.0301E-01	2.83E 00	40	4.1062E-10
3.0300318E-01		1.2120126E 01	4.8480509E 02		
(X2)	5	1.1876E 00	4.95E-01	10	6.9811E-11
1.0450575E 00		1.1876340E 01	1.0450575E 02		
(X2)	5	1.2487E 00	1.62E 00	20	3.7958E-10
1.2487153E 00		2.4974306E 01	4.9948611E 02		
(X2)	5	5.5787E-01	2.41E 00	30	4.7511E-10
5.5786723E-01		1.6735896E 01	5.0208051E 02		
(X2)	5	2.8339E-01	2.67E 00	40	3.6502E-10
2.8339281E-01		1.1335712E 01	4.5342850E 02		
(X2)	6	1.1187E 00	5.94E-01	10	6.1826E-11
9.2733658E-01		1.1187406E 01	9.2733658E 01		
(X2)	6	9.9934E-01	1.61E 00	20	2.7805E-10
9.9933122E-01		1.9986623E 01	3.9973249E 02		
(X2)	6	4.9856E-01	2.30E 00	30	3.5297E-10
4.9855481E-01		1.4955778E 01	4.4869933E 02		
(X2)	6	2.6830E-01	2.58E 00	40	3.4573E-10

TABLE 4 (CONTINUED)

2.6830270E-01		1.0732108E 01	4.2928432E 02		
(X2)	7	1.0489E 00	6.81E-01	10	6.1955E-11
8.1511352E-01		1.0488686E 01	8.1511352E 01		
(X2)	7	8.3295E-01	1.60E 00	20	2.9755E-10
8.3295236E-01		1.6659048E 01	3.3318094E 02		
(X2)	7	4.4663E-01	2.21E 00	30	3.4147E-10
4.4662542E-01		1.3398431E 01	4.0196288E 02		
(X2)	7	2.5277E-01	2.49E 00	40	3.3459E-10
2.5275993E-01		1.0110396E 01	4.0441589E 02		
(X2)	8	9.6804E-01	7.71E-01	10	6.7696E-11
6.9432069E-01		9.6804108E 00	6.9432069E 01		
(X2)	8	6.9440E-01	1.60E 00	20	1.7937E-10
6.9438816E-01		1.3887765E 01	2.7775526E 02		
(X2)	8	3.9417E-01	2.12E 00	30	3.0287E-10
3.9416069E-01		1.1824923E 01	3.5474462E 02		
(X2)	8	2.3452E-01	2.40E 00	40	2.8902E-10
2.3450284E-01		9.3801115E 00	3.7520454E 02		
(X2)	9	9.1709E-01	8.24E-01	10	6.1918E-11
6.6792998E-01		9.1709075E 00	6.6792998E 01		
(X2)	9	6.2484E-01	1.59E 00	20	1.9507E-10
6.2482436E- 1		1.2496486E 01	2.4992974E 02		
(X2)	9	3.6434E-01	2.08E 00	30	2.5342E-10
3.6434065E-01		1.0930220E 01	3.2790658E 02		
(X2)	9	2.2288E-01	2.35E 00	40	3.0981E-10
2.2286695E-01		8.9146792E 00	3.5658712E 02		
(X2)	10	8.0348E-01	9.33E-01	10	4.3958E-11
6.4180896E-01		8.0348255E 00	6.4180896E 01		
(X2)	10	4.9992E-01	1.59E 00	20	1.3911E-10
4.9991633E-01		9.9983263E 00	1.9996653E 02		
(X2)	10	.0467E-01	1.99E 00	30	1.9112E-10
3.0466856E-01		9.1396672E 00	2.7420170E 02		
(X2)	10	1.9653E-01	2.24E 00	40	2.4083E-10
1.9652231E-01		7.8608916E 00	3.1443570E 02		
(X3)	1	1.3497E 00	0	10	1.1767E-10
1.3496503E 00		1.3496087E 01	1.3496503E 02		
(X3)	1	2.7571E 01	3.14E 00	20	9.5963E-09
2.7571428E 01		5.5142856E 02	1.1028571E 04		
(X3)	1	7.5097E-01	3.14E 00	30	5.5567E-10
7.5097276E-01		2.2528482E 01	6.7587549E 02		
(X3)	1	3.1796E-01	3.14E 00	40	4.2251E-10
3.1795717E-01		1.2718287E 01	5.0873147E 02		
(X3)	2	1.3496E 00	4.64E-03	10	6.6391E-04
1.3496210E 00		1.3496286E 01	1.3496210E 02		

TABLE 4 (CONTINUED)

(X3)	2	9.5937E 00	1.93E 00	20	1.3412E-01
9.5935709E 00		1.9187144E 02	3.8374284E 03		
(X3)	2	7.5091E-01	3.13E 00	30	1.8413E-03
7.5090710E-01		2.2527016E 01	6.7581639E 02		
(X3)	2	3.1795E-01	3.14E 00	40	5.8928E-04
3.1795185E-01		1.2718075E 01	5.0872296E 02		
(X3)	3	1.3457E 00	7.69E-02	10	1.1360E-02
1.3416772E 00		1.3456570E 01	1.3416772E 02		
(X3)	3	2.4223E 00	1.66E 00	20	1.4251E-01
2.4222876E 00		4.8445757E 01	9.6891504E 02		
(X3)	3	7.3483E-01	2.93E 00	30	2.8906E-02
7.3482130E-01		2.2043353E 01	6.6133917E 02		
(X3)	3	3.1721E-01	3.07E 00	40	9.7756E-03
3.1720922E-01		1.2688370E 01	5.0753475E 02		
(X3)	4	1.3164E 00	2.22E-01	10	3.3402E-02
1.2840150E 00		1.3164222E 01	1.2840150E 02		
(X3)	4	1.4008E 00	1.62E 00	20	1.4288E-01
1.4007534E 00		2.8015067E 01	5.6030136E 02		
(X3)	4	6.5444E-01	2.63E 00	30	7.2164E-02
6.5443369E-01		1.9632081E 01	5.8899033E 02		
(X3)	4	3.1168E-01	2.94E 00	40	2.8295E-02
3.1165918E-01		1.2466369E 01	4.9865469E 02		
(X3)	5	1.3164E 00	2.22E-01	10	3.3420E-02
1.2839435E 00		1.3163852E 01	1.2839435E 02		
(X3)	5	1.4003E 00	1.62E 00	20	1.4288E-01
1.4003337E 00		2.8006673E 01	5.6013350E 02		
(X3)	5	6.5436E-01	2.63E 00	30	7.2194E-02
6.5435721E-01		1.9629754E 01	5.8892149E 02		
(X3)	5	3.1167E-01	2.94E 00	40	2.8311E-02
3.1165176E-01		1.2466073E 01	4.9864282E 02		
(X3)	6	1.2415E 00	4.03E-01	10	5.5816E-02
1.1419842E 00		1.2414831E 01	1.1419842E 02		
(X3)	6	9.9081E-01	1.61E 00	20	1.4297E-01
9.9079891E-01		1.9815977E 01	3.9631956E 02		
(X3)	6	5.4696E-01	2.39E 00	30	1.0396E-01
5.4695877E-01		1.6408373E 01	4.9226289E 02		
(X3)	6	2.9680E-01	2.77E 00	40	5.1316E-02
2.9678356E-01		1.1871341E 01	4.7485370E 02		
(X3)	7	1.2414E 00	4.03E-01	10	5.5834E-02
1.1418014E 00		1.2413831E 01	1.1418014E 02		
(X3)	7	9.9051E-01	1.61E 00	20	1.4297E-01
9.9050186E-01		1.9810036E 01	3.9620075E 02		
(X3)	7	5.4685E-01	2.39E 00	30	1.0398E-01

TABLE 4 (CONTINUED)

5.4685377E-01		1.6405249E 01	4.9216839E 02		
(X3)	7	2.9678E-01	2.77F 00	40	5.1340E-02
2.9676378E-01		1.1870549E 01	4.7482205E 02		
(X3)	8	1.1686E 00	5.24F-01	10	6.5323E-02
1.0117952E 00		1.1685785E 01	1.0117952E 02		
(X3)	8	8.2586E-01	1.60F 00	20	1.4300E-01
8.2586078E-01		1.6517216E 01	3.3034431E 02		
(X3)	8	4.8218E-01	2.27F 00	30	1.1575E-01
4.8217993E-01		1.4465154E 01	4.3396194E 02		
(X3)	8	2.8155E-01	2.66F 00	40	6.6479E-02
2.8152524E-01		1.1261012E 01	4.5044038E 02		
(X3)	9	1.1323E 00	5.75F-01	10	6.8228E-02
9.4998566E-01		1.1323235E 01	9.4998566E 01		
(X3)	9	7.6735E-01	1.60F 00	20	1.4301E-01
7.6734145E-01		1.5346830E 01	3.0693658E 02		
(X3)	9	4.5606E-01	2.22F 00	30	1.1932E-01
4.5606261E-01		1.3681371E 01	4.1045635E 02		
(X3)	9	2.7373E-01	2.61E 00	40	7.2790E-02
2.7372589E-01		1.0949035E 01	4.3796142E 02		
(X3)	10	1.0829E 00	6.40E-01	10	7.1391E-02
8.6883547E-01		1.0828779E 01	8.6883547E 01		
(X3)	10	7.0072E-01	1.60F 00	20	1.4302E-01
7.0070838E-01		1.4014169E 01	2.8028335E 02		
(X3)	10	4.2438E-01	2.17F 00	30	1.2289E-01
4.2437690E-01		1.2731331E 01	3.8193921E 02		
(X3)	10	2.6285E-01	2.54F 00	40	8.0497E-02
2.6285082E-01		1.0514033E 01	4.2056131E 02		
(X4)	1	1.3497E 00	0	10	1.1767E-10
1.3496503E 00		1.3496087E 01	1.3496503E 02		
(X4)	1	2.7571E 01	3.14E 00	20	9.5963E-09
2.7571428E 01		5.5142856E 02	1.1028571E 04		
(X4)	1	7.5097E-01	3.14E 00	30	5.5567E-10
7.5097276E-01		2.2528482E 01	6.7587549E 02		
(X4)	1	3.1796E-01	3.14E 00	40	4.2251E-10
3.1795717E-01		1.2718287E 01	5.0873147E 02		
(X4)	2	1.3447E 00	8.57E-02	10	6.9422E-02
1.3397577E 00		1.3446956E 01	1.3397577E 02		
(X4)	2	1.3648E 01	2.09E 00	20	7.4429E-01
1.3648370E 01		2.7296740E 02	5.4593480E 03		
(X4)	2	7.5012E-01	3.09E 00	30	4.1417E-02
7.5011587E-01		2.2502891E 01	6.7510428E 02		
(X4)	2	3.1789E-01	3.12E 00	40	1.7333E-02
3.1787214E-01		1.2714883E 01	5.0859542E 02		

TABLE 4 (CONTINUED)

(X4)	3	1.3302E 00	1.70F-01	10	1.2912F-01
1.3109347E 00		1.3301490E 01	1.3109347F 02		
(X4)	3	7.5535E 00	1.85F 00	20	8.2377E-01
7.5533914E 00		1.5106784E 02	3.0213565F 03		
(X4)	3	7.4756E-01	3.05F 00	30	8.3348E-02
7.4756281E-01		2.2426377E 01	6.7280653E 02		
(X4)	3	3.1770E-01	3.10F 00	40	3.4647E-02
3.1768408E-01		1.2707365E 01	5.0829452F 02		
(X4)	4	1.3069E 00	2.52F-01	10	1.7845E-01
1.2655580E 00		1.3069301E 01	1.2655580E 02		
(X4)	4	5.1441E 00	1.76F 00	20	8.4155E-01
5.1440490E 00		1.0288098E 02	2.0576196E 03		
(X4)	4	7.4337E-01	3.00F 00	30	1.2546F-01
7.4336547E-01		2.2300460E 01	6.6902892E 02		
(X4)	4	3.1737E-01	3.08F 00	40	5.1926E-02
3.1737177E-01		1.2694870E 01	5.0779484E 02		
(X4)	5	1.2764E 00	3.31F-01	10	2.1790E-01
1.2070645E 00		1.2763706E 01	1.2070645E 02		
(X4)	5	3.8878E 00	1.71F 00	20	8.4804E-01
3.8877548E 00		7.7755097E 01	1.5551019E 03		
(X4)	5	7.3761E-01	2.95F 00	30	1.6743E-01
7.3760655E-01		2.2127588E 01	6.6384590E 02		
(X4)	5	3.1692E-01	3.06F 00	40	6.9120E-02
3.1689129E-01		1.2675649E 01	5.0702606E 02		
(X4)	6	1.2401E 00	4.06F-01	10	2.4884F-01
1.1393584E 00		1.2400546E 01	1.1393584E 02		
(X4)	6	3.1214E 00	1.68F 00	20	8.5105E-01
3.1213761E 00		6.2427518E 01	1.2485504E 03		
(X4)	6	7.3039E-01	2.91F 00	30	2.0890E-01
7.3039447E-01		2.1910985E 01	6.5735502E 02		
(X4)	6	3.1634E-01	3.04F 00	40	8.6251E-02
3.1633429E-01		1.2653373E 01	5.0613486E 02		
(X4)	7	1.1996E 00	4.76E-01	10	2.7315F-01
1.0662596E 00		1.1996149E 01	1.0662596E 02		
(X4)	7	2.6063E 00	1.67F 00	20	8.5276E-01
2.6062708E 00		5.2125416E 01	1.0425083E 03		
(X4)	7	7.2186E-01	2.86F 00	30	2.4958E-01
7.2185698E-01		2.1654460E 01	6.4967128E 02		
(X4)	7	3.1564E-01	3.02F 00	40	1.0328E-01
3.1563415E-01		1.2625365E 01	5.0501464E 02		
(X4)	8	1.1566E 00	5.41E-01	10	2.9285E-01
9.9111076E-01		1.1565751E 01	9.9111076E 01		
(X4)	8	2.2366E 00	1.65F 00	20	8.5374E-01

TABLE 4 (CONTINUED)

2.2365913E 00		4.4731824E 01	8.9463652E 02	
(X4)	8	7.1215E-01	2.82E 00	30 2.8919E-01
7.1215131E-01		2.1363730E 01	6.4093618E 02	
(X4)	8	3.1481E-01	3.00E 00	40 1.2016E-01
3.1477704E-01		1.2591085E 01	5.0364326E 02	
(X4)	9	1.1389E 00	5.66E-01	10 2.9984E-01
9.6109799E-01		1.1389288E 01	9.6109799E 01	
(X4)	9	2.1164E 00	1.65E 00	20 8.5405E-01
2.1164316E 00		4.2328632E 01	8.4657262E 02	
(X4)	9	7.0797E-01	2.80E 00	30 3.0467E-01
7.0796208E-01		2.1239134E 01	6.3716587E 02	
(X4)	9	3.1445E-01	2.99E 00	40 1.2688E-01
3.1443800E-01		1.2577518E 01	5.0310079E 02	
(X4)	10	1.1212E 00	5.90E-01	10 3.0649E-01
9.3132872E-01		1.1211509E 01	9.3132872E 01	
(X4)	10	2.0085E 00	1.64E 00	20 8.5426E-01
2.0084591E 00		4.0169187E 01	8.0338366E 02	
(X4)	10	7.0364E-01	2.78E 00	30 3.1992E-01
7.0363682E-01		2.1109028E 01	6.3327314E 02	
(X4)	10	3.1407E-01	2.98E 00	40 1.3361E-01
3.1406670E-01		1.2562668E 01	5.0250672E 02	

The steady-state response diagrams from the computer program are given in Figs. 2 through 9. The damping coefficients used were calculated by the equivalent energy methods, assuming the viscous coefficients would give a complete response diagram above critical damping and an output amplitude of unity. These assumptions are seen to give excellent coverage of the response.

The response curves can be used to study the effects of damping. The variation in the functional relationship as the damping coefficient is increased can be estimated when compared with the numerical solution in Chapter IV.

The values of the damping coefficients used for plotting the following response diagrams are:

Damping Coefficient	Coulomb	Velocity	Velocity Squared	Displacement Squared
BETA 1	0	0	0	0
BETA 2	0.10000	0.01000	0.00050	0.50000
BETA 3	0.30000	0.03000	0.00200	1.50000
BETA 4	0.50000	0.05000	0.00400	2.50000
BETA 5	0.70000	0.08000	0.00600	3.50000
BETA 6	0.78000	0.10000	0.00800	4.50000.

The frequency ratios for the plotted points are:

OMGP = .10180
OMGP = .20359
OMGP = .30539
OMGP = .40719
OMGP = .50899
OMGP = .61078
OMGP = .71258
OMGP = .81438
OMGP = .91618
OMGP = 1.01797
OMGP = 1.11977
OMGP = 1.22157
OMGP = 1.32337
OMGP = 1.42516
OMGP = 1.52696
OMGP = 1.62876
OMGP = 1.73055
OMGP = 1.83235
OMGP = 1.93415
OMGP = 2.03595
OMGP = 2.13774
OMGP = 2.23954
OMGP = 2.34134
OMGP = 2.44314
OMGP = 2.54493

where OMGP = $\frac{\omega}{\omega_n}$.

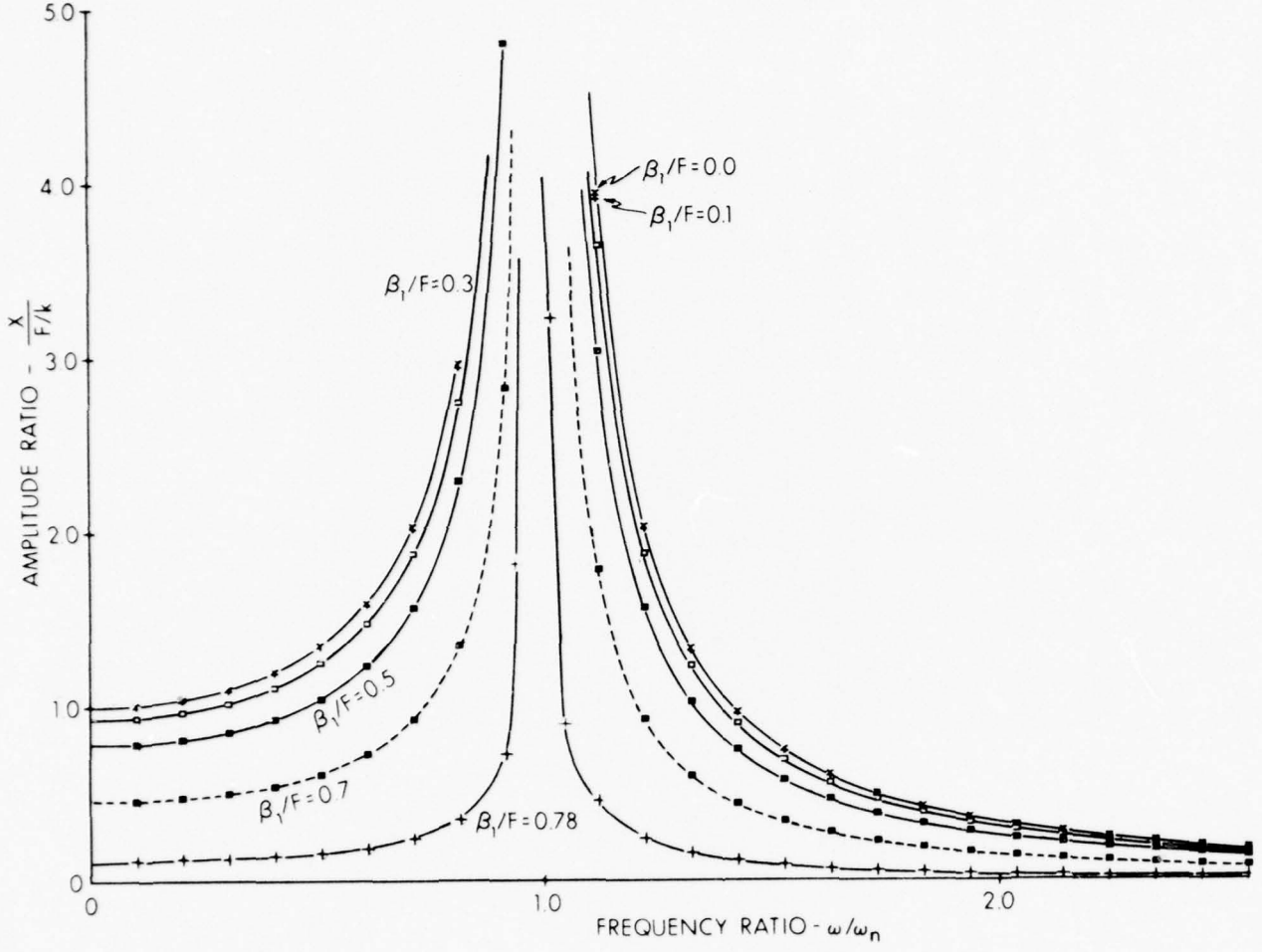

FIGURE 2
LINEARIZED RESONANCE CURVES OF SYSTEM WITH COULOMB DAMPING
AS A FUNCTION OF DAMPING RATIOS

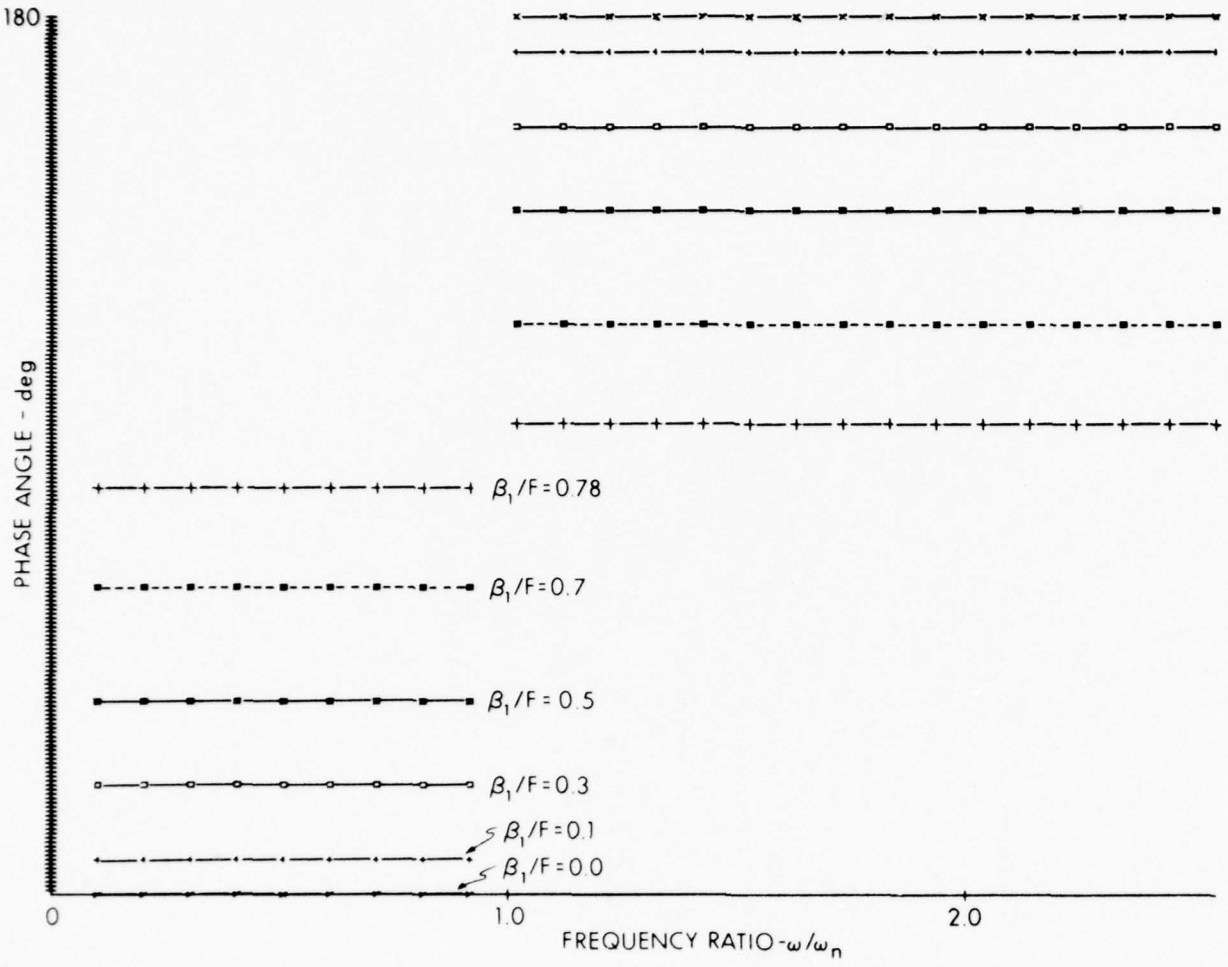

FIGURE 3
LINEARIZED PHASE ANGLES OF SYSTEM WITH COULOMB DAMPING
AS A FUNCTION OF DAMPING RATIOS

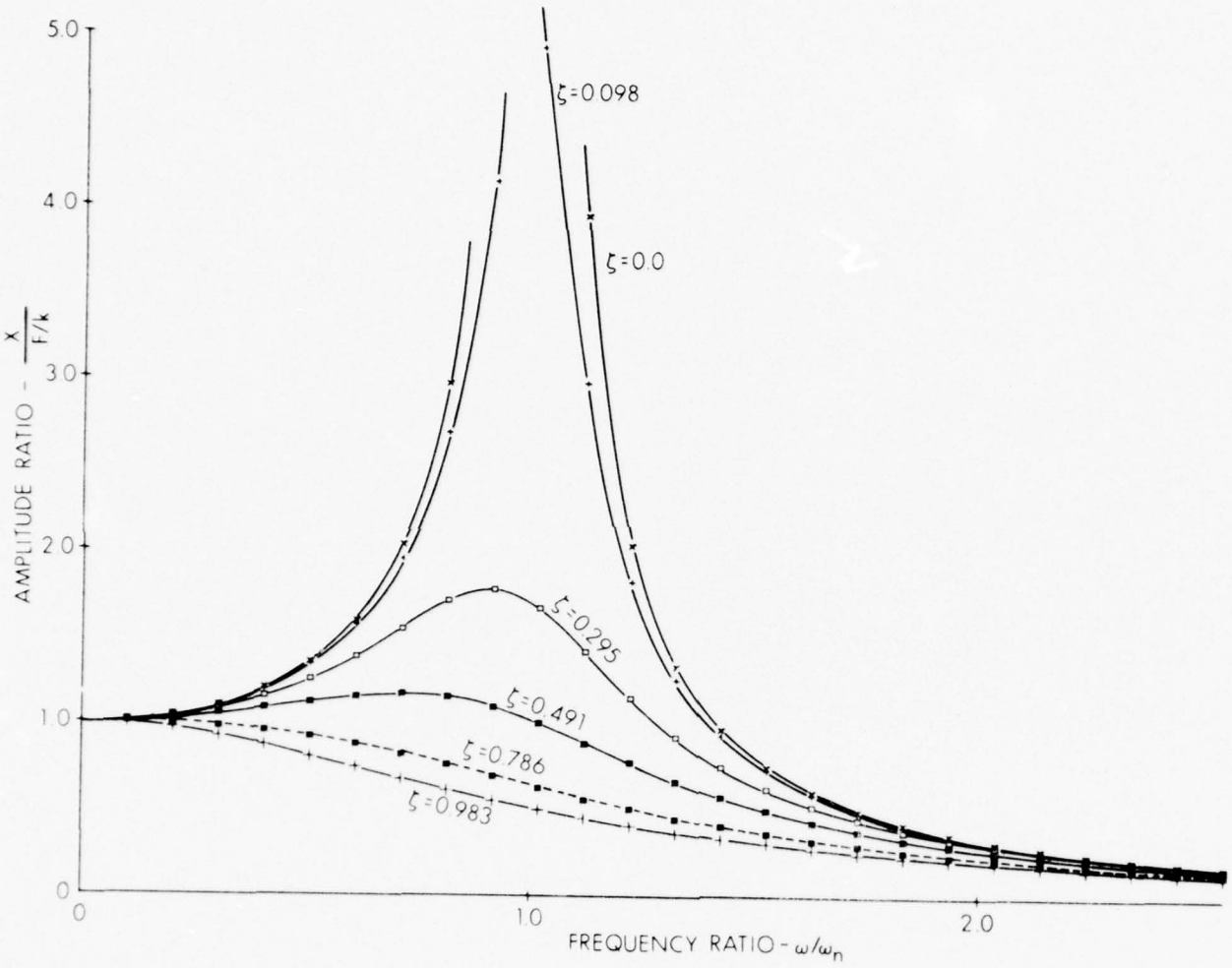

FIGURE 4
LINEARIZED RESONANCE CURVES OF SYSTEM WITH VISCOUS DAMPING
AS A FUNCTION OF DAMPING RATIOS

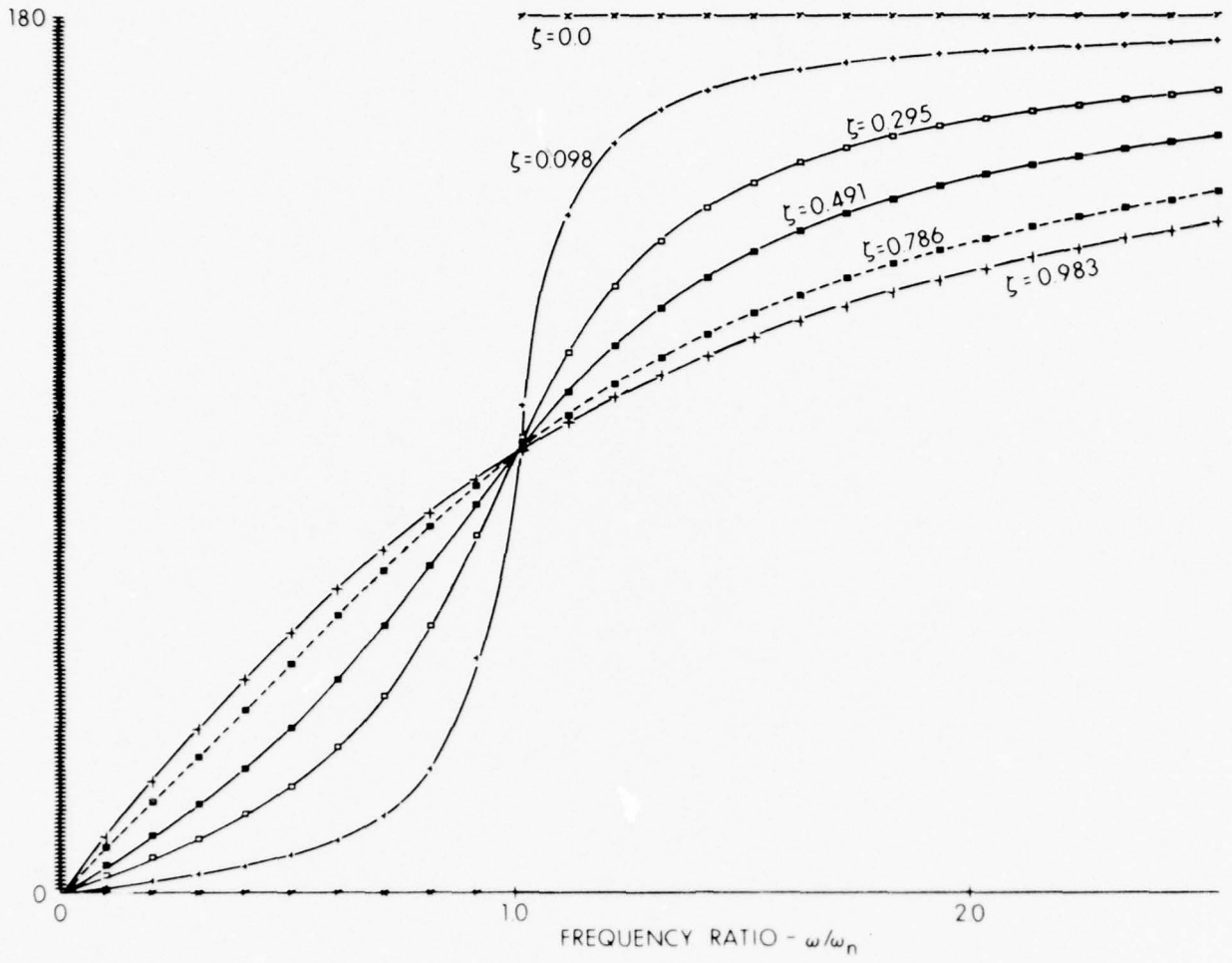

FIGURE 5
LINEARIZED PHASE ANGLE CURVES OF SYSTEM WITH VISCOUS DAMPING
AS A FUNCTION OF DAMPING RATIOS

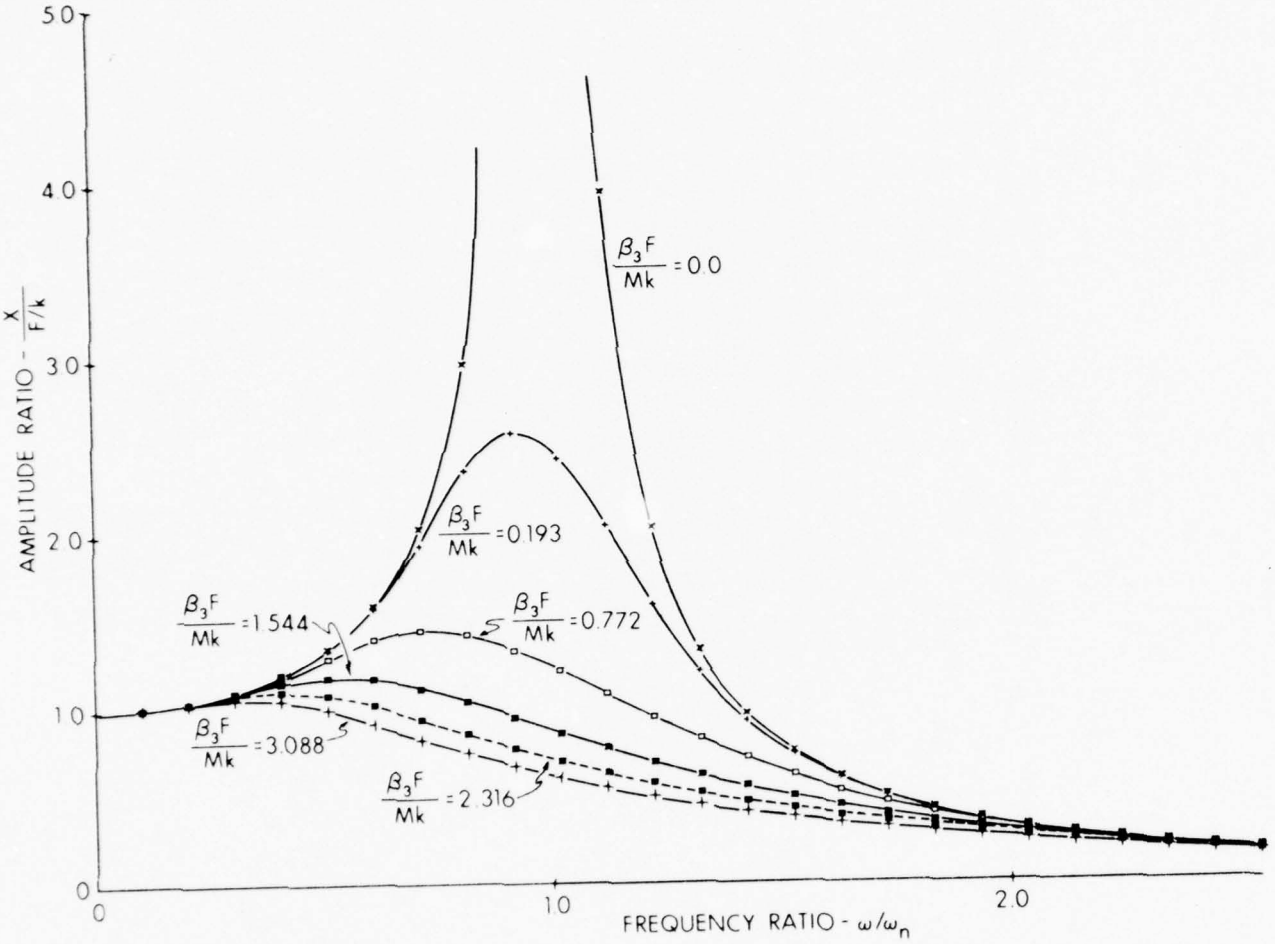

FIGURE 6
LINEARIZED RESONANCE CURVES OF SYSTEM WITH
VELOCITY-SQUARED DAMPING AS A FUNCTION OF DAMPING RATIOS

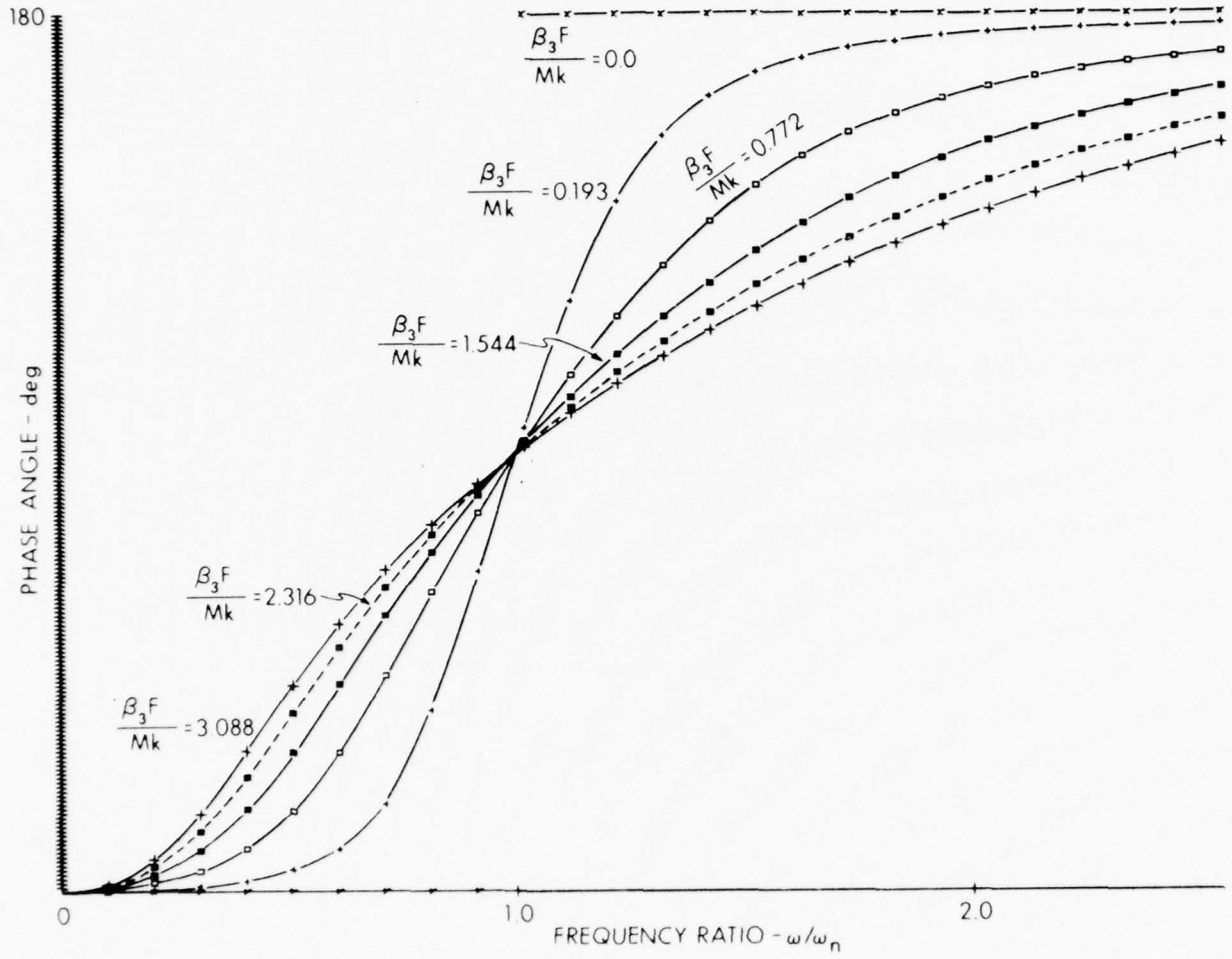

FIGURE 7
LINEARIZED PHASE ANGLE CURVES OF SYSTEM WITH
VELOCITY-SQUARED DAMPING AS A FUNCTION OF DAMPING RATIOS

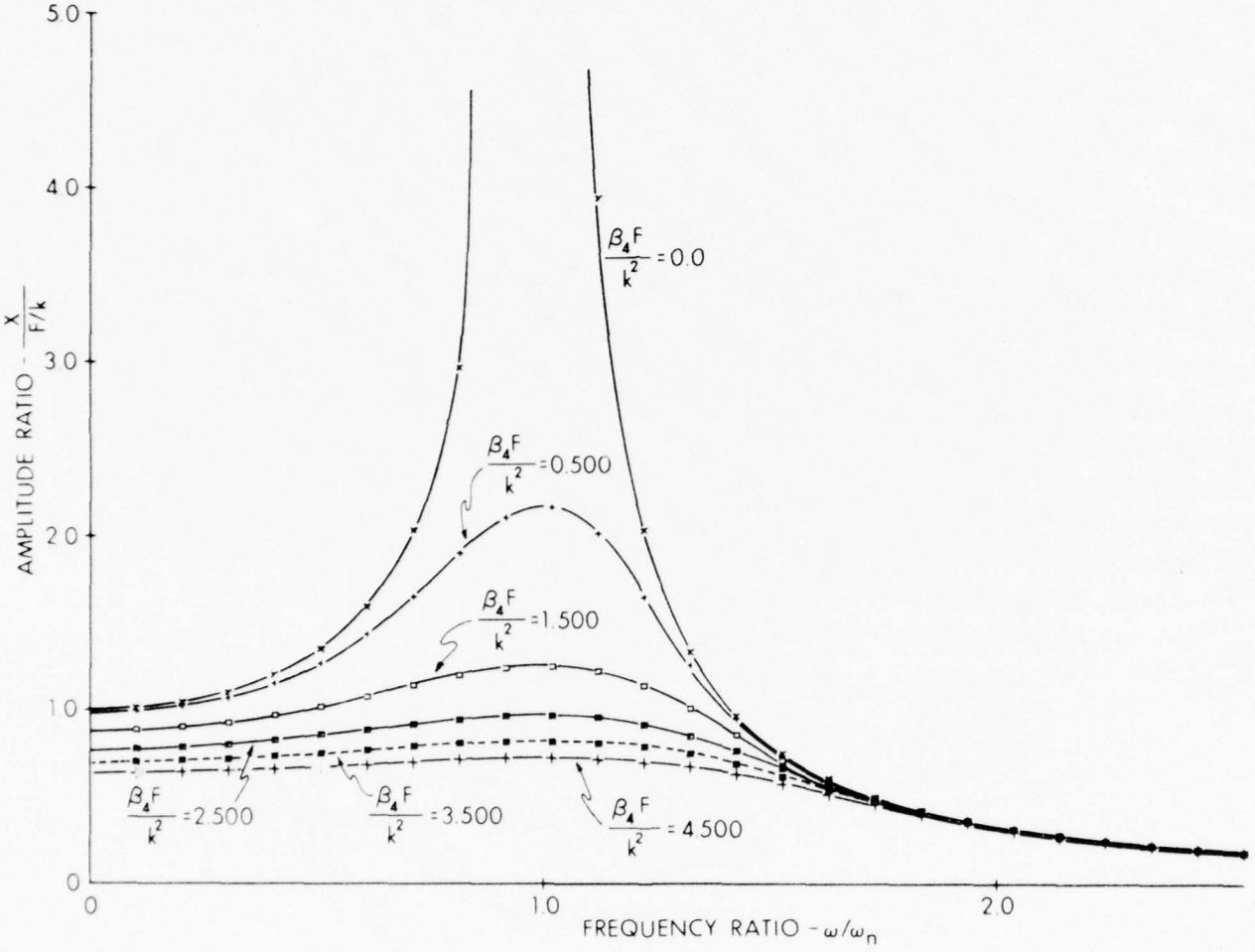

FIGURE 8
LINEARIZED RESONANCE CURVES OF SYSTEM WITH
DISPLACEMENT-SQUARED DAMPING AS A FUNCTION OF DAMPING RATIOS

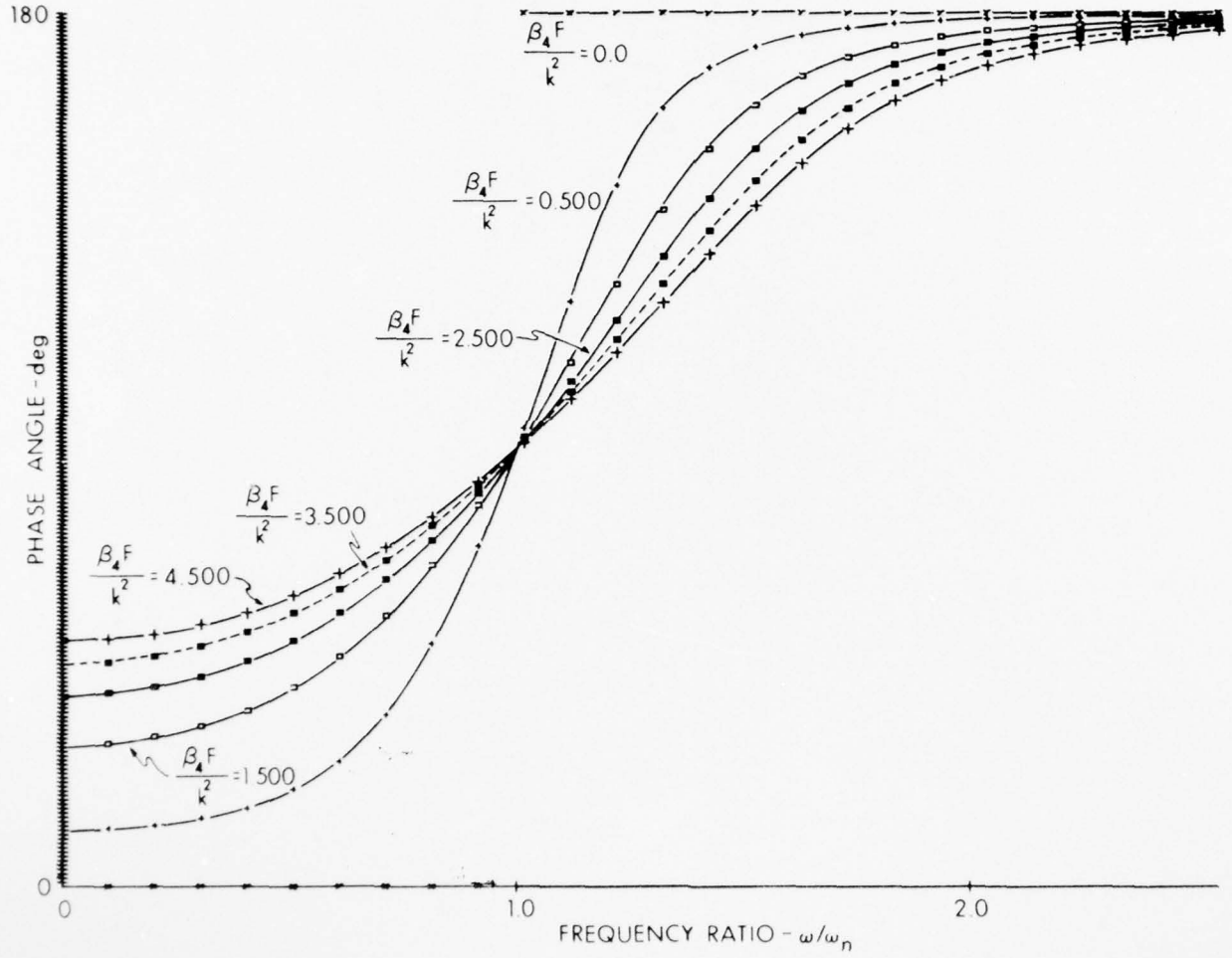

FIGURE 9
LINEARIZED PHASE ANGLE CURVES OF SYSTEM WITH
DISPLACEMENT-SQUARED DAMPING AS A FUNCTION OF DAMPING RATIOS

CHAPTER III

DIMENSIONAL ANALYSIS

A. Introduction

Dimensional analysis of any physical problem can be utilized to great advantage, the only requirement being that one have sufficient knowledge of the physical variables to apply the procedure. The requirements do not demand a complete understanding of the functional relations but rather a knowledge of the most important physical variables. Full use of dimensional analysis has not been made in vibration problems. It is believed that the section on dimensional analysis is unique and indicates the general conclusions that can be drawn from analysis in the case of a damped system. To the knowledge of this author no one has presented an analysis of this type.

The uniqueness of the analysis is the application of dimensional analysis to the dimensionless ratios to use in the response diagram. The analysis includes the definition of the critical damping ratios. This allows significant general conclusions to be drawn from the response curve without knowing the exact functional relationship of the variables. Also, the fundamental linearization of the system can be used to interpret the results. For example, a comparison of the equivalent linear relationships and the dimensional relations reveals a basic agreement of the results. The exact range of this agreement is indicated in the section on the analysis of the results.

B. Results Obtained

Considering the single-degree-of-freedom system shown in Fig. 1, the following physical variables completely describe the system behavior (expressed in terms of the units force F, length L, and time T).

$$M \doteq \frac{FT^2}{L}$$

$$k \doteq \frac{F}{L}$$

$$F \doteq F$$

$$\omega \doteq \frac{1}{T}$$

$$X \doteq L$$

$$B_2 \doteq \frac{FT}{L},\ B_3 \doteq \frac{FT^2}{L^2},\ B_1 \doteq F,\ B_4 \doteq \frac{F}{L^2}\ .$$

It should be noted that all of the variables appear in the differential equation of motion. A dimensionally homogeneous equation exists if the variables are independent according to the Buckingham phi theorem.[9] Any relationships that are deductible from the resulting equations are consequently dimensionally homogeneous. There exists a general equation of the form

$$f(M,k,F,\omega,X,C) = 0\ .$$

By virtue of Buckingham's theorem, the following complete set of dimensionless independent ratios exists:

$$\frac{\omega}{\sqrt{\frac{k}{M}}}, \frac{X}{\frac{F}{k}}, \frac{\beta_2}{\sqrt{MK}} \qquad \frac{\omega}{\sqrt{\frac{k}{M}}}, \frac{X}{\frac{F}{k}}, \frac{\beta_1}{F}$$

$$\frac{\omega}{\sqrt{\frac{k}{M}}}, \frac{X}{\frac{F}{k}}, \frac{\beta_3 F}{Mk} \qquad \frac{\omega}{\sqrt{\frac{k}{M}}}, \frac{X}{\frac{F}{k}}, \frac{\beta_4 F}{k^2} .$$

Dimensional ratios other than the ones above do exist; however, the ratios shown are the most useful because of their independence of amplitude. A comparison of the viscous ratios and the other ratios (in Table 5) can be used to interpret the general areas of the response diagrams.

General conclusions concerning the various areas of the response diagram may be drawn if it can be shown that the ratios are independent. The dimensionless ratios for C, as shown in Table 5, indicate the general trend of the function if C_x is independent of the variables considered. In the case of viscous damping (C_x is equal to 2), C_x is known to be independent of the other physical variables. If the same independence can be established for the other cases of damping, then general conclusions can be drawn concerning the response diagrams.

Upon close inspection of the ratios shown in Table 5, the similarity of the expressions for C would suggest that the ratios in column 1 are the critical damping ratios. The dominant physical variables in the viscous critical case are the mass and spring constant. The other viscous ratios may be observed as dominating the spring-controlled portion, the damping-controlled portion, and the mass-controlled portion of the diagram. Similar general conclusions can be reached concerning the other damping cases. For example, the spring controlled portion of the response diagram for velocity-squared-damping will vary directly as the spring constant and inversely as ω_n^2 and X.

TABLE 5

POSSIBLE DIMENSIONLESS DAMPING RATIOS

DAMPING FUNCTION	CRITICAL DAMPING RATIO	SPRING CONTROLLED RATIO	MASS CONTROLLED RATIO
COULOMB	$C_x F$	$C_x Xk$	$C_x M\omega^2 X$
VISCOUS	$C_x\sqrt{Mk}$	$C_x k/\omega_n$	$C_x M\omega_n$
VELOCITY SQUARED	$C_x Mk/F$	$C_x k/X\omega^2$	$C_x M/X$
DISPLACEMENT SQUARED	$C_x k^2/F$	$C_x k/X$	$C_x \omega^2 M/X$

A summary of the normalized damping coefficients for both the equivalent energy method and the dimensionless ratios is shown in Table 5. The coefficients are normalized to the viscous coefficient so that the equivalent damping coefficient for each case can be compared. The numerical value of the damping coefficients for the various cases are shown. These values are calculated at the resonant peak of 19.646 radians/second. These values indicate the range of damping coefficients at resonance and are calculated disregarding any dependence on C_x and assuming an amplitude at resonance of one.

The analytic methods of investigating the response of the damping cases do not give one a clear and explicit feeling for the meaning of stability. The energy method suggests the correct interpretation to place on the meaning of stability. The procedure is to calculate the equivalent damping coefficients for the various cases and to compare these coefficients with the viscous case. This method would show the areas of the response diagram that are underdamped and overdamped. Thus, a general interpretation of stability in terms of underdamping and overdamping is possible.

The equivalent energy coefficients for the cases as shown in Chapter II indicate that the stability is no more complicated than the linear case. The magnitude of the damping coefficient that is required for stable motion in the viscous case is greater than 0.0005 of critical. This gives uniform steady-state motion and fairly short transients.

The discontinuities in the damping force would be expected to excite all harmonics. The combination of these harmonics could cause instability.

For velocity-squared damping, the magnitude of the damping coefficient over the frequency range considered indicates that the response is stable for all values of $\frac{\beta_3 F}{Mk}$ between 0.6 and 2.0 (predicted by equal energy).

For displacement-squared damping the coefficients are seen to vary considerably with frequency, i.e., a stable system cannot be constructed unless the damping is varied with frequency.

For Coulomb damping the coefficient varies approximately as for displacement-squared damping, i.e., the response diagram should contain a subresonance above and below the natural frequency. Stable response should occur for values of $\frac{\beta_1}{F}$ between 0.39 and 1.5 (predicted by equal energy).

The principle of similarity was combined with the equivalent linearization technique to interpret the response of the damped systems. The dimensional analysis of the problem revealed some of the ways in which the constants enter into the solution. Although mathematical derivations are frequently attacked with this general method, the interpretation of the results is unique in that they have not been applied to the vibration damping cases.

If the problem is solved for the case in which these constants are specified numerical values (i.e., unity), the solution may be immediately generalized to cover the case in which the constants have arbitrary values. These solutions, along with the proof of independence, are given in Chapter VII.

CHAPTER IV

ADAMS-MOULTON NUMERICAL ANALYSIS

A. Introduction

The method of obtaining the solution to ordinary first and second order differential equations by the fourth order Runge-Kutta and Adams formulas[4] can be found in books giving a discussion of numerical approximations. The Adams-Moulton method for continuation of the increments of the function with the existing slopes is found in most advanced numerical analysis texts.[4] The Adams-Moulton procedure provides a method of predicting the error after each integration step. The procedure is inherently more accurate than the Runge-Kutta method if there are no abrupt discontinuities in the solution. When a discontinuity occurs, the derivative at that point does not exist. The existence of all the derivatives of all orders up to and including the order of the solution must exist; otherwise the formulas do not apply.

The numerical solution to the second order ordinary differential equations is accomplished by reducing the equations to two simultaneous first-order equations and solving these simultaneous equations with Adams-Moulton equations. The starting values for the Adams-Moulton procedure are obtained with the Runge-Kutta formulas and the initial conditions.

The fourth order Runge-Kutta formula used to obtain the starting values is

$$y_{i,1} = y_i + \frac{1}{6}\left[K_{0,i} + 2K_{1,i} + 2K_{2,i} + K_{3,i}\right]$$

$$i = 1,2,3,\ldots,N. \qquad (26)$$

There are two Adams-Moulton formulas.[4] One is the prediction equation

$$y_{i,1} = y_i + \frac{h}{24}\left[55\ F_i - 59\ F_{i,-1} + 37\ F_{i,-2} - 9\ F_{i,-3}\right] \qquad (27)$$

and the correction equation

$$y_{i,1} = y_i + \frac{h}{24}\left[9\ F_{i,1} + 19\ F_i - 5\ F_{i,-1} + F_{i,-2}\right] . \qquad (28)$$

The addition of the step values of $h\Delta y_i$ to the correct value of y_i is carried out in double precision, i.e., 72 bit word length (all the precision available on the CDC 3200 computer). All other operations are done in single precision, i.e., 24 bit word length. This conserves the accuracy of the above methods which have errors less than $\left[h\right]^5$. (Note: For the equation used, the program will not run with any repeatable accuracy without the double precision arithmetic.)

The error analysis consists of checking the relative magnitude of the corrected value at each step by the following formula:

$$\text{error} = \max \left| \frac{-19\left[y^C_{i,-1} - y^P_{i,1}\right]}{270\left[y^C_{i,1}\right]} \right|^4 \qquad (29)$$

where C and P refer to corrected and predicted, respectively. Equation (29) represents the error due to the truncation of Eqs. (27) and (28).

This procedure provides some estimate of the number of significant digits obtained in the corrected solution as the calculations are performed. This procedure will not guarantee the accuracy of the solution since accumulative errors cannot be detected. Also, the specifications of the limit values of the error are critical, and will vary with the rate of change of the derivatives. The exact solution of Eq. (1) is obtained if the following identity is satisfied:

$$M\ddot{x} + C\ f(x,\dot{x}) + kx - F \sin \omega t \equiv 0 .$$

Therefore, the determination of the residual in the above equation will indicate the accuracy of the solution. The root-mean-square (RMS) value of the residual is determined over the steady-state period. This residual was found to be small for a minimum of 150 points per cycle. The minimum and maximum number of points per cycle is fixed for each frequency so that the accuracy and storage space requirements are preserved. A table of the integration steps versus frequency was compiled for this purpose. The numerical value of the RMS residual is less than 10^{-8} for all the equations.

The steady-state condition exists if the wave form of the solution and all of the derivatives vary in a continuing periodic manner, i.e., $f(x) = f(x+\tau)$. The steady-state check is performed once per cycle when the displacement changes sign from negative to positive. When this amplitude sign change occurs all of the calculated values over a cycle are checked for maximum value by substitution into subroutine AMV. The maximum value is stored and compared to the previous maximum values, as shown in Fig. 10. The amplitudes are compared with the following formula:

$$\left| \left| \frac{Dx(i) - Dx(i-1)}{Dx(i)} \right| - 0.005 \right| .$$

If the amplitude check falls within the defined limits the periodicity is checked by the following formula:

$$\left| \left| \frac{Bz(i) - Bz(i-1)}{Bz(i)} \right| - 0.005 \right| .$$

If the motion does not cross the time axis, a storage limit stops the program and the data is printed and plotted. (Note: Both positive and negative values of the amplitude and period are permitted.)

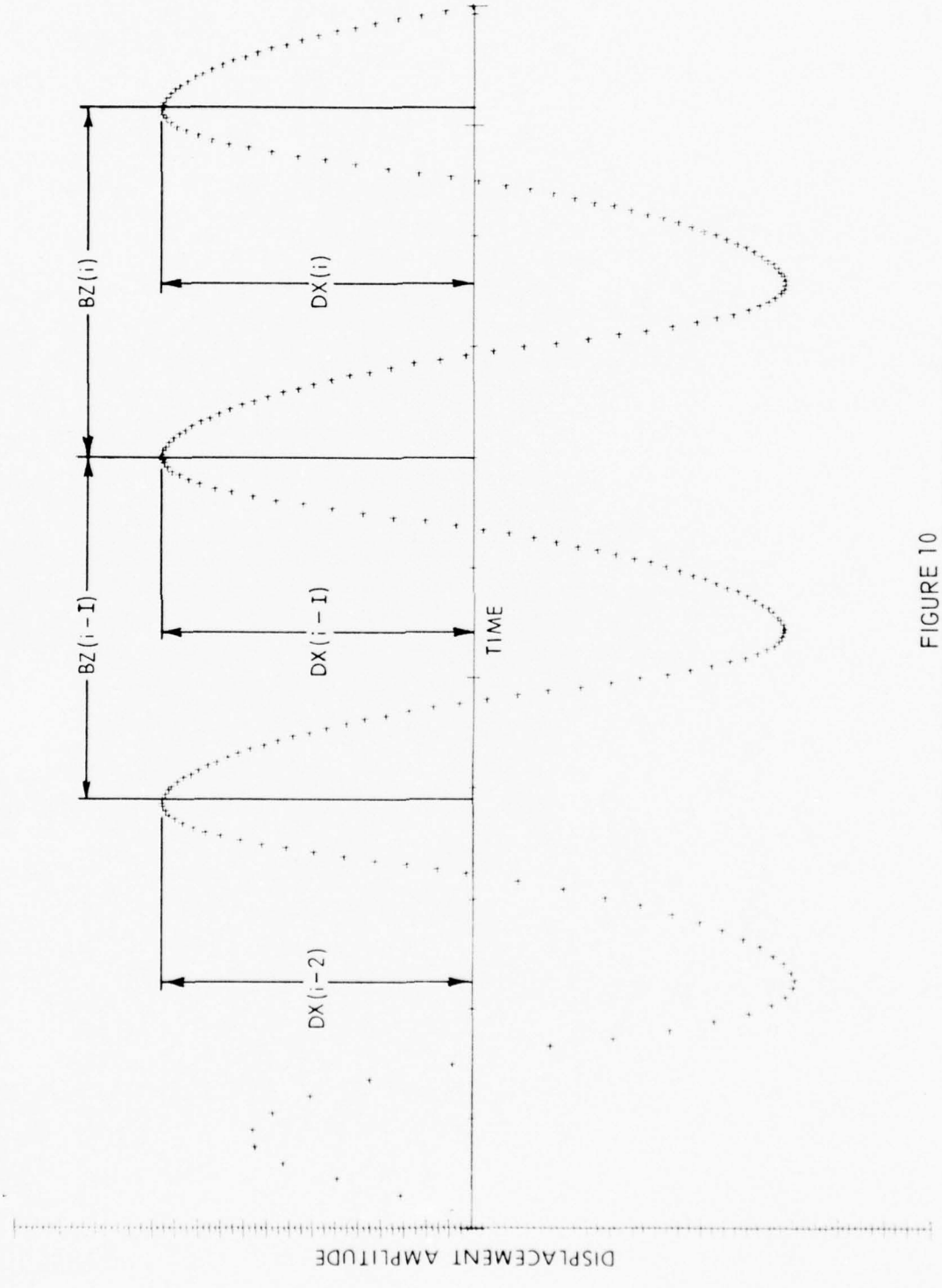

FIGURE 10
DEFINITION OF STEADY-STATE CONDITIONS

When the continuing periodicity of the wave form is established, the steady-state and transient data are printed. All of the calculations are self-explanatory except the energy dissipated per cycle and the phase angle.

The actual damping energy per cycle is calculated with the formulas given in Chapter III. The correct expression for each damping case must be used; therefore, a program was written for each damping function.

The areas under the curves are determined by Simpson's 1/3 rule. The justification for using the 1/3 rule, rather than a higher approximation, is the inherent accuracy of the calculated values (see section above). Also, the number of calculated points per cycle is not necessarily an even number as required by other procedures such as the 3/8 rule. For an RMS error of 10^{-10}, the value of the energy calculation is accurate to four places (a relative error of 0.01% for the viscous case).

The phase angle between the forcing function and the displacement amplitude is calculated at the zero crossing and at the peak amplitudes. This is done by comparing the angular travel of the forcing function to the resulting displacement travel with time equal to zero as a reference. The phase angle at the zero crossing was used as an aid in reducing the data. Unless otherwise specified, all reference to phase angle will mean phase angle at the positive peaks.

The values printed under transient response are cyclic values, and are printed without regard to sign.

A complete time-history of the displacement, velocity, and acceleration is plotted at the end of each run. Every tenth value of the data is plotted on a 6-in. by 8-in. axis the scale of which is determined by

subroutine Largest. The original program contained a routine to plot the complete steady-state and transient response diagrams; however, this was found to be impractical because of the computer time required (eight hours for viscous damping). The program is given in the Appendix, p. 128.

B. Numerical Results

The computer program described above is used to solve the equations of motion. With the exception of additional values of the damping coefficients, the parameters (shown in Table 3) are used for all damping cases. The equations for Coulomb, velocity-squared, and displacement-squared are presented since the viscous case is given in Chapter II.

The viscous case was used as a base for comparing the accuracy of the other equations. A direct comparison of equivalent energy method, the numerical method, and the results from a desk calculator revealed no distinguishable error in the maximum values of the displacement, velocity, and acceleration. Several different frequencies were checked on either side of resonance. Also, the values of the RMS error are of the same magnitude (10^{-10}) for each integration step as it is over a cycle of motion. It should be noted that the CDC 3200 computer has only 10 digits of accuracy. Therefore, RMS errors in the same order of magnitude are considered sufficiently accurate.

The steady-state response characteristics of Coulomb, velocity-squared, and displacement-squared damping are given in Figs. 11 through 40. The RMS error is in the order of 10^{-10} for all cases. They are plotted as a function of the damping ratios given in Chapter III. The displacement, phase angle, velocity, acceleration, and the damping energy per cycle are given. The values plotted are for the steady-state conditions defined in

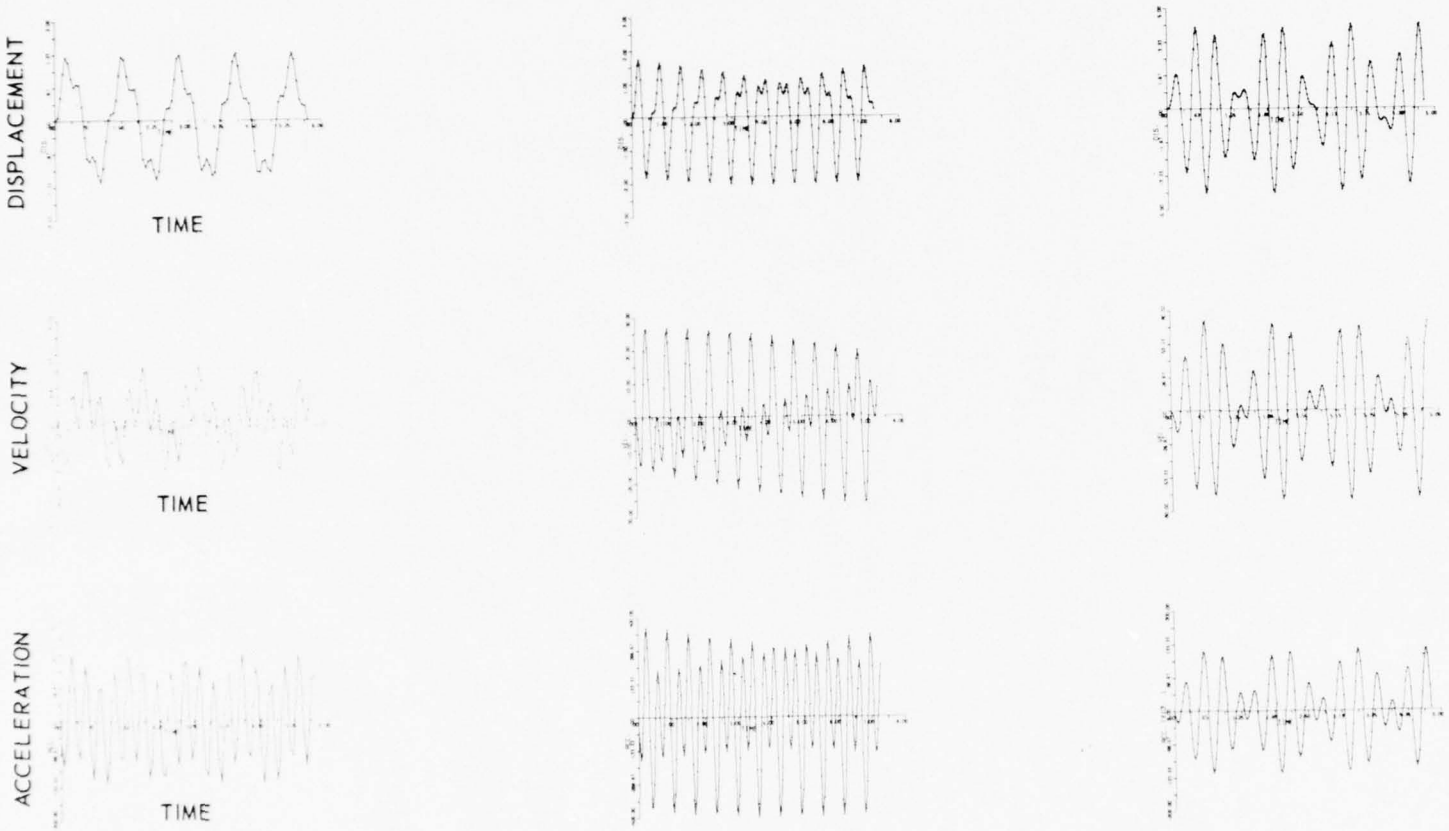

FIGURE 11
TIME-HISTORIES OF DISPLACEMENT, VELOCITY,
AND ACCELERATION FOR NO DAMPING,
$\omega/\omega_n = 0.255$, $\omega/\omega_n = 0.509$, AND $\omega/\omega_n = 0.764$

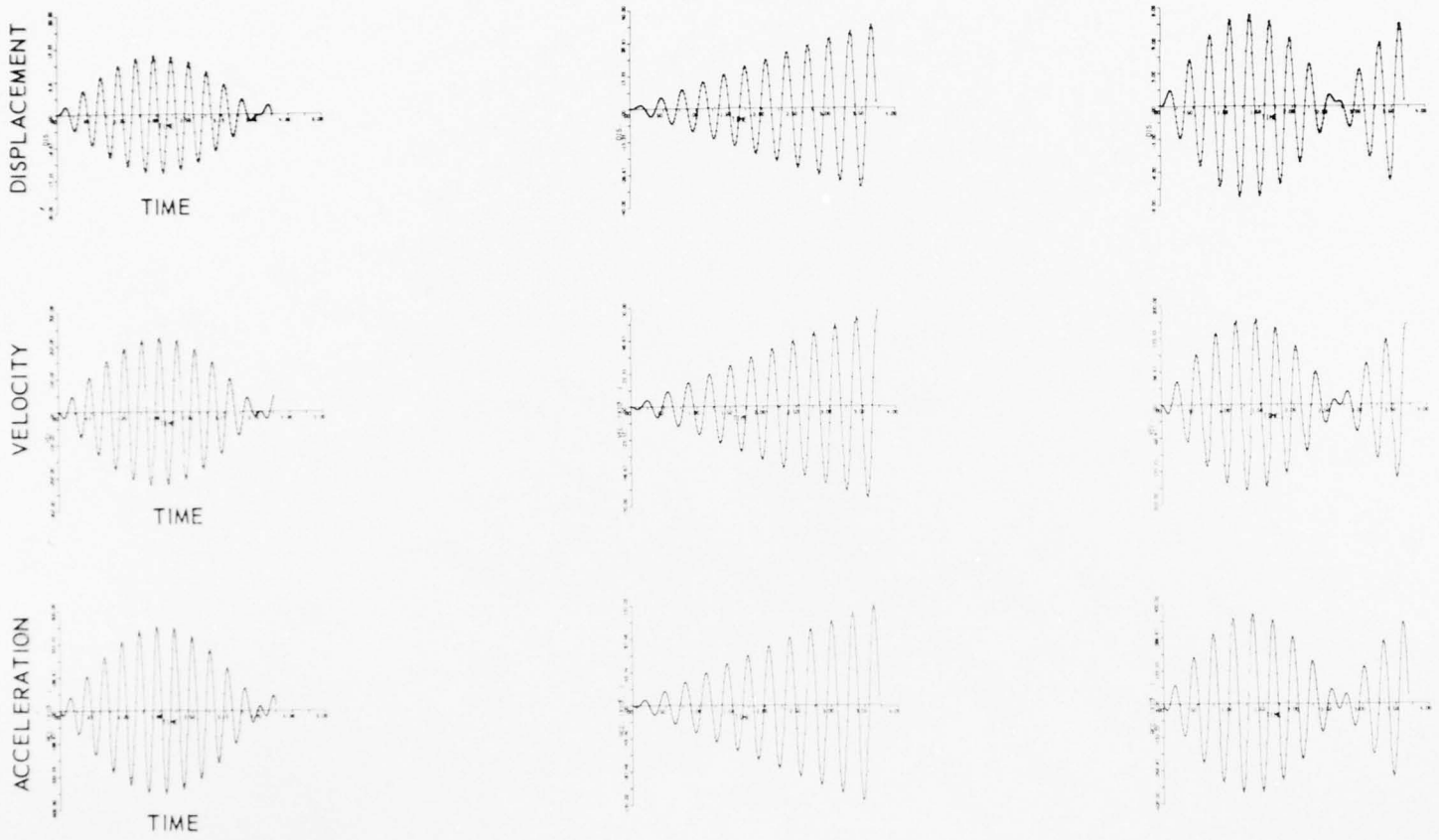

FIGURE 12
TIME-HISTORIES OF DISPLACEMENT, VELOCITY, AND ACCELERATION FOR NO DAMPING, $\omega/\omega_n = 0.916$, $\omega/\omega_n = 1.018$, AND $\omega/\omega_n = 1.120$

FIGURE 13
TIME-HISTORIES OF DISPLACEMENT, VELOCITY,
AND ACCELERATION FOR NO DAMPING,
ω/ω_n = 1.272, ω/ω_n = 1.527, AND ω/ω_n = 2.545

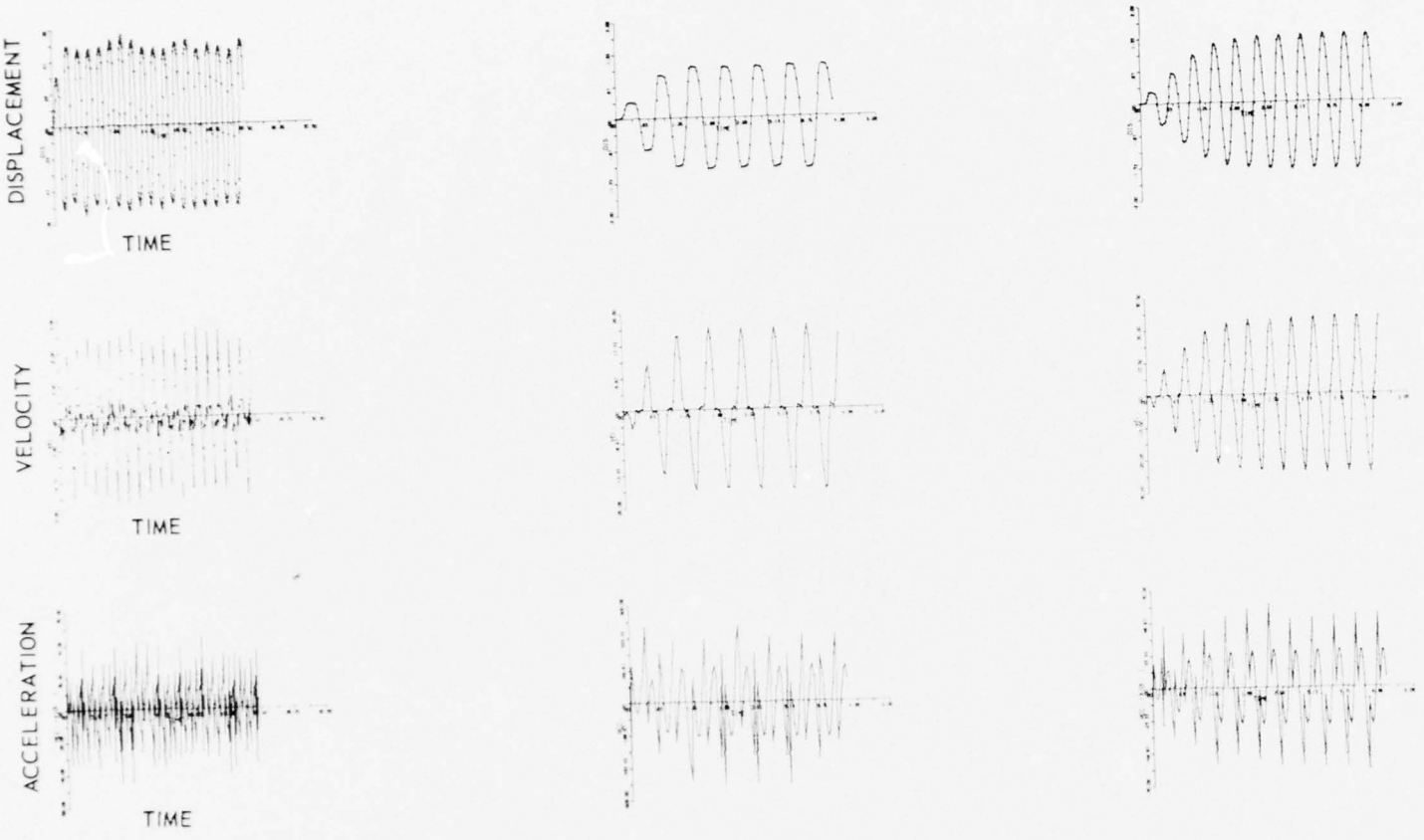

FIGURE 14
TIME-HISTORIES OF DISPLACEMENT, VELOCITY,
AND ACCELERATION FOR COULOMB DAMPING WITH $\beta_1/F = 0.77$,
$\omega/\omega_n = 0.255$, $\omega/\omega_n = 0.509$, AND $\omega/\omega_n = 0.764$

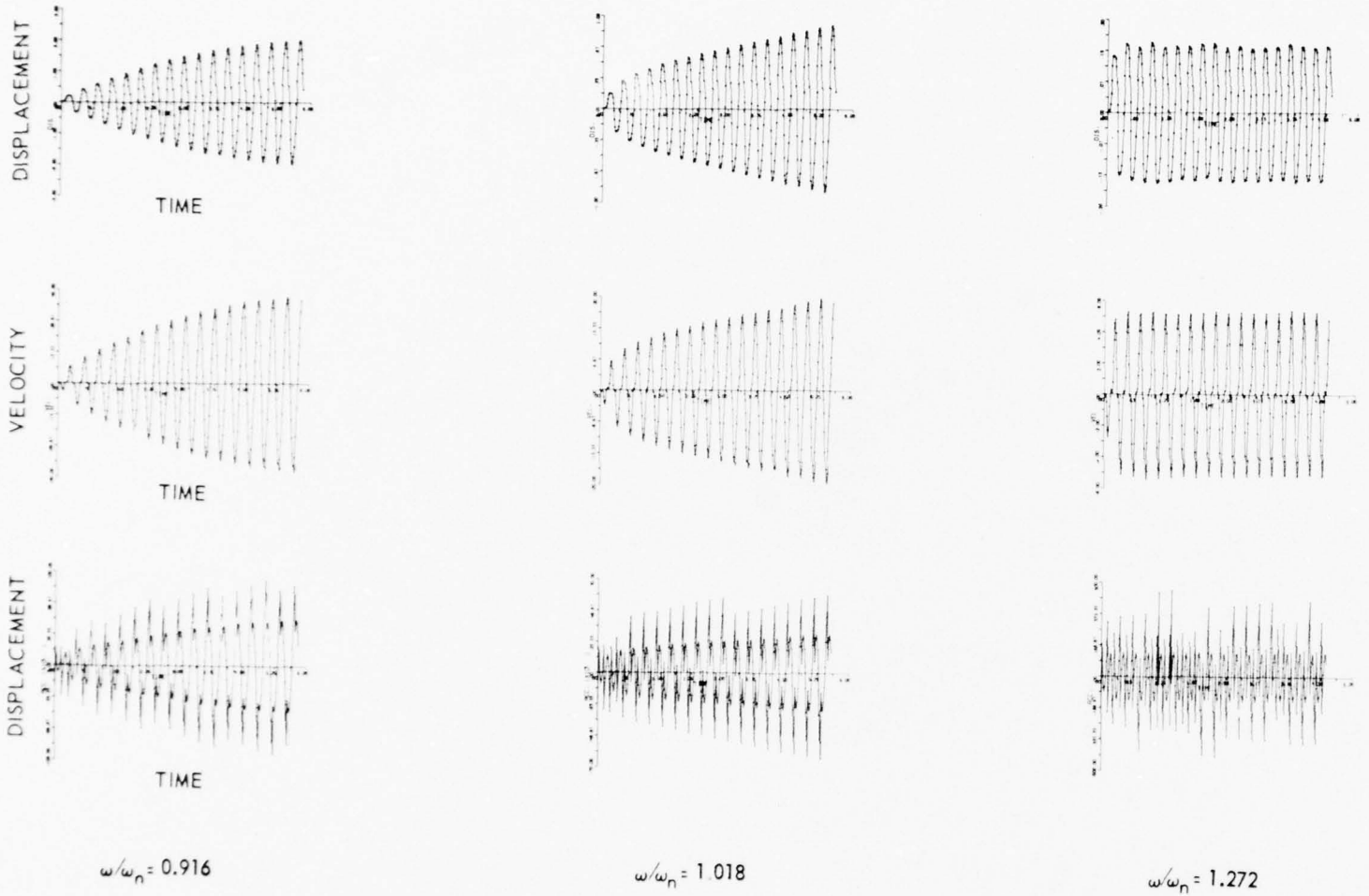

FIGURE 15
TIME-HISTORIES OF DISPLACEMENT, VELOCITY,
AND ACCELERATION FOR COULOMB DAMPING WITH $\beta_1/F = 0.77$,
$\omega/\omega_n = 0.916$, $\omega/\omega_n = 1.018$, AND $\omega/\omega_n = 1.272$

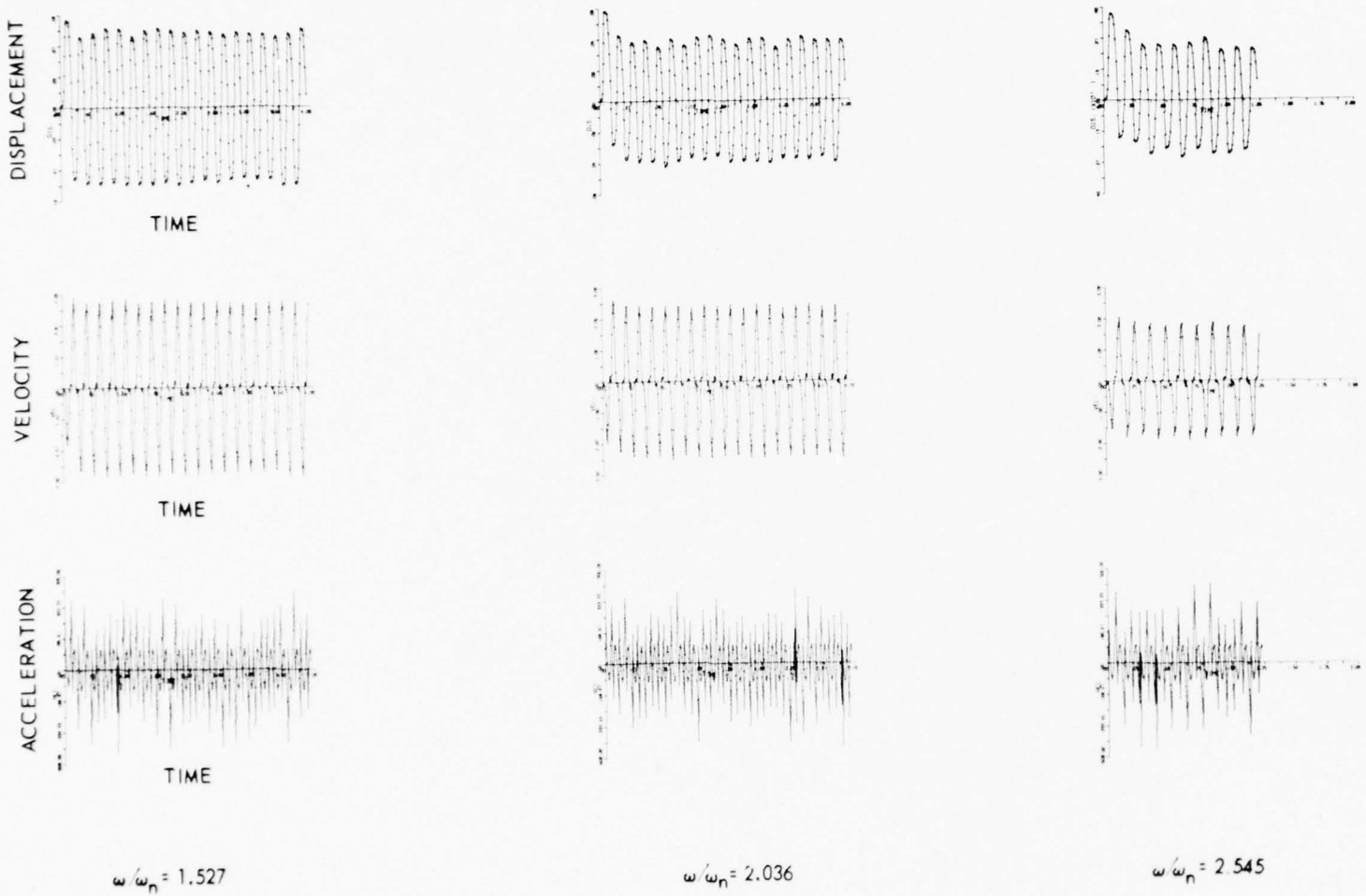

FIGURE 16
TIME-HISTORIES OF DISPLACEMENT, VELOCITY,
AND ACCELERATION FOR COULOMB DAMPING WITH $\beta_1/F = 0.77$,
$\omega/\omega_n = 1.527$, $\omega/\omega_n = 2.036$, AND $\omega/\omega_n = 2.545$

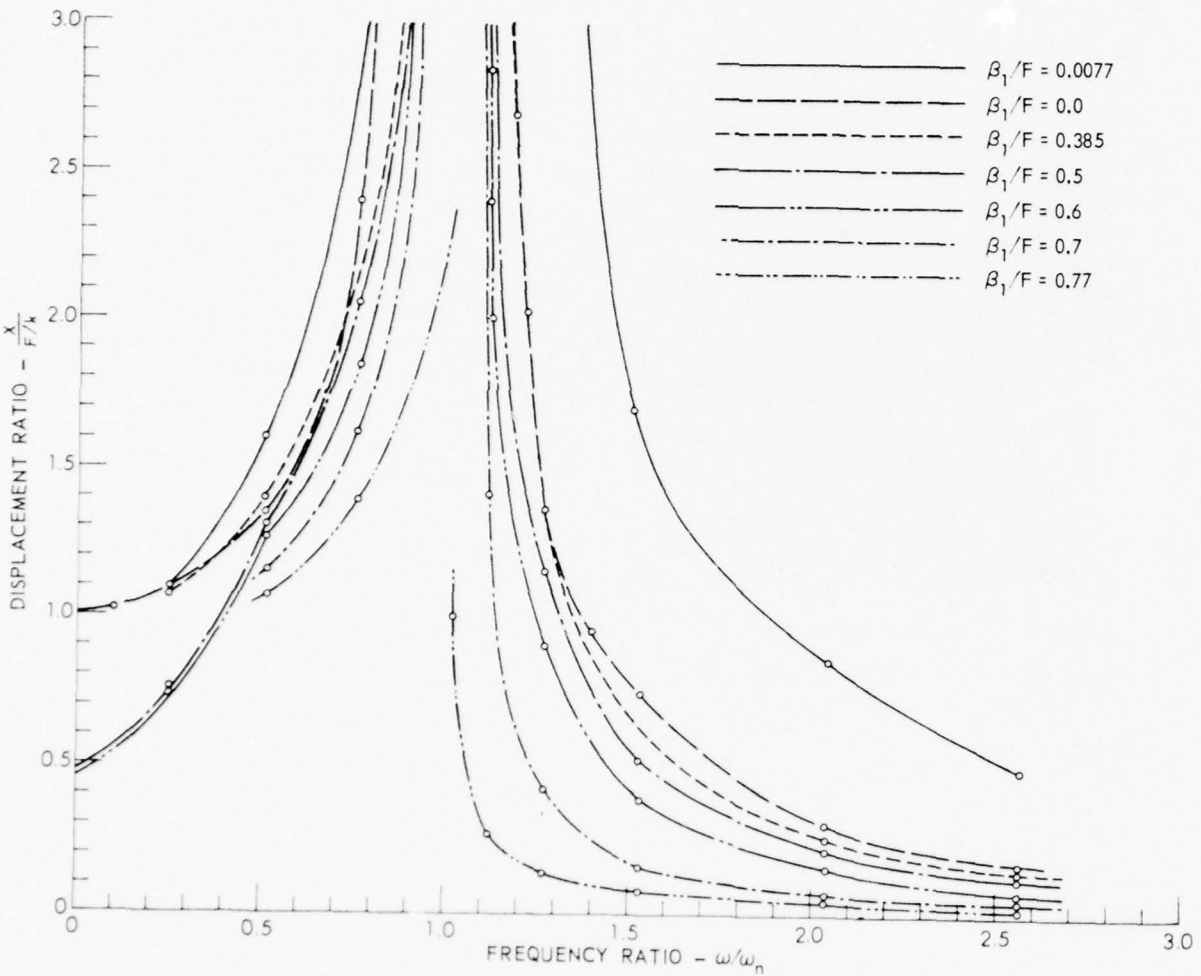

FIGURE 17
COULOMB DISPLACEMENT CURVES BY NUMERICAL PROCEDURE,
AS A FUNCTION OF DAMPING RATIOS

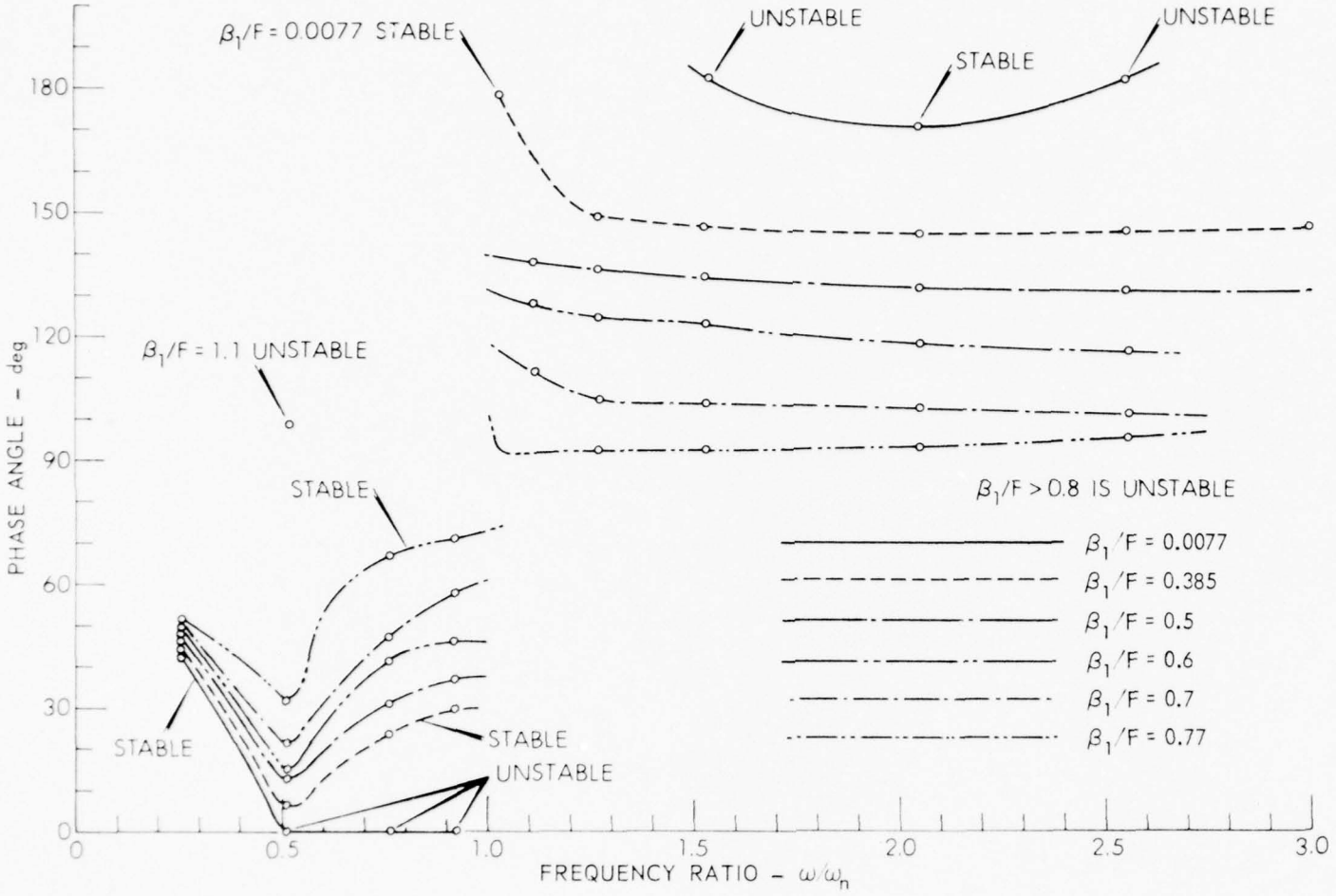

FIGURE 18
COULOMB PHASE ANGLE CURVES BY NUMERICAL PROCEDURE,
AS A FUNCTION OF DAMPING RATIOS

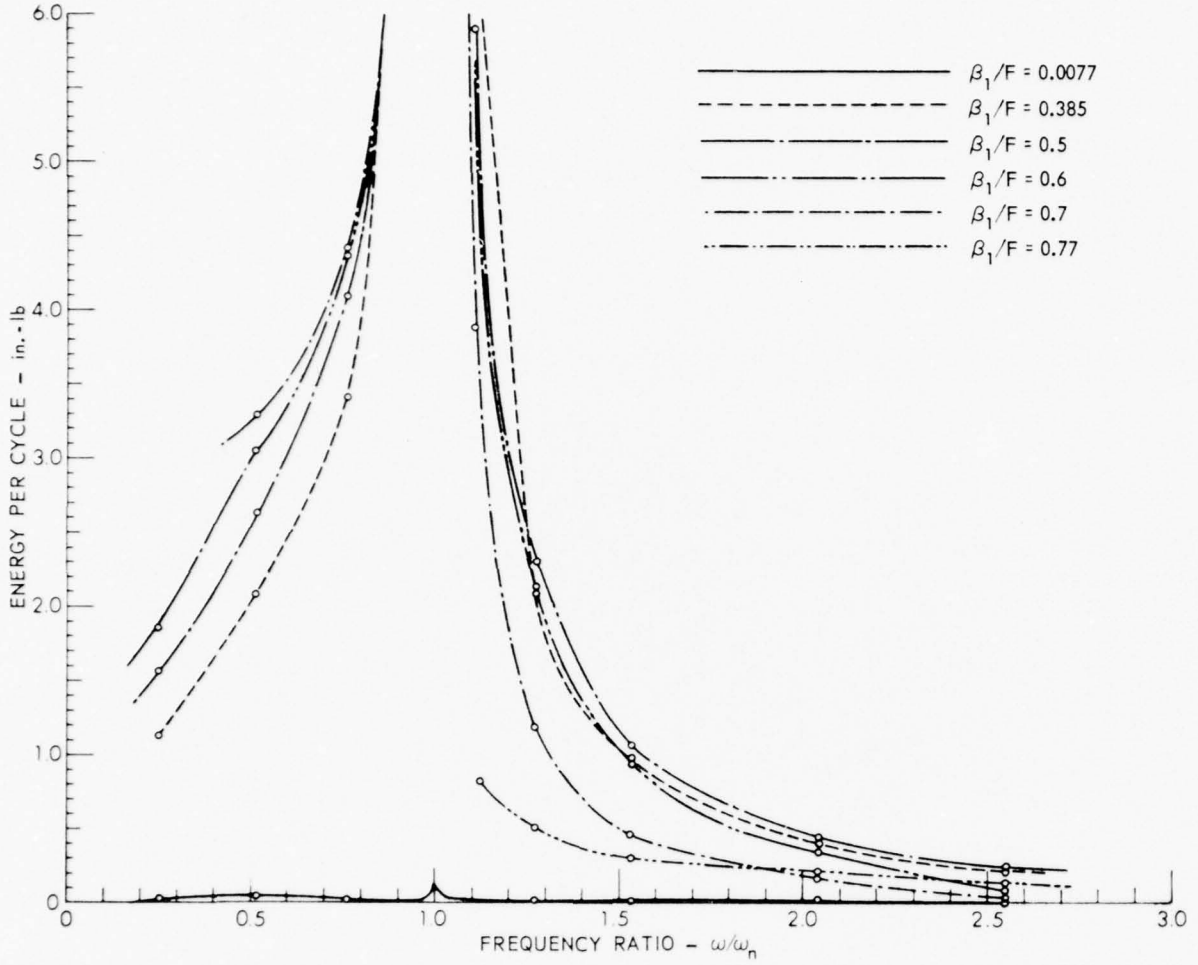

FIGURE 19
COULOMB ENERGY CURVES BY NUMERICAL PROCEDURE,
AS A FUNCTION OF DAMPING RATIOS

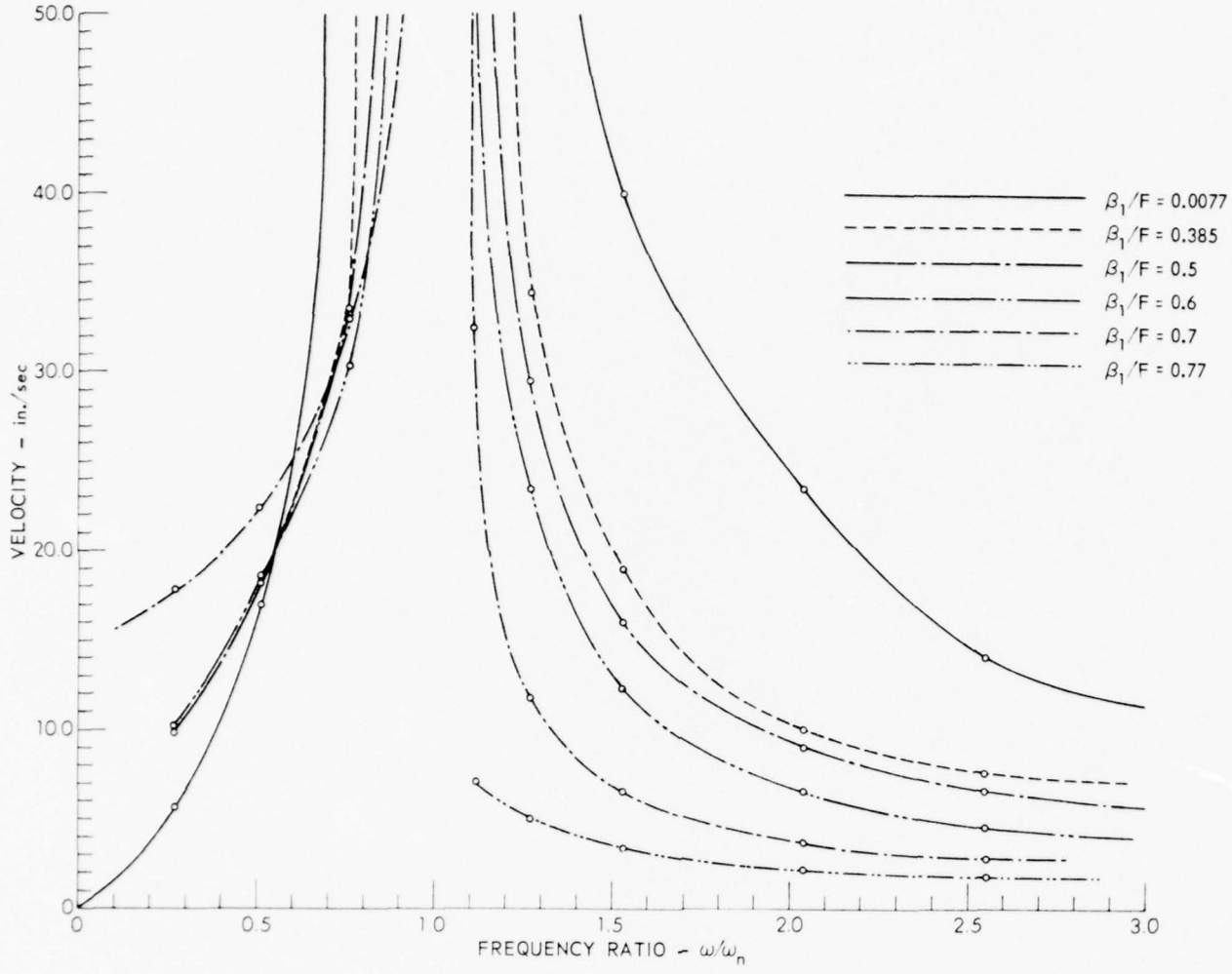

FIGURE 20
COULOMB VELOCITY CURVES BY NUMERICAL PROCEDURE,
AS A FUNCTION OF DAMPING RATIOS

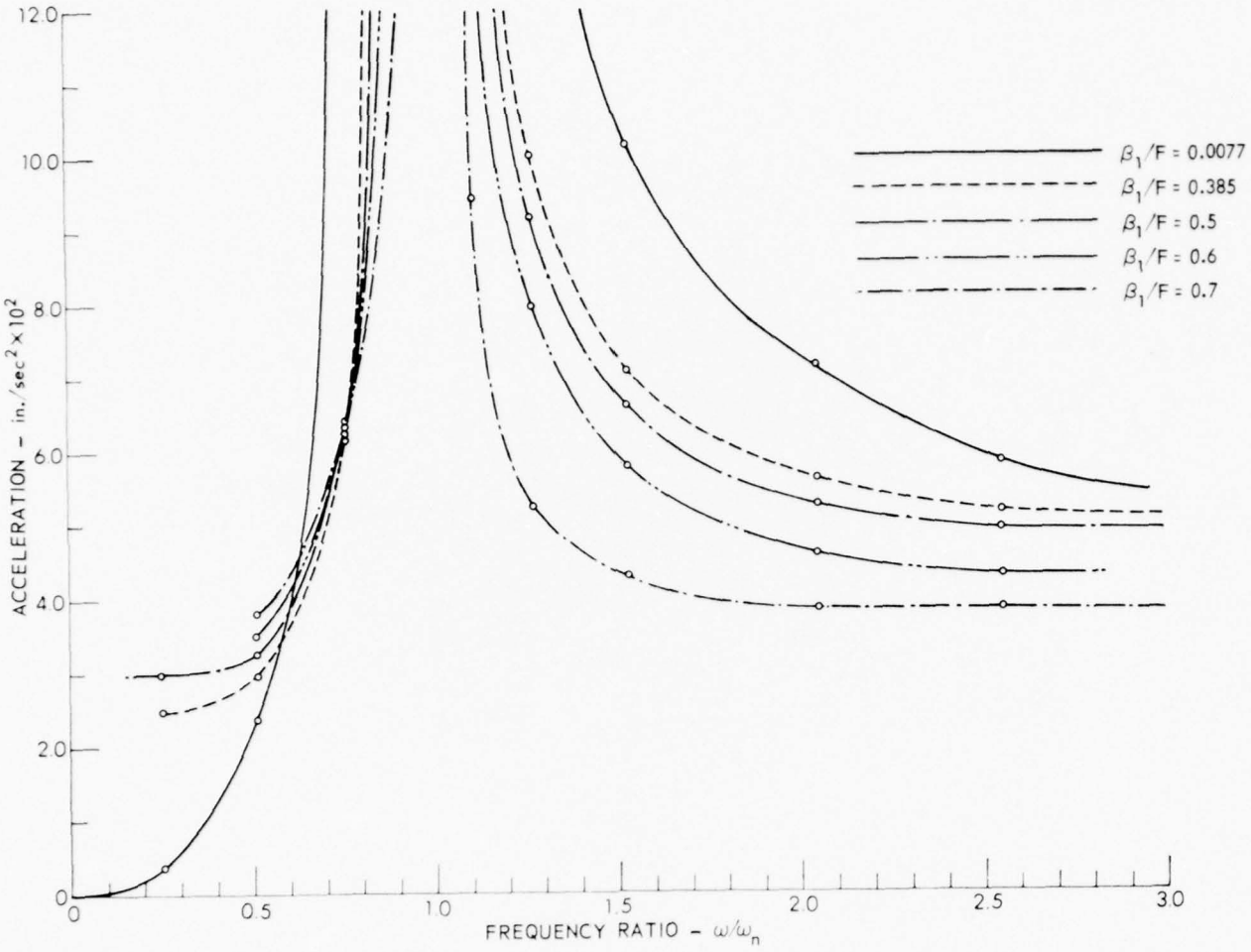

FIGURE 21
COULOMB ACCELERATION CURVES BY NUMERICAL PROCEDURE,
AS A FUNCTION OF DAMPING RATIOS

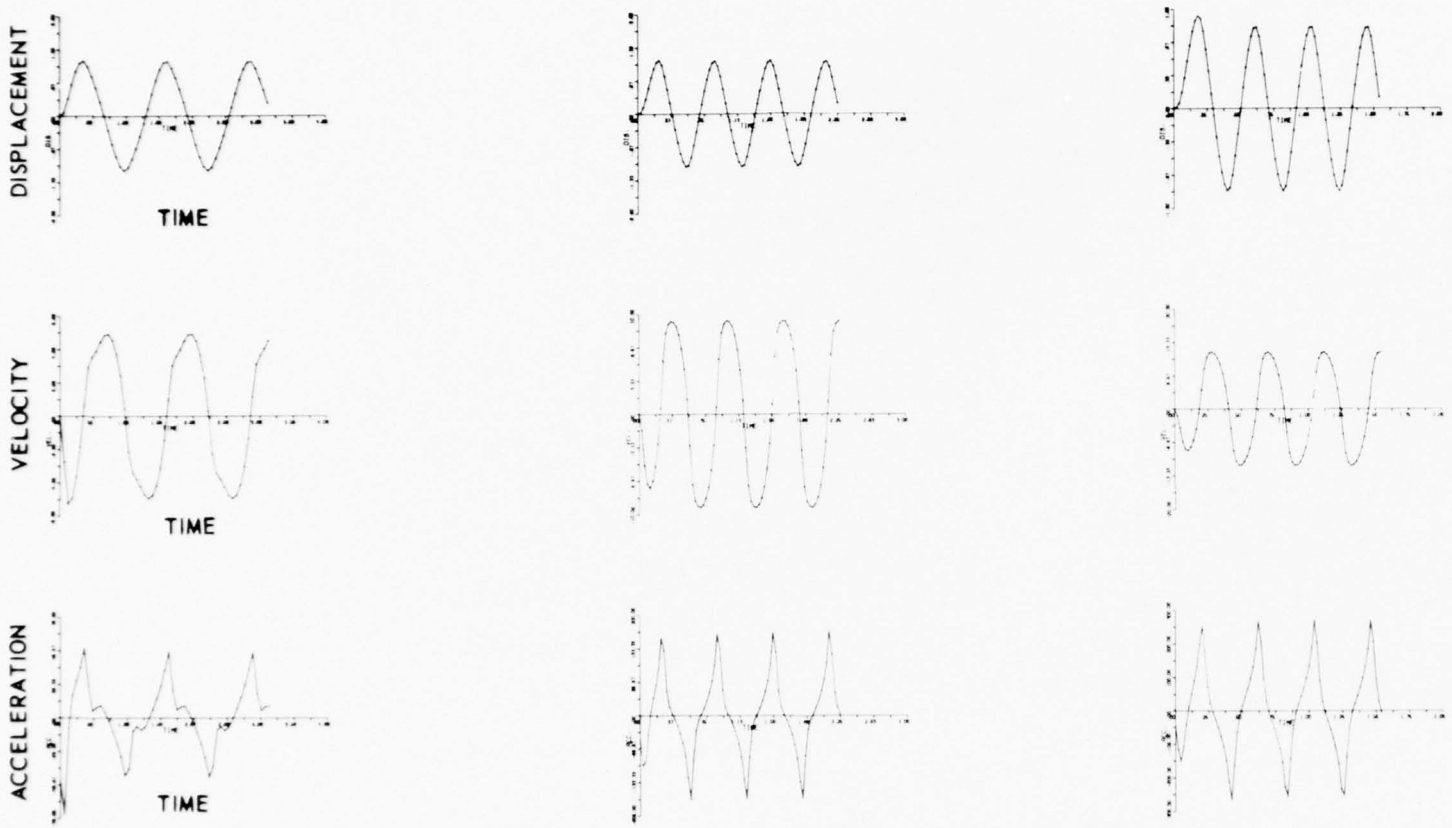

FIGURE 22
TIME-HISTORIES OF DISPLACEMENT, VELOCITY, AND ACCELERATION
FOR VELOCITY-SQUARED DAMPING WITH $\beta_3 F/Mk = 3.09$,
$\omega/\omega_n = 0.255$, $\omega/\omega_n = 0.509$. AND $\omega/\omega_n = 0.764$

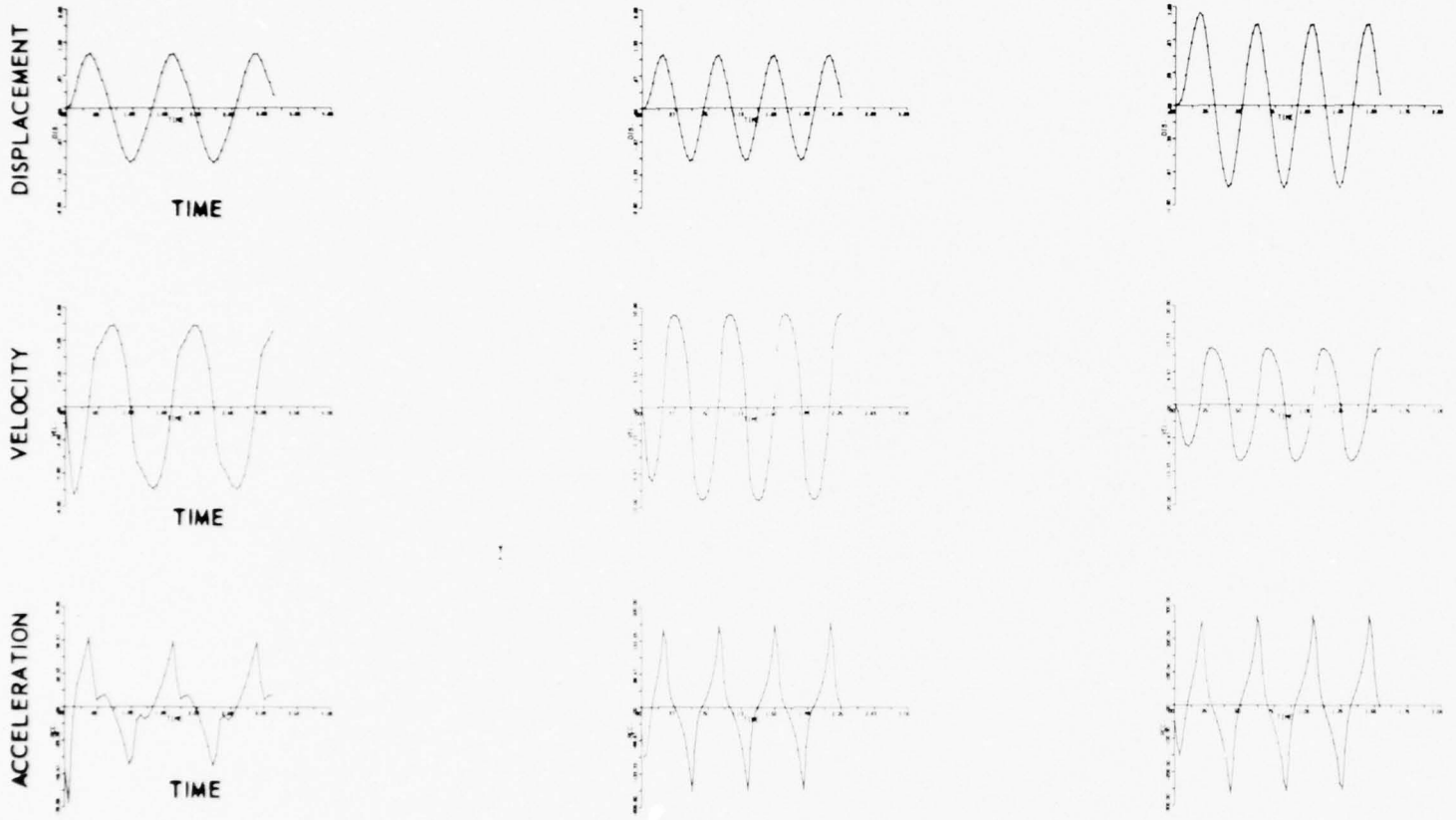

FIGURE 23
TIME-HISTORIES OF DISPLACEMENT, VELOCITY, AND ACCELERATION
FOR VELOCITY-SQUARED DAMPING WITH $\beta_3 F/Mk = 3.09$,
$\omega/\omega_n = 0.916$, $\omega/\omega_n = 1.018$, AND $\omega/\omega_n = 1.120$

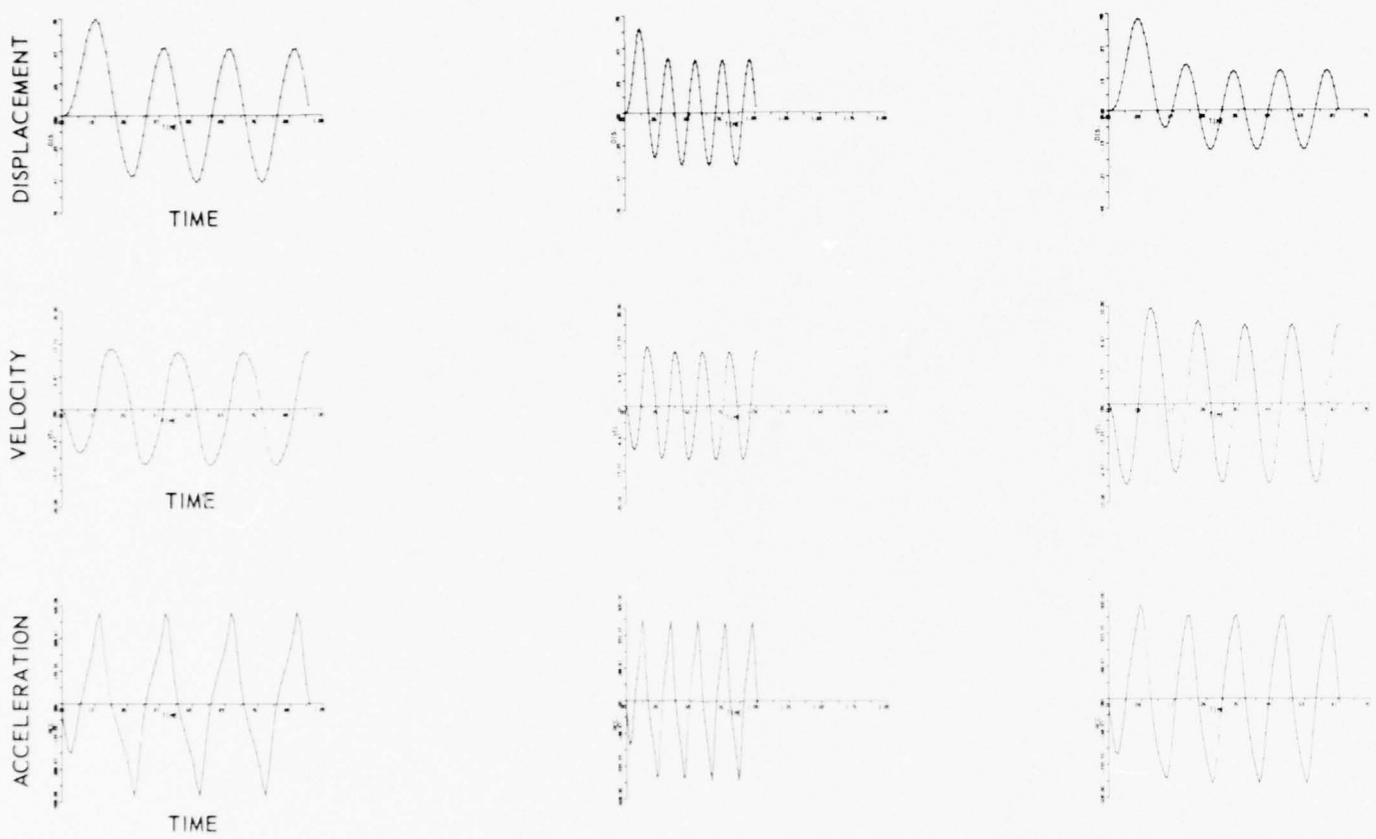

FIGURE 24
TIME-HISTORIES OF DISPLACEMENT, VELOCITY, AND ACCELERATION
FOR VELOCITY-SQUARED DAMPING WITH $\beta_3 F/Mk = 3.09$,
$\omega/\omega_n = 1.272$, $\omega/\omega_n = 1.527$, AND $\omega/\omega_n = 2.545$

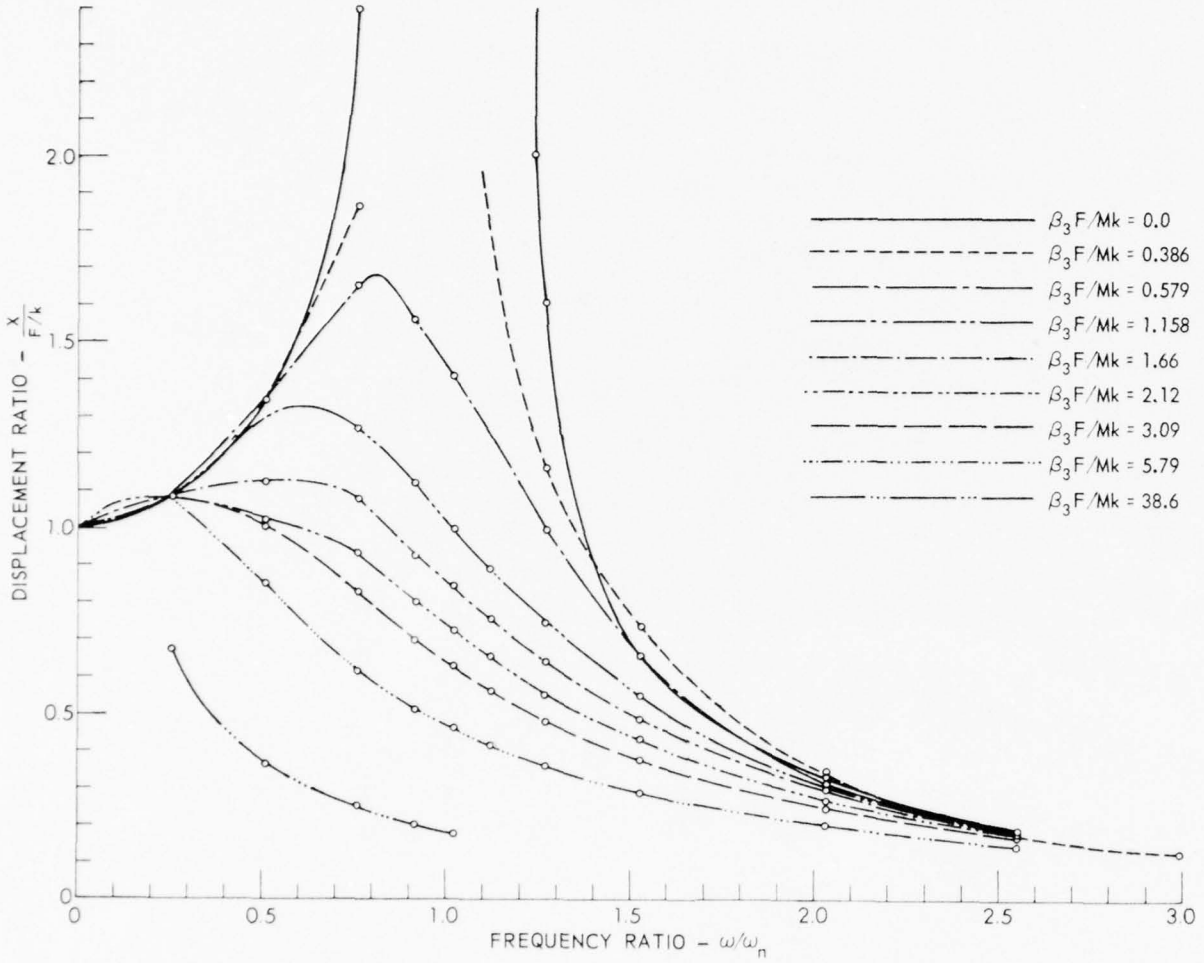

FIGURE 25
VELOCITY-SQUARED DISPLACEMENT CURVES BY NUMERICAL PROCEDURE,
AS A FUNCTION OF DAMPING RATIOS

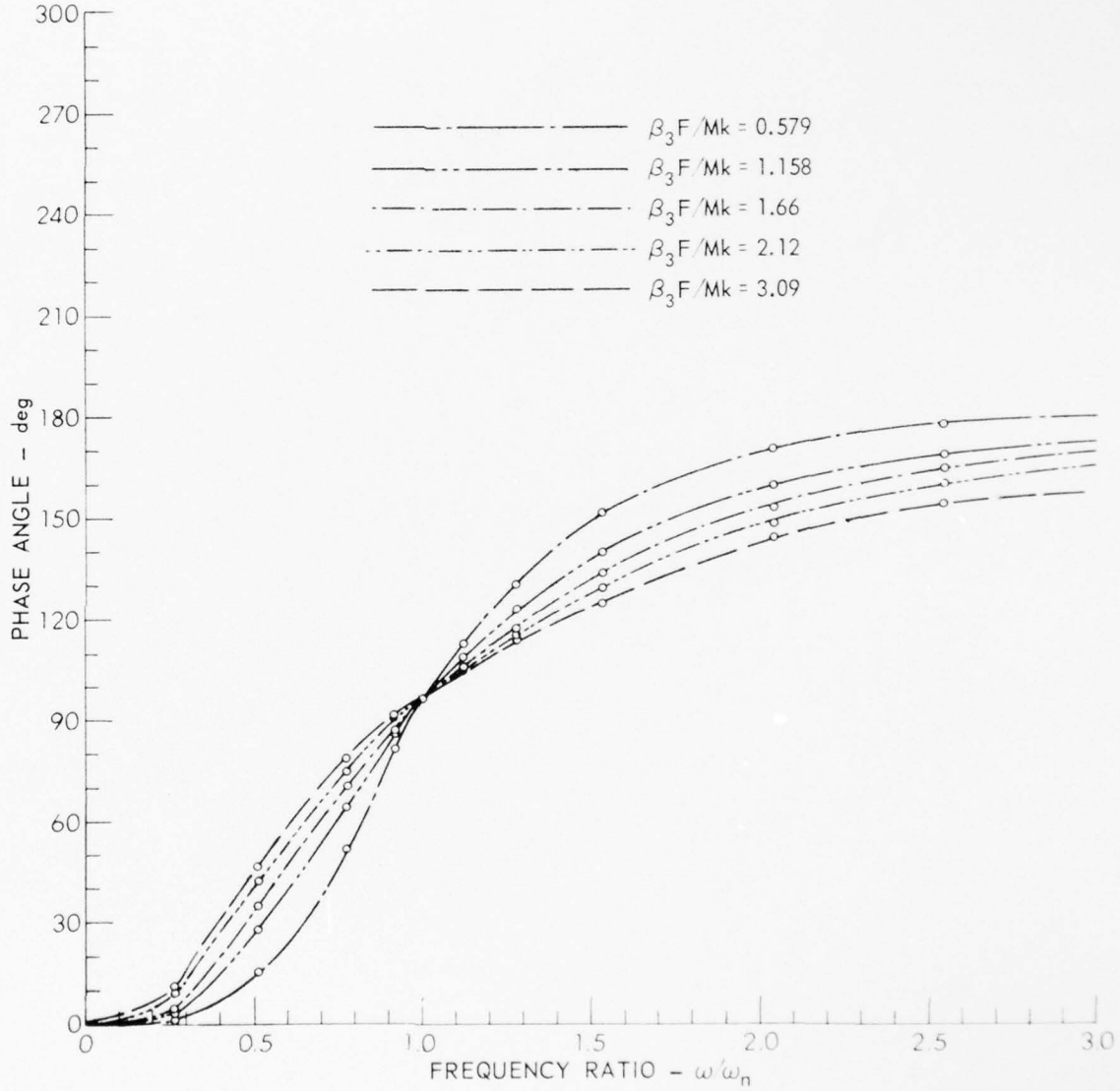

FIGURE 26
VELOCITY-SQUARED PHASE ANGLE CURVES BY NUMERICAL PROCEDURE,
AS A FUNCTION OF DAMPING RATIOS

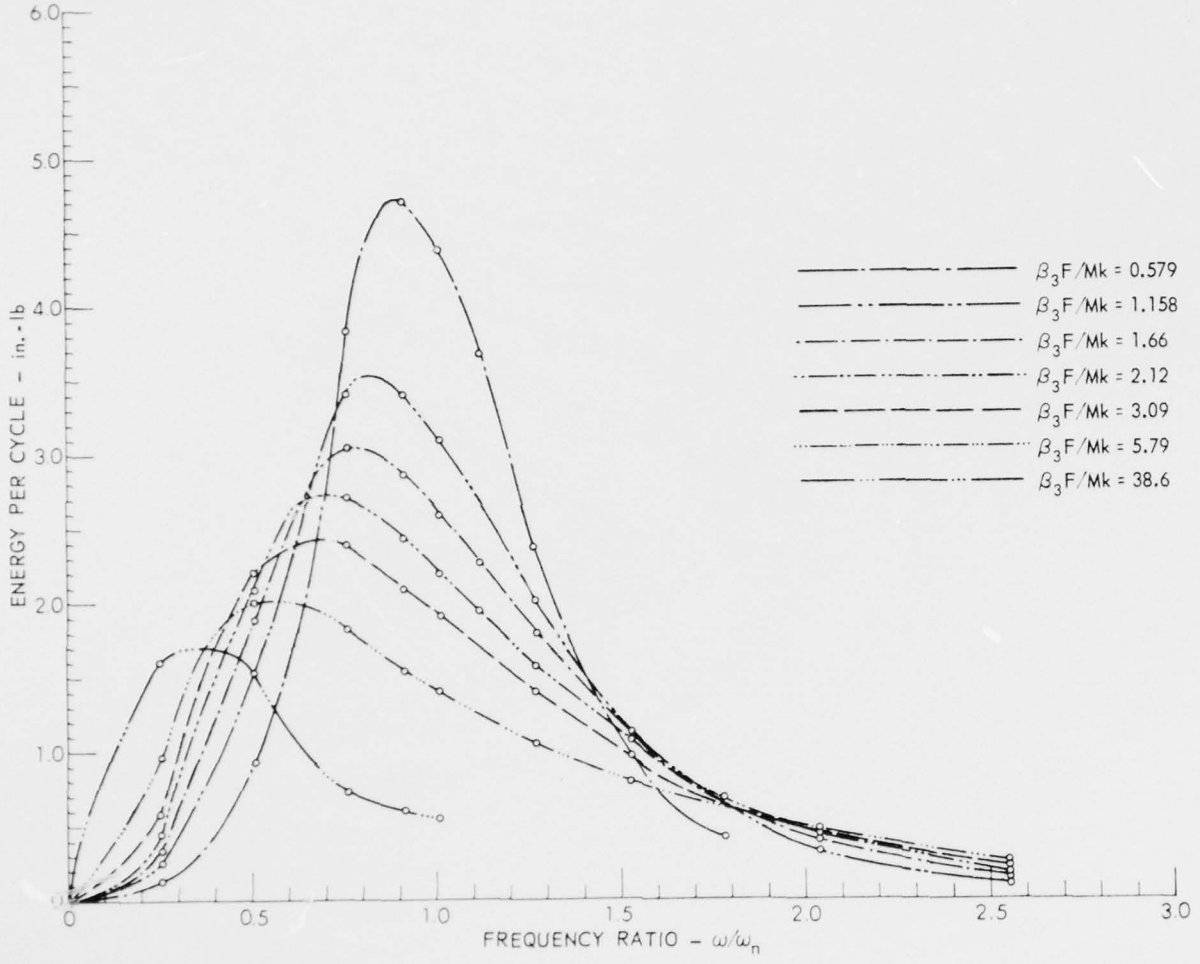

FIGURE 27
VELOCITY-SQUARED ENERGY CURVES BY NUMERICAL PROCEDURE,
AS A FUNCTION OF DAMPING RATIOS

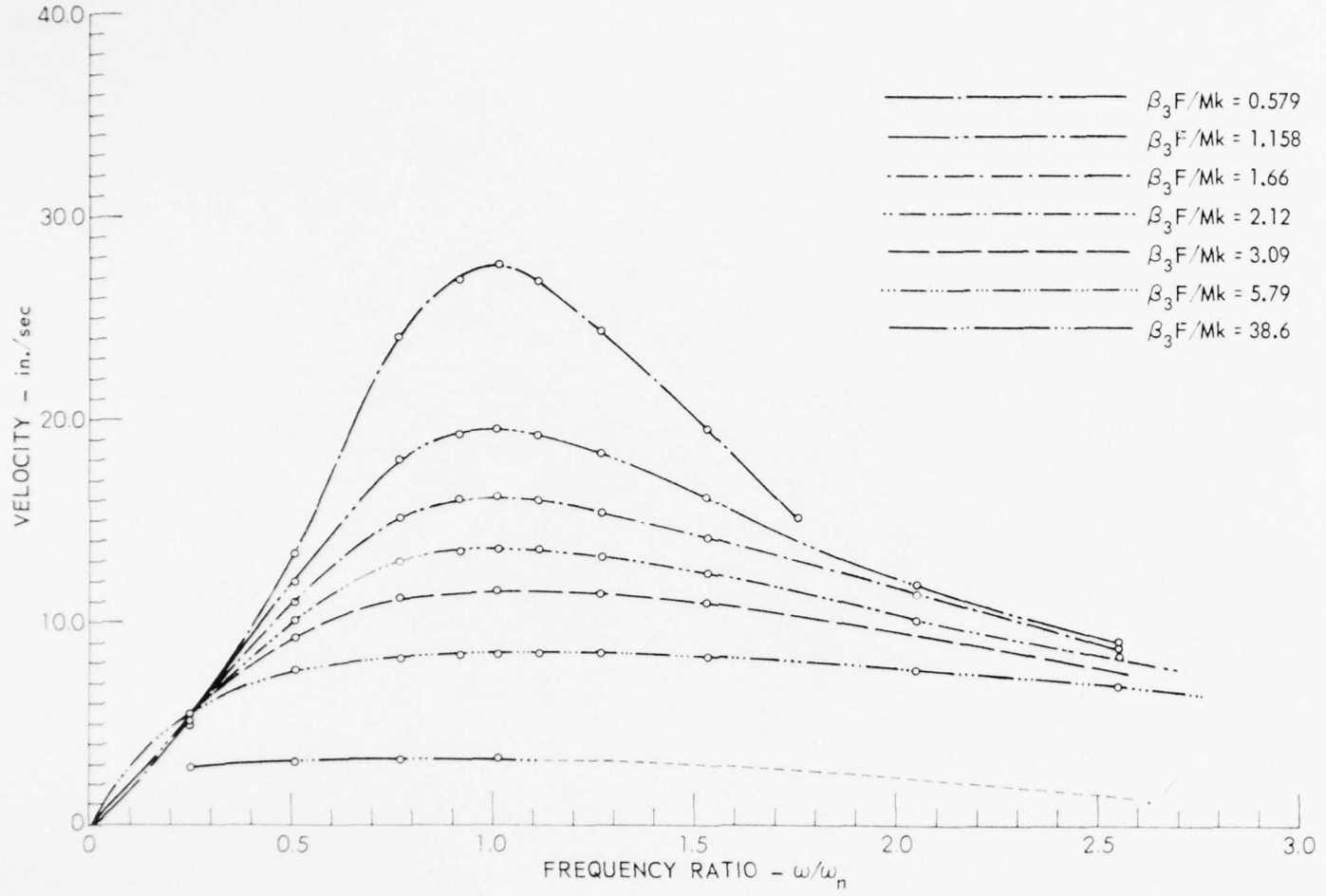

FIGURE 28
VELOCITY-SQUARED VELOCITY CURVES BY NUMERICAL PROCEDURE,
AS A FUNCTION OF DAMPING RATIOS

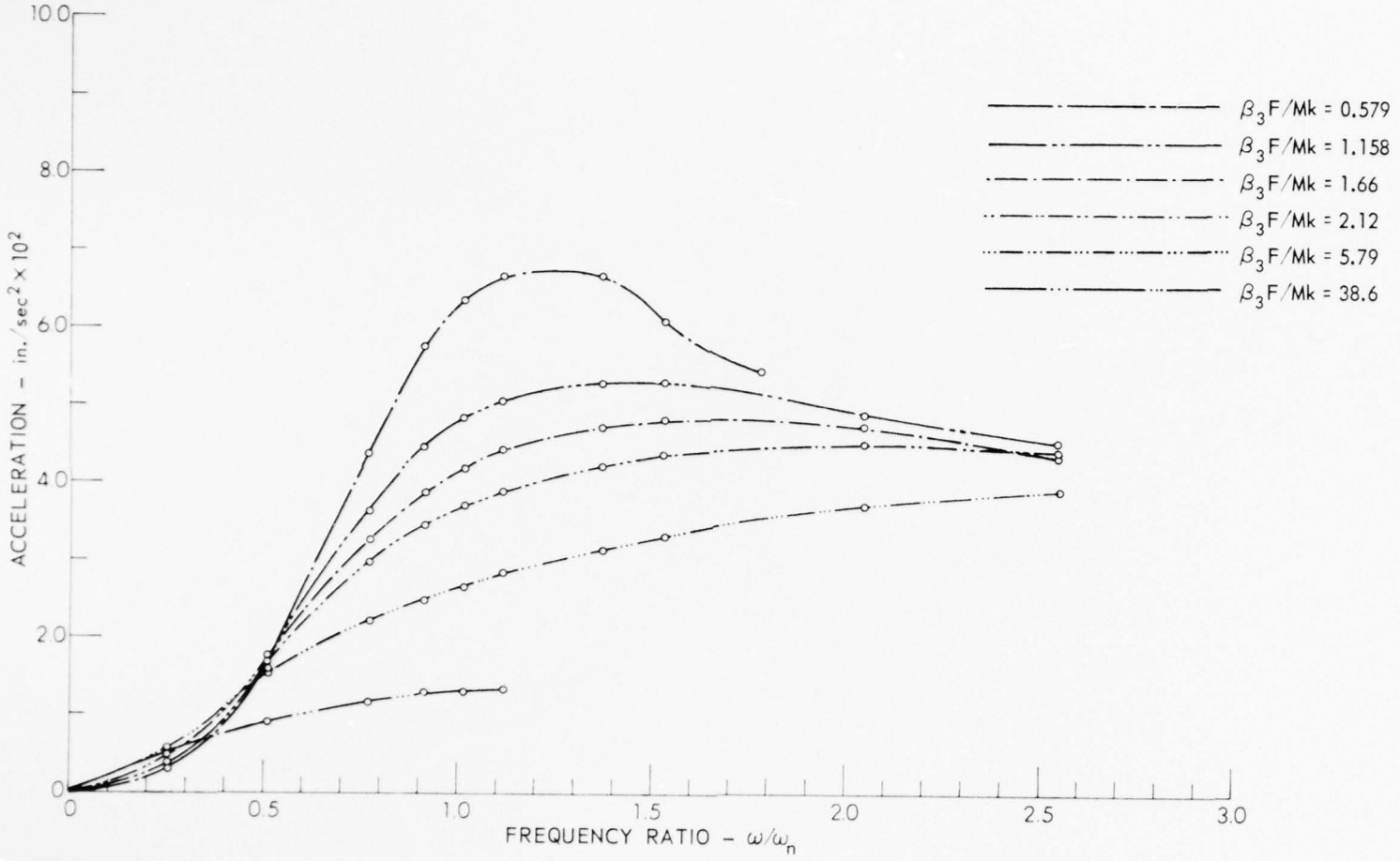

FIGURE 29
VELOCITY-SQUARED ACCELERATION CURVES BY NUMERICAL PROCEDURE,
AS A FUNCTION OF DAMPING RATIOS

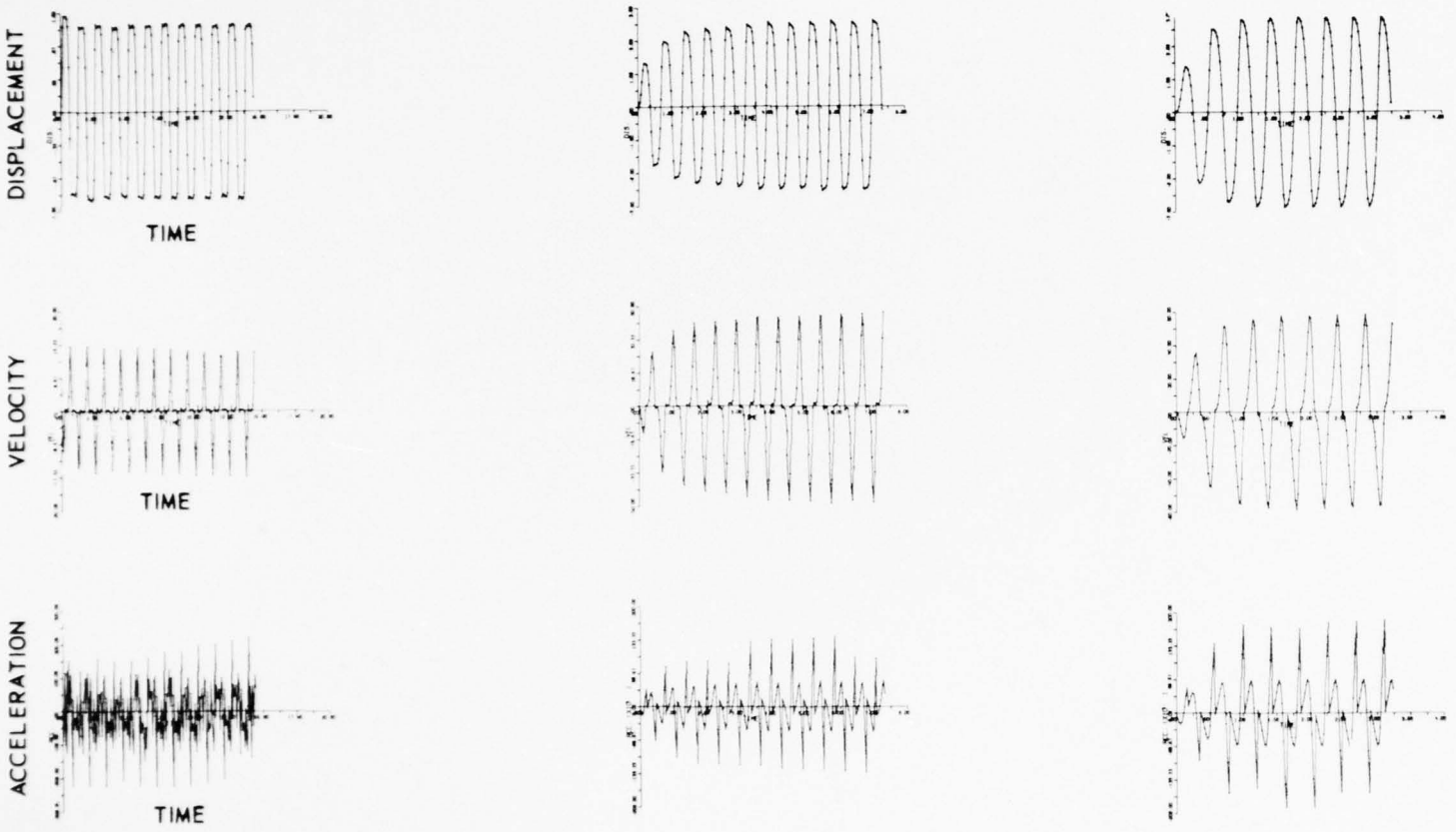

FIGURE 30
TIME-HISTORIES OF DISPLACEMENT, VELOCITY, AND ACCELERATION
FOR DISPLACEMENT-SQUARED DAMPING WITH $\beta_4 F/k^2 = 0.308$,
$\omega/\omega_n = 0.255$, $\omega/\omega_n = 0.509$, AND $\omega/\omega_n = 0.764$

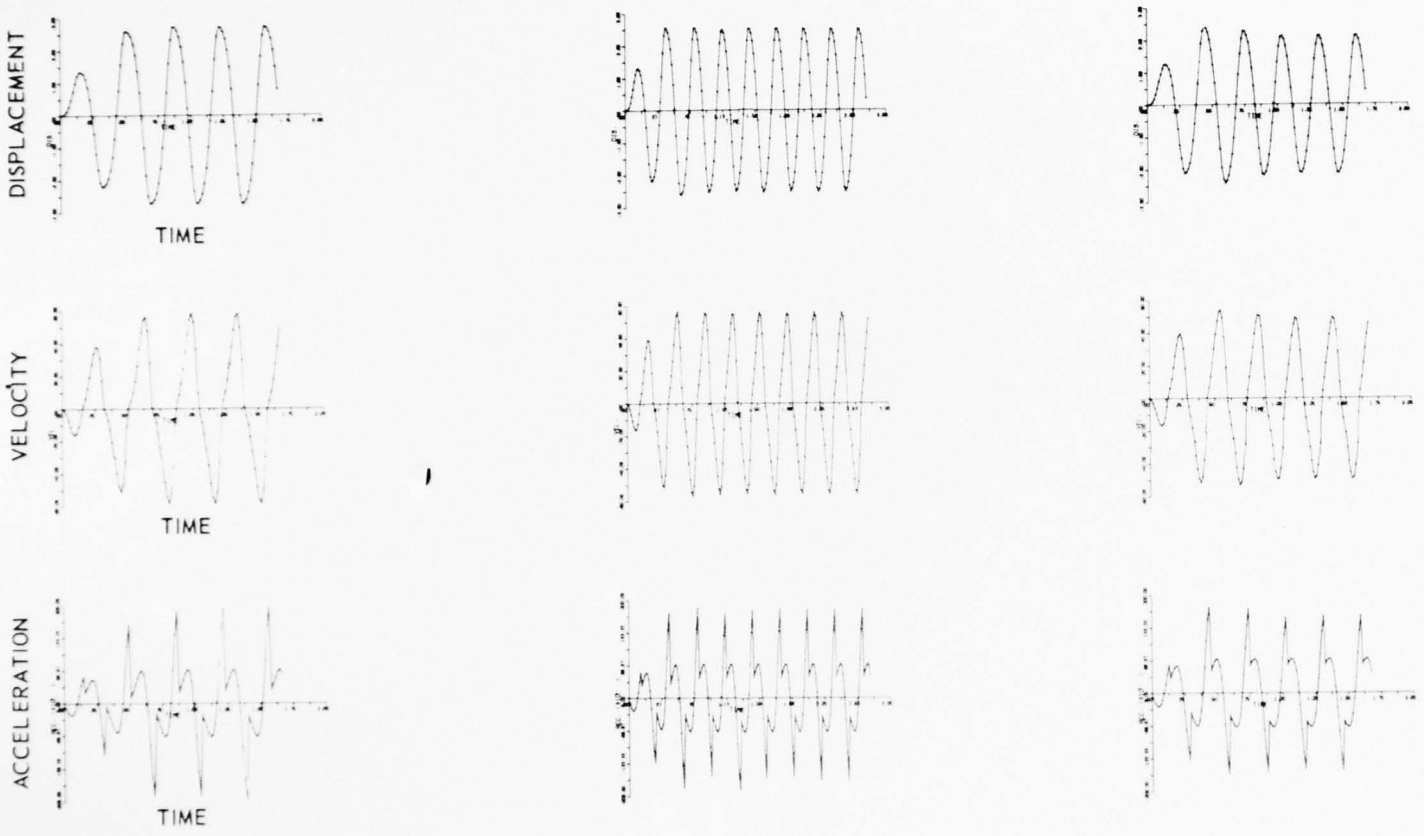

FIGURE 31
TIME-HISTORIES OF DISPLACEMENT, VELOCITY, AND ACCELERATION
FOR DISPLACEMENT-SQUARED DAMPING WITH $\beta_4 F/k^2 = 0.308$,
$\omega/\omega_n = 0.916$, $\omega/\omega_n = 1.018$, AND $\omega/\omega_n = 1.120$

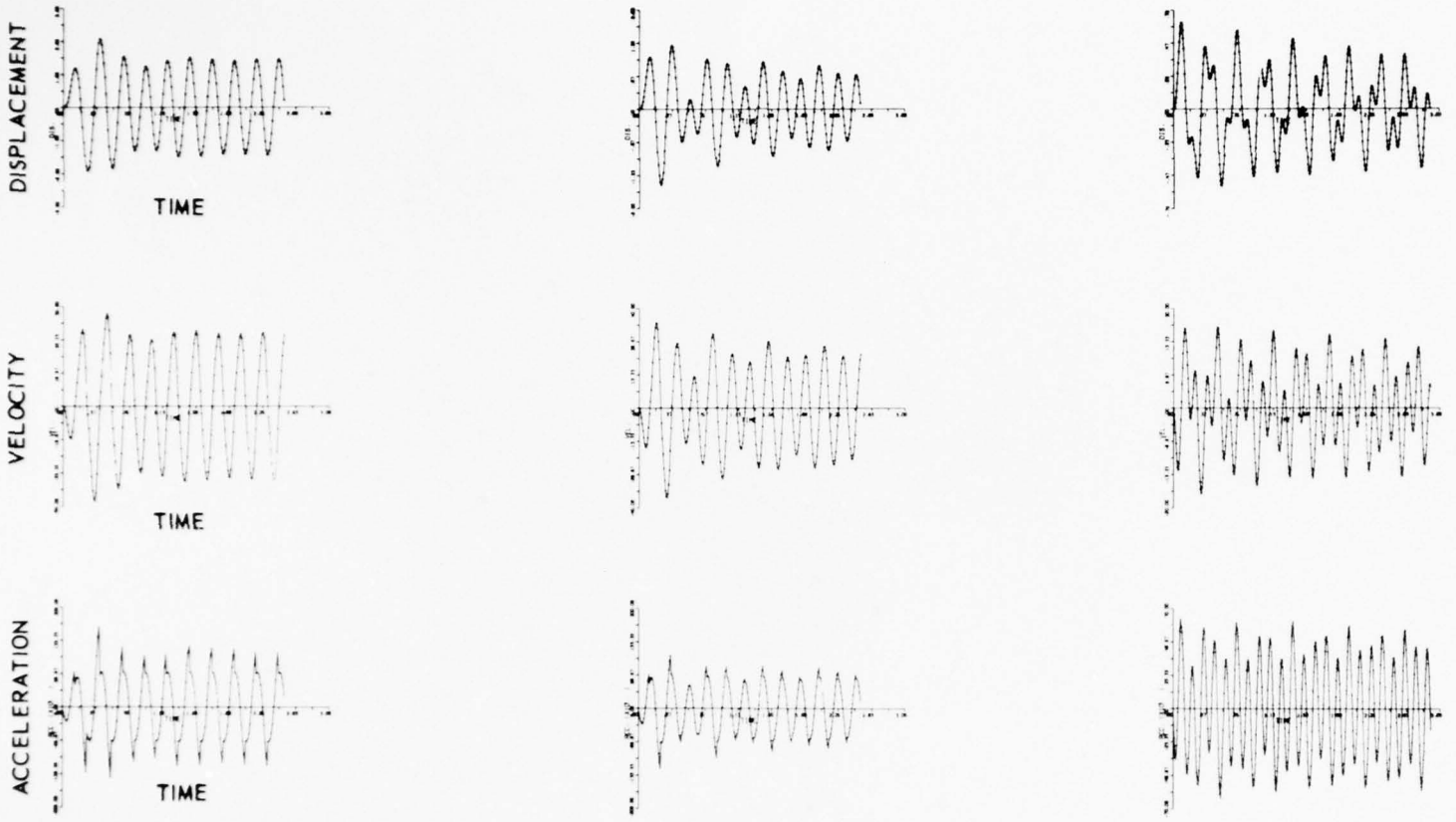

FIGURE 32
TIME-HISTORIES OF DISPLACEMENT, VELOCITY, AND ACCELERATION
FOR DISPLACEMENT-SQUARED DAMPING WITH $\beta_4 F/k^2 = 0.308$,
$\omega/\omega_n = 1.527$, $\omega/\omega_n = 2.036$, AND $\omega/\omega_n = 2.345$

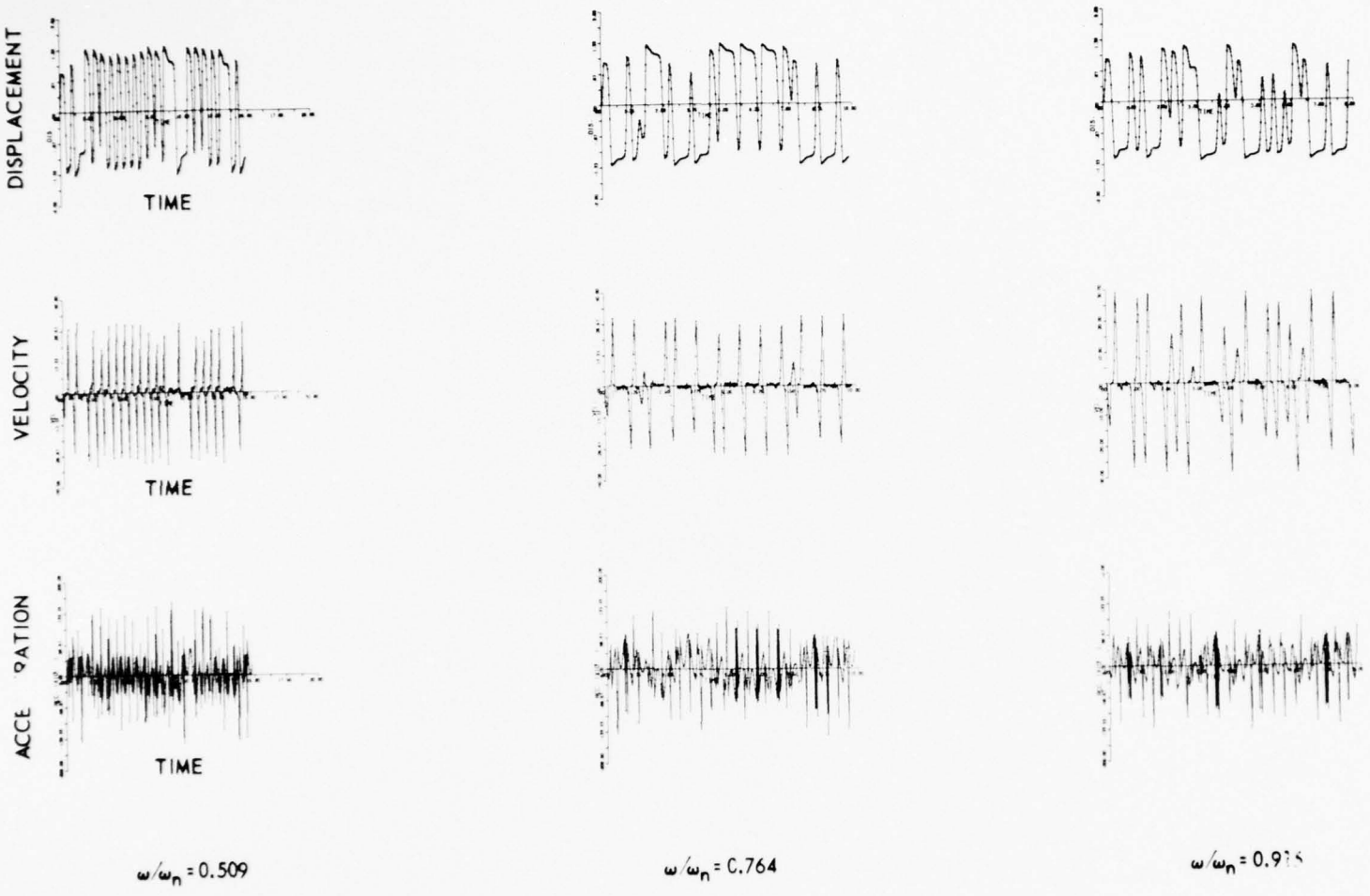

FIGURE 33
TIME-HISTORIES OF DISPLACEMENT, VELOCITY, AND ACCELERATION
FOR DISPLACEMENT-SQUARED DAMPING WITH $\beta_4 F/k^2 = 1.5$,
$\omega/\omega_n = 0.509$, $\omega/\omega_n = 0.764$, AND $\omega/\omega_n = 0.916$

FIGURE 34
TIME-HISTORIES OF DISPLACEMENT, VELOCITY, AND ACCELERATION
FOR DISPLACEMENT-SQUARED DAMPING WITH $\beta_4 F/k^2 = 1.5$,
$\omega/\omega_n = 1.018$, $\omega/\omega_n = 1.120$, AND $\omega/\omega_n = 1.272$

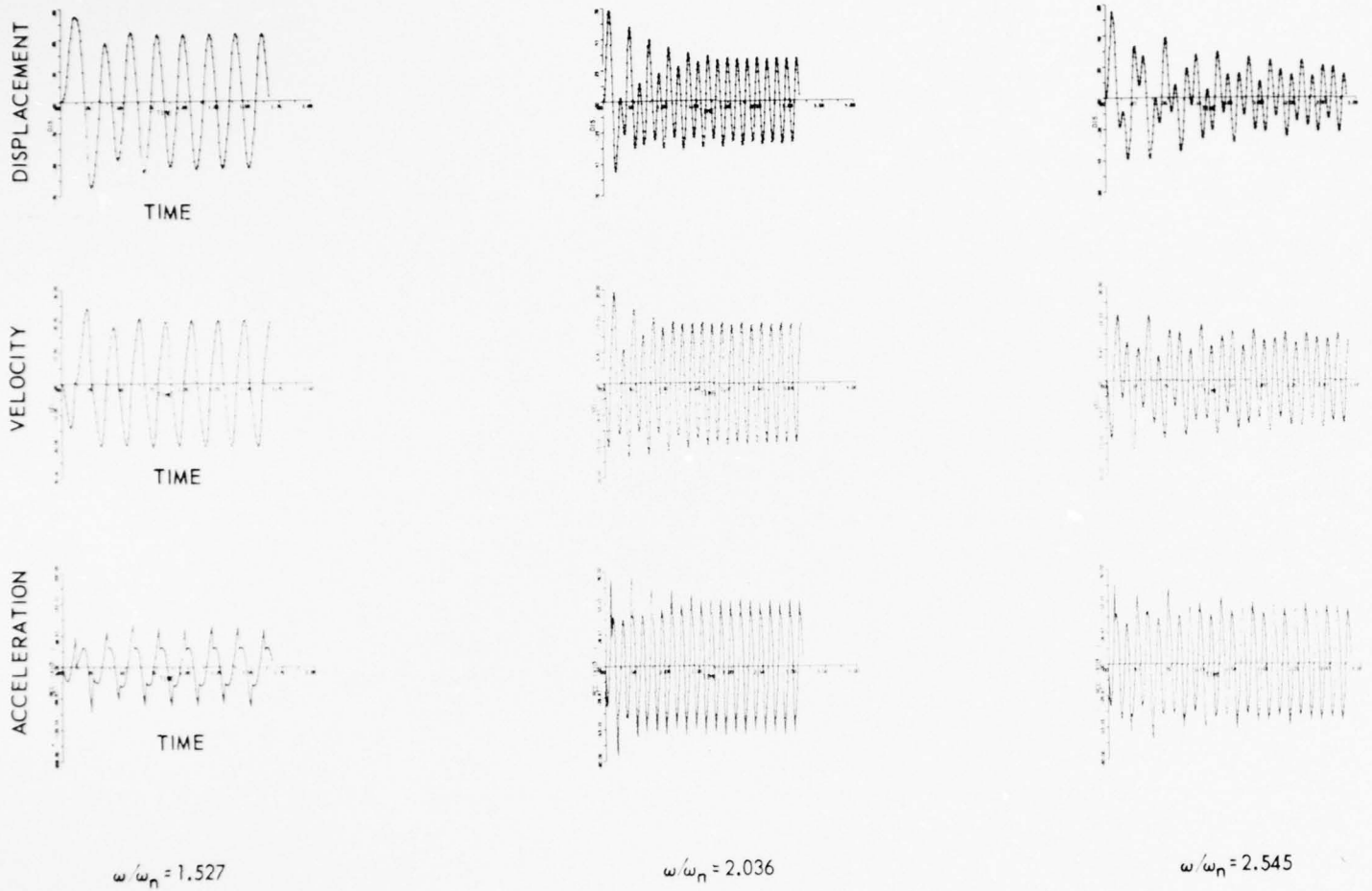

FIGURE 35
TIME-HISTORIES OF DISPLACEMENT, VELOCITY, AND ACCELERATION
FOR DISPLACEMENT-SQUARED DAMPING WITH $\beta_4 F/k^2 = 1.5$,
$\omega/\omega_n = 1.527$, $\omega/\omega_n = 2.036$, AND $\omega/\omega_n = 2.545$

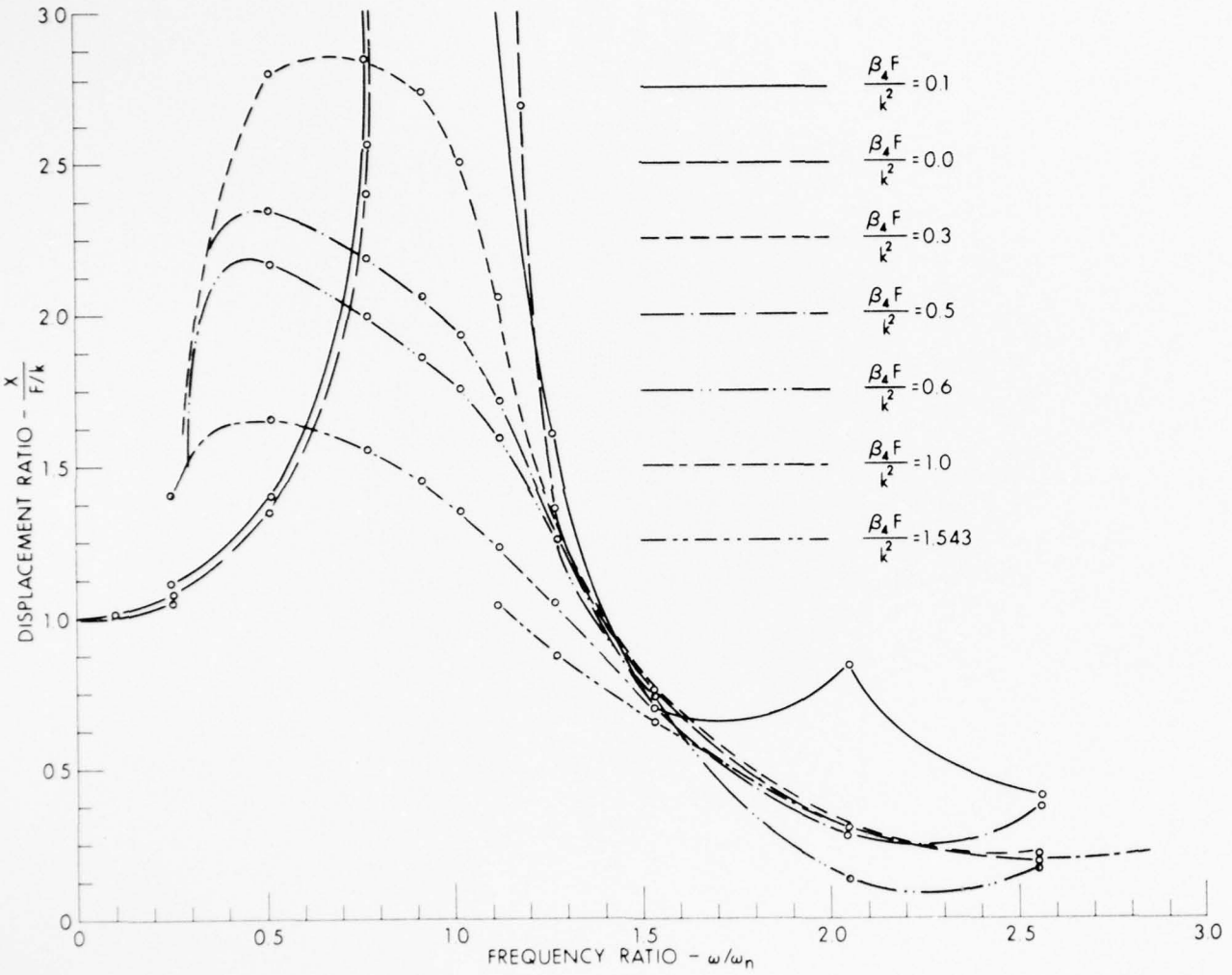

FIGURE 36
DISPLACEMENT-SQUARED DISPLACEMENT CURVES
BY NUMERICAL PROCEDURE, AS A FUNCTION OF DAMPING RATIOS

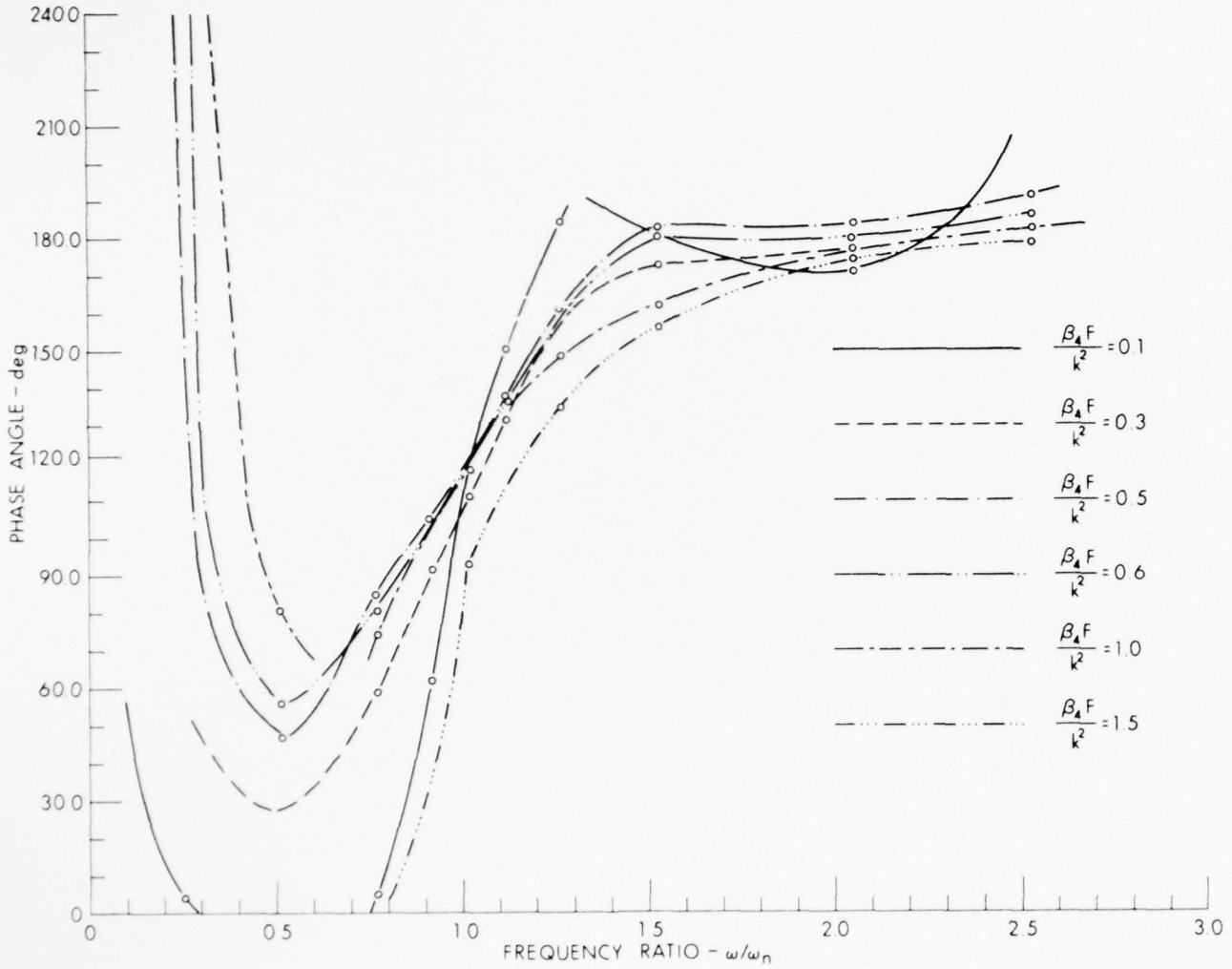

FIGURE 37
DISPLACEMENT-SQUARED PHASE ANGLE CURVES
BY NUMERICAL PROCEDURE, AS A FUNCTION OF DAMPING RATIOS

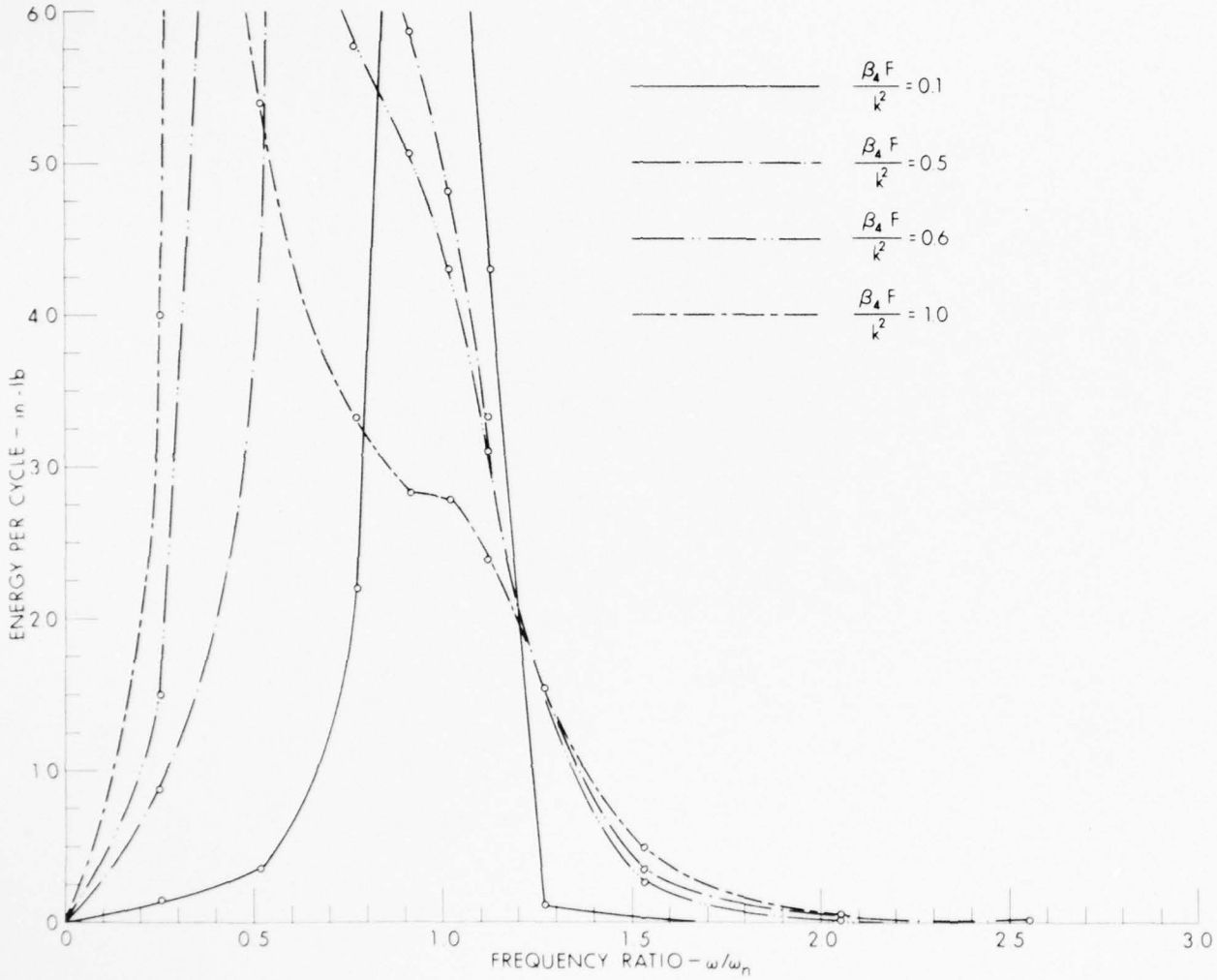

FIGURE 38
DISPLACEMENT-SQUARED ENERGY CURVES
BY NUMERICAL PROCEDURE, AS A FUNCTION OF DAMPING RATIOS

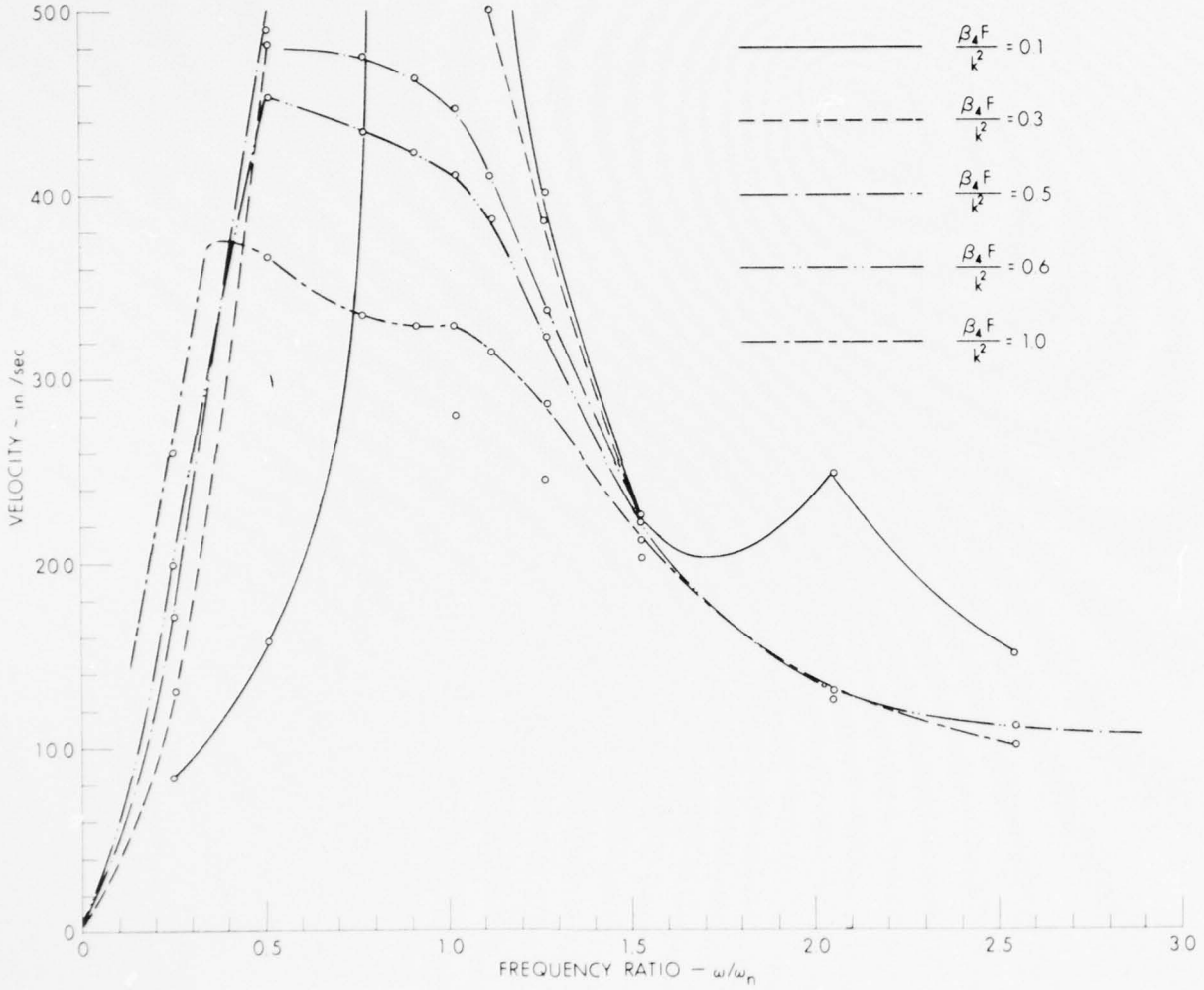

FIGURE 39
DISPLACEMENT-SQUARED VELOCITY CURVES
BY NUMERICAL PROCEDURE, AS A FUNCTION OF DAMPING RATIOS

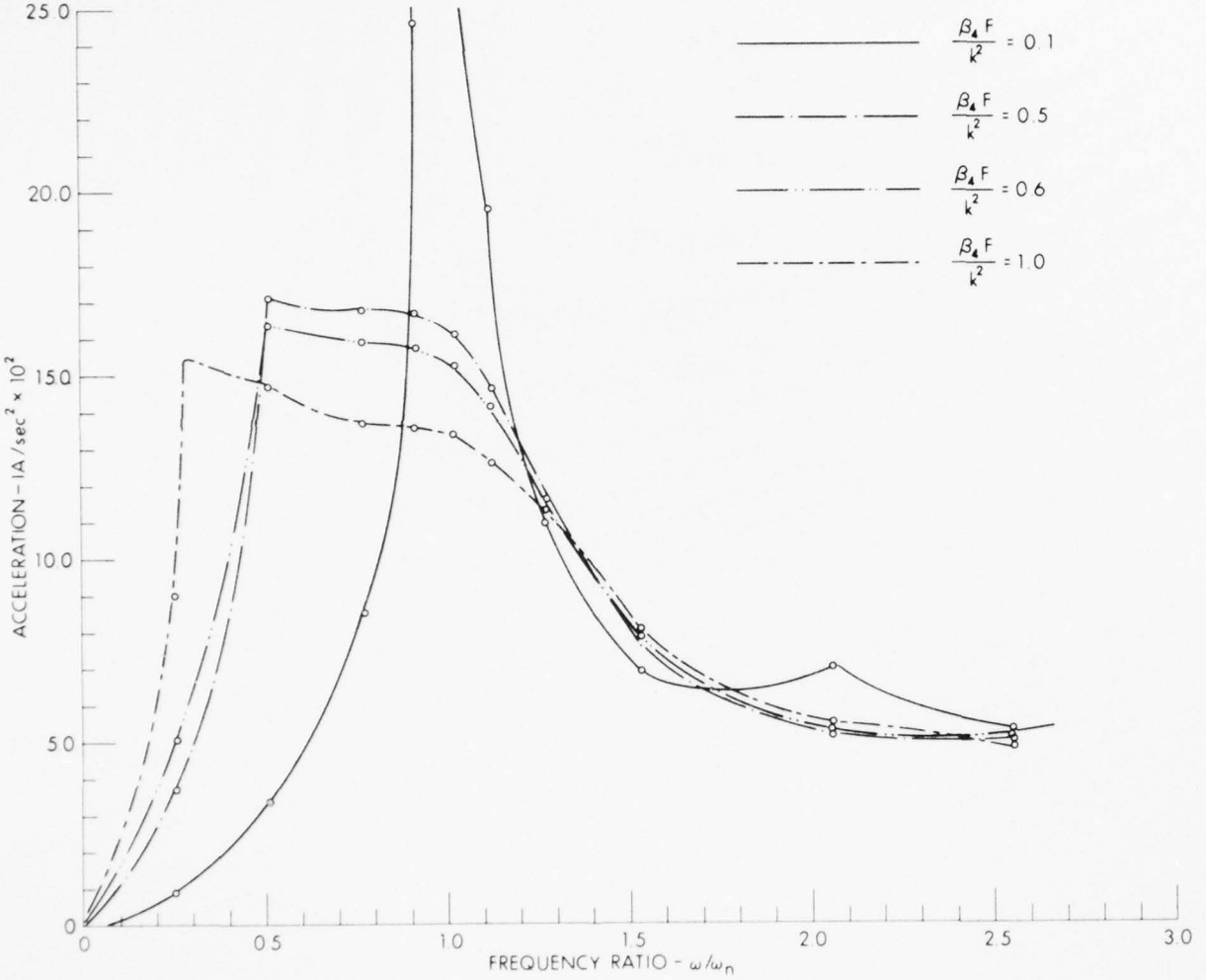

FIGURE 40
DISPLACEMENT-SQUARED ACCELERATION CURVES
BY NUMERICAL PROCEDURE, AS A FUNCTION OF DAMPING RATIOS

AD-A036 695 TEXAS UNIV AT AUSTIN DEFENSE RESEARCH LAB F/G 12/1
EFFECTS OF SEVERAL TYPES OF DAMPING ON THE DYNAMICAL BEHAVIOR O--ETC(U)
JAN 67 J F BYERS NOBSR-93125
UNCLASSIFIED DRL-A-272 NL

2 OF 2
ADA036695

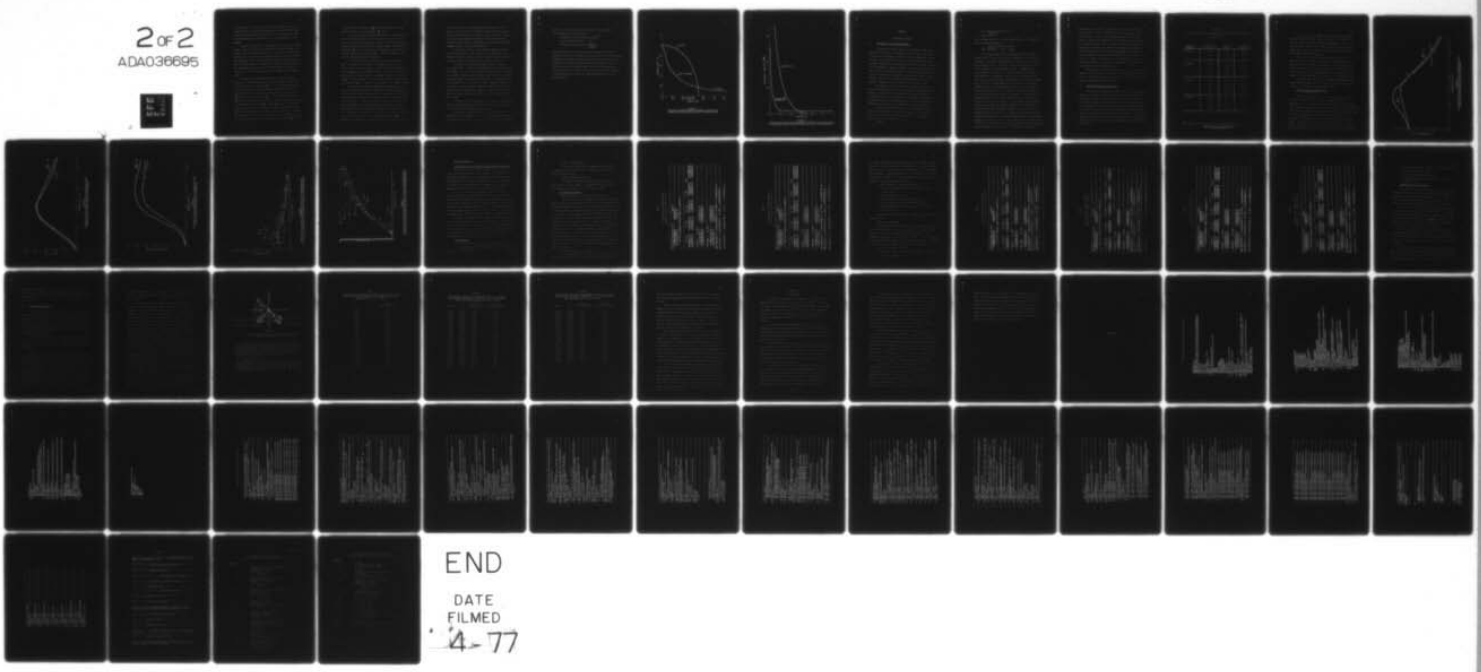

END

DATE FILMED
4-77

2 OF 2

ADA036695

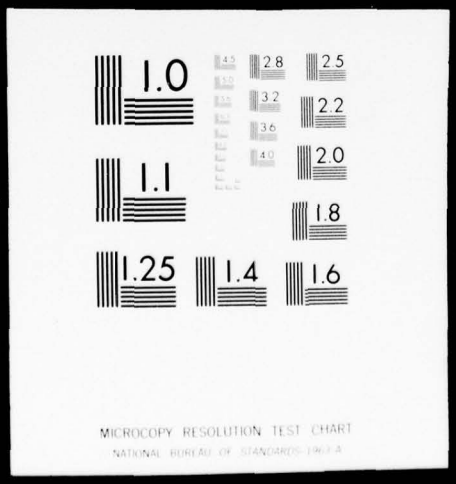

the Introduction. The curves are extended by interpreting the time-histories where the steady-state conditions are not well defined. Where insufficient repeatability of the motion exists, no points are plotted. The curve extensions are intended to aid in the interpretation of the response.

Typical time-histories for each damping case precedes the response curves. These curves show the steady-state and transient response for average values of the damping coefficients. In general, the displacement, velocity, and acceleration curves differ significantly for each case and each frequency. In all cases the higher derivatives cannot be related with the simple algebraic or trigonometric equations indicated by Eq. (2). The corresponding time-histories for no damping are given in Figs. 11 through 13. These curves are presented for comparison with the damped cases.

Typical Coulomb damped time-histories are given in Figs. 14 through 16. The displacement wave forms seem to vary as expected with the stick-slip motion occurring at $\frac{\omega}{\omega_n} = 0.5$ and smooth uniform motion at the higher frequencies. The velocity and acceleration curves are not uniform. The effect of the discontinuities may occur in the velocity ($\frac{\omega}{\omega_n} = 0.255$) or the acceleration ($\frac{\omega}{\omega_n} = 1.272$ and higher ratios). The presence of low frequencies in the output is most evident in the acceleration for frequency ratios from $\frac{\omega}{\omega_n} = 0.764$ to $\frac{\omega}{\omega_n} = 1.018$. The envelope appears to be described by a straight line with sharp discontinuities. This is not the case for viscous damping where the envelope is sinusoidal. The wave shape of the third derivative could be estimated from the curves of velocity and acceleration. For example, the velocity for $\frac{\omega}{\omega_n} = 0.509$

is similar to the acceleration at $\frac{\omega}{\omega_n} = 0.764$, which suggests the "jerk" would be similar to the acceleration at $\frac{\omega}{\omega_n} = 0.509$.

The velocity-squared time-histories (Figs. 22 through 24) are more uniform than Coulomb. The wave forms are practically identical for all coefficients and frequencies considered. The velocity peaks are smoothly rounded and the acceleration peaks are sharp. The acceleration wave form at $\frac{\omega}{\omega_n} = 0.255$ is similar to the displacement wave form (the negative peak being disregarded) for $\frac{\omega}{\omega_n} = 0.255$ and no damping. Therefore, the higher derivatives are suggested.

The displacement-squared time-histories curves are given in Figs. 30 through 35 . In general, the response is similar to the Coulomb curves. The motion appears to have the stick-slip type motion for small damping and low frequencies (Figs. 36 and 40). At higher frequency ratios the system appears to be undamped. Figs. 11, 32, and 35 for $\frac{\omega}{\omega_n} = 2.545$ are identical. The low frequency response for high damping coefficient (Fig. 33) seems to be dissimilar to the undamped response.

The phase angle response diagram for Coulomb damping gives a better understanding of the motion characteristics than the displacement, velocity, and acceleration response curves. The phase angle curves (Fig. 18) show that the response has a subresonant peak at a frequency ratio of 0.5; however, Fig. 14 shows that stick-slip motion occurs at this frequency and damping ratio. The phase angle in this region undergoes a smooth change in slope for values of the damping ratio between 0.38 and 0.77. For values in the order of 0.0077 the system is unstable for frequency ratios of 0.5 through 1.0. The reversal in phase at $\frac{\omega}{\omega_n} = 1.0$ appears to be instantaneous. For frequencies near resonance, instability

occurs for all values of the phase angle that are greater than 180 degrees. Also, the motion is completely stable when the phase angle drops below 180 degrees for the frequency ratios considered. However, as the phase angle approaches 90 degrees for the higher frequency ratios, the motion becomes unstable again. The other Coulomb response diagrams indicate no unusual characteristics.

The response curves for velocity-squared damping indicate no characteristics similar to the Coulomb case. The phase angle curves (Fig. 28) are smooth, continuous curves. The phase shift is practically constant for values of the damping ratio between 1.158 and 2.12.

In general, the displacement-squared response is similar to the Coulomb curves. The phase angle diagram (Fig. 37) indicates a phase shift at $\frac{\omega}{\omega_n} = 0.5$, and the same instability comments apply. The motion is unstable for frequency ratios between 0.5 and 1.0 if the curve drops below zero degrees. For frequency ratios above 1.0 and damping coefficients greater than 0.5, the motion is stable. Damping coefficients in the range of 0.1 have a completely different shape that would seem to indicate another resonance point at $\frac{\omega}{\omega_n} = 2.0$. Again, all values of the phase angle larger than 180 degrees and less than 90 degrees give unstable motion.

In general, the Coulomb damping has the narrowest resonant peak, and the displacement-squared the widest. The velocity-squared response is smoother and has the highest energy dissipation.

The position of maximum frequency response as a function of damping ratio for the damping cases can be determined by differentiating the equation of motion with respect to the frequency ratio and equating

the result to zero. The displacement, velocity, and acceleration viscous damped natural frequencies are:

Displacement resonant frequency $\omega_n(1-2\zeta^2)^{\frac{1}{2}}$

Velocity resonant frequency ω_n

Acceleration resonant frequency $\dfrac{\omega_n}{(1-2\zeta^2)^{\frac{1}{2}}}$.

This frequency ratio can be substituted into the equation of motion to determine the value of the maximum response amplitude. Since the functional relationship is unknown, these values may be obtained from the response diagrams. The results for displacement are shown in Figs. 41 and 42 for the viscous and velocity-squared cases. The Coulomb and displacement-squared cases are not plotted. The Coulomb response curve shows resonance at a frequency ratio of one and the displacement-squared case is frequency-dependent.

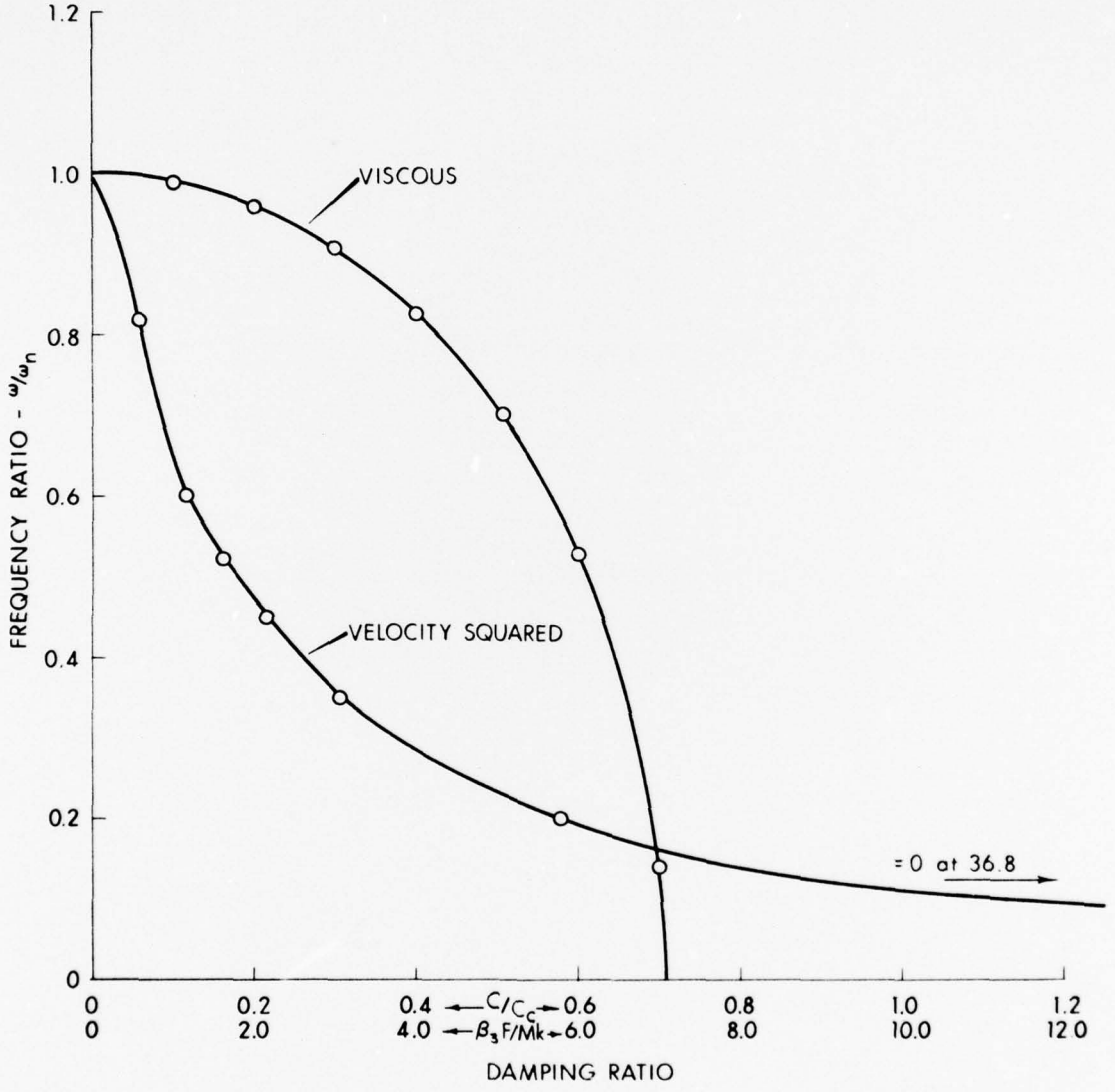

FIGURE 41
POSITION OF MAXIMUM FREQUENCY RESPONSE AS A FUNCTION OF DAMPING RATIO FOR VISCOUS AND VELOCITY-SQUARED DAMPING

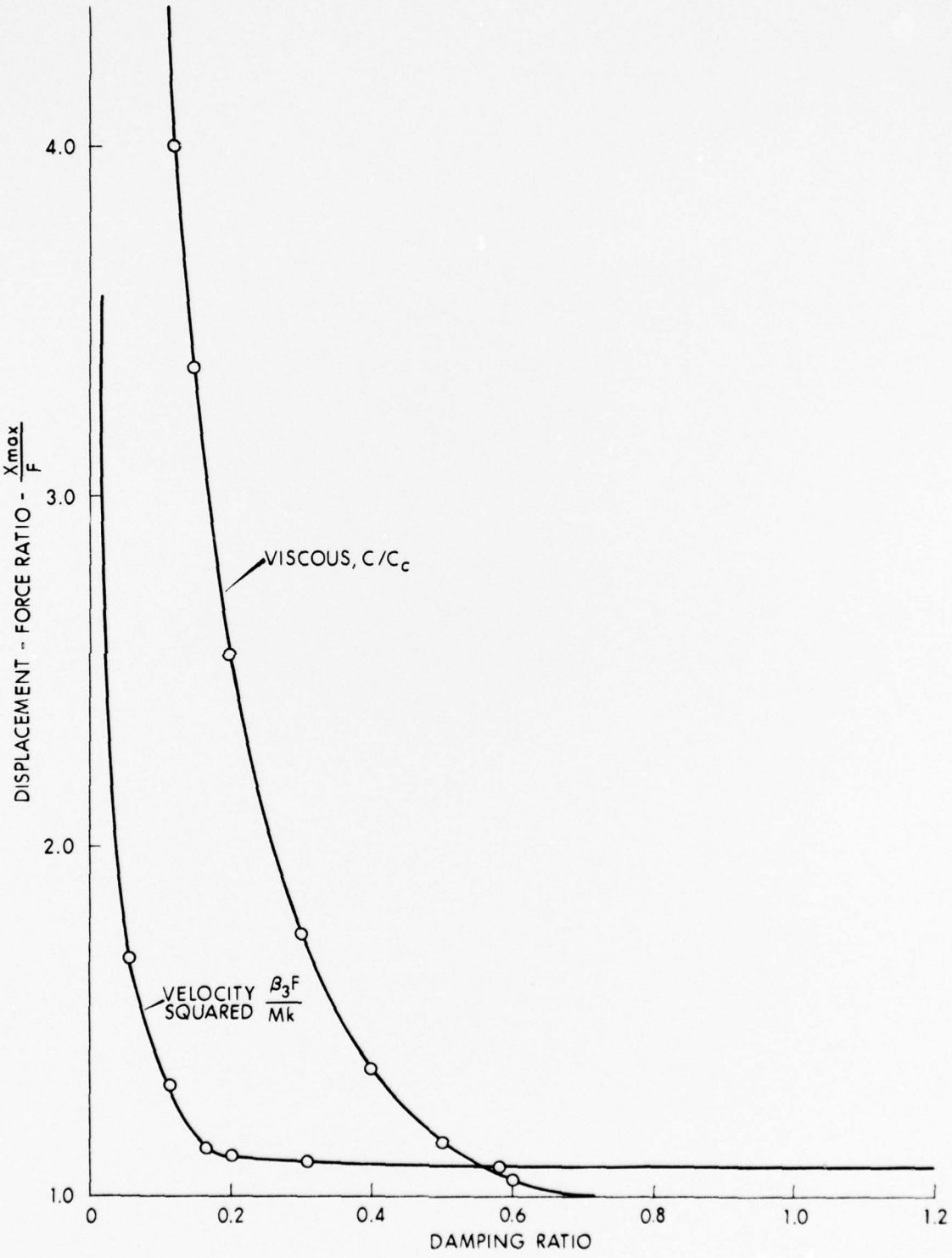

FIGURE 42
RATIO OF AMPLITUDE OF MAXIMUM FREQUENCY RESPONSE TO INPUT AMPLITUDE AS A FUNCTION OF DAMPING RATIO FOR VISCOUS AND VELOCITY-SQUARED DAMPING

CHAPTER V

DISCUSSION OF RESULTS

A. Discussion of Root-Mean-Square Error

The accuracy of the solutions to the differential equations is based on the evaluation of the magnitude of the residual. The residual is defined as the arithmetic difference between the approximate and true solution. It is obtained by substituting the estimated values of the dependent variables (for corresponding values of the independent variable) into the differential equation; therefore, it represents an aggregate of the deviation of the dependent variables. Also, the residual represents the sum of both positive and negative terms which are either very large or small. The sign of the terms are not random since the values of the dependent variables are in the neighborhood of the correct value.

The deviation of one of the independent variables from the exact value will vary from point to point over the cycle. The magnitude of the residual will depend upon the integration method and the step-size. If the analytic procedure is legitimate and the integration interval is infinitesimally small, the approximate value will yield a small residual. Therefore, analytic methods of evaluating the error may be applied.

In general, the residuals will be of either algebraic sign with respect to the true values. Therefore, the square of the residual can be used to represent the error. By the principle of least squares, the expression for the error over a cycle is

$$\int \epsilon^2(t)dt.$$

The value of the average error is

$$\epsilon_{rms} = \sqrt{\frac{1}{n} \sum_{1}^{n} \epsilon_i^2}$$

or the root-mean-square error. By the same reasoning, the average error of all the dependent variables is

$$\epsilon_{rms} = \sqrt{\frac{1}{3} \left(\epsilon^2_{rms_x} + \epsilon^2_{rms_{\dot{x}}} + \epsilon^2_{rms_{\ddot{x}}}\right)} \quad .$$

The root-mean-square error was calculated at each integration interval (not less than 150 points) and the magnitude of the error did not change. The total root-mean-square error over the cycle was equal to the point-by-point value. Therefore, neither the calculation procedure nor the equipment caused any propagation errors. The RMS error for viscous damping is less than 10^{-10}. Also, the errors in the steady-state amplitudes, displacements, velocities, and accelerations for the viscous case is less than 0.06%. Therefore, it is concluded that an RMS error of 10^{-10} is a reliable measure of the accuracy of the solution. The RMS error for the nonlinear damped solutions by the linearized procedure is in the order of 10^{-3}. In general, results with residuals of this order of magnitude are completely unreliable. It is impossible to ascertain whether the error of the linear procedures occurs in the displacement, velocity, or acceleration. The steady-state velocity-squared displacement and phase angle response diagrams for the linearized solutions are shown in Figs. 46 and 47, respectively. The errors in the diagrams are given as a percent of the numerical values. Errors (by the linearized procedure) in the steady-state amplitudes for velocity-squared damping are as high as 6 per cent. (Note: The errors in the linearized procedure for the Coulomb curves are as large as 500 per cent.) The phase angle response diagrams show similar errors. A comparison of steady-state

displacement errors with the corresponding velocity and acceleration errors is given in Table 6. The errors in the displacement, velocity, and acceleration seem to vary in a random manner with no particular pattern. Although these comments refer to maximum steady-state values, the instantaneous values vary in the same way. The instantaneous root-mean-square errors are of the same order of magnitude as the RMS total error. The wave forms for velocity-squared damping differs somewhat from sine waves, and the Coulomb wave forms bear little resemblance to a sine wave. Perhaps the explanation for equal RMS values is that the Coulomb case has many solutions due to the variable initial conditions at discontinuities in the damping function.

These comments would seem to indicate that no matter what linear analytic form of the solution is assumed, the error would be large. The method of optimizing the coefficients and functions of Eq. (2) is not as important as having the correct functions.

B. Equivalent Energy and Ritz Methods

The accuracy of the equivalent energy concept is investigated by comparing the results in Table 4 with the accurate value determined by the computer program. The calculation procedure and accuracy used in the computer program is discussed in Section A. The procedure was to choose coefficients at the resonant frequency based on equal energy and to compare the results with the values obtained with the numerical procedure. The equivalence of energy requires the assumption of the steady-state amplitude. If the wave forms of displacement and velocity are sine waves, the coefficient will give the same amplitude for the assumed damping function.

Table 6

Velocity and Acceleration Errors Corresponding to Displacement Errors in Fig. 46, p.

Damping Coeffieient	Frequency Ratio ω/ω_n	Velocity* Error	Acceleration* Error
0.0014991	0.509	+1.14	-24.2
	1.081	+0.89	-13.4
	1.527	+0.61	-3.44
0.0029982	0.509	+3.22	-52.5
	1.081	+1.61	-22.2
	1.527	+1.22	- 7.7
	2.036	+0.25	- 2.88
0.0043163	0.509	+4.6	-75
	1.081	+2.1	-26.6
	1.527	+1.59	-11.3
	2.036	+0.62	- 5.12
0.0059964	0.509	+5.7	-102
	1.081	+2.5	-32
	1.527	+1.9	-15
	2.036	+0.95	-7

*The errors are given as a per cent of the numerical value, i.e.,

$$\frac{\text{Numerical Value - Linearized Value}}{\text{Numerical Value}}$$.

The accuracy of these assumptions for velocity-squared damping and viscous damping is shown in Figs. 43, 44, and 45. An amplitude of unity was assumed, and Fig. 43 indicates the assumption is correct for the displacement; however, the velocity and acceleration values differ significantly. Also, it should be noted that the "fit" of the curves is for an insignificant frequency range.

Since the wave form is the most important consideration for equality of motion, the equality of energy is a good approximation for first order accuracy. If the correct amplitude could be determined, the energy procedure will give accurate results for a fixed frequency. The energies are equal for the same damping function if the wave form is not changed. The only requirement is the equality of the dimensional ratios.

The representative errors in the linearized steady-state velocity-squared response diagrams are shown in Figs. 46 and 47. The errors are expressed as a percentage of the numerical value, i.e.,

$$\frac{\text{Numerical Value - Linearized Value}}{\text{Numerical Value}} .$$

The errors are representative of the variation from the assumed solution. In those areas of the response diagrams where the error approaches zero, the functional variations are negligible. The most significant deviations are indicated by errors as large as 6 per cent and as small as 0.01 per cent, depending upon frequency. Typical velocity and acceleration errors for the displacement are given in Table 6. The velocity errors are positive and the acceleration errors are negative for all frequency ratios. The larger errors occur at the lower frequencies in all cases. Because of the wide variation of the errors, full coverage of the diagrams was considered unnecessary since accurate curves are given in Chapter IV.

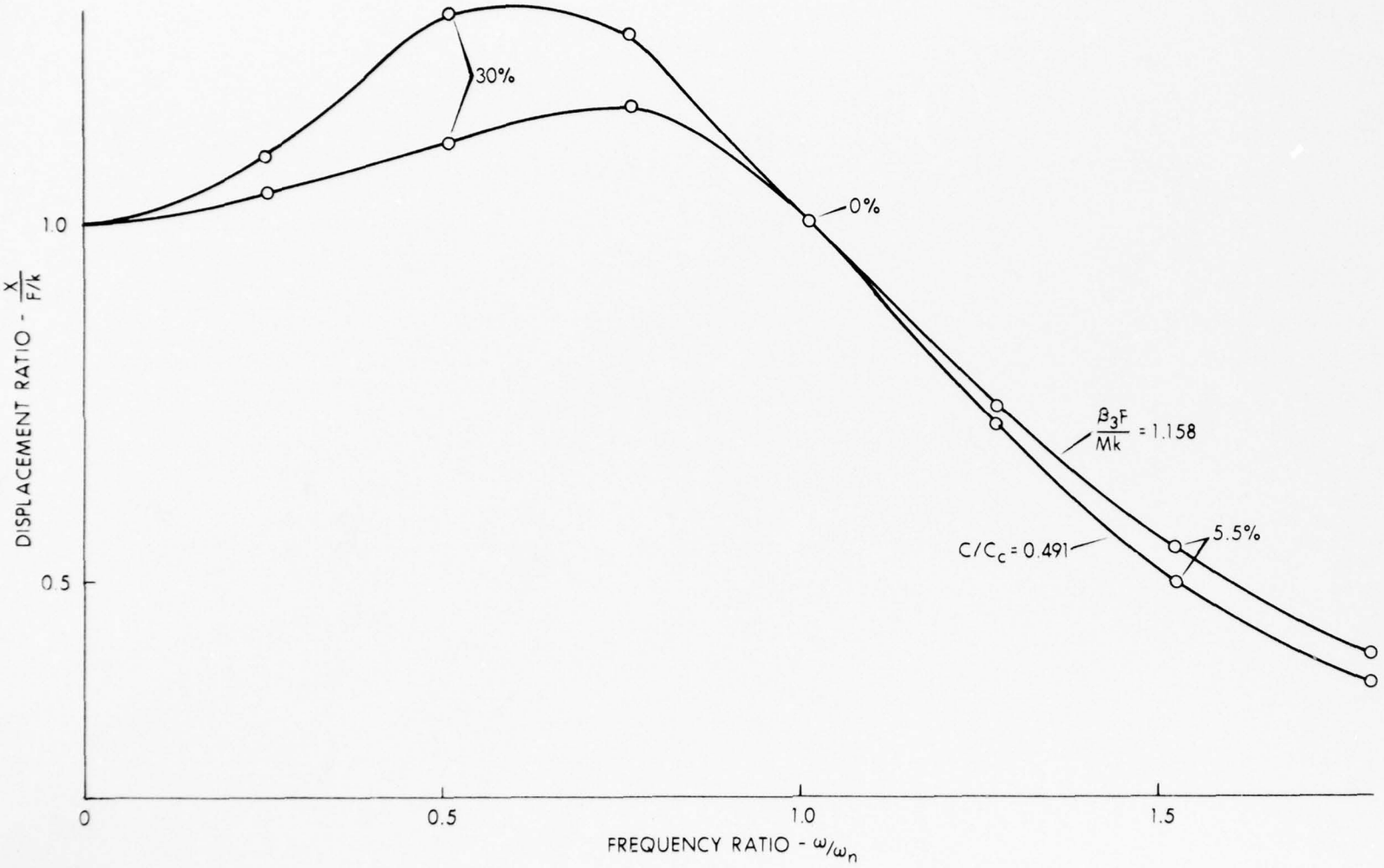

FIGURE 43
COMPARISON OF DISPLACEMENTS OF VELOCITY-SQUARED AND VISCOUS DAMPING FOR EQUAL ENERGY DISSIPATED AT RESONANCE

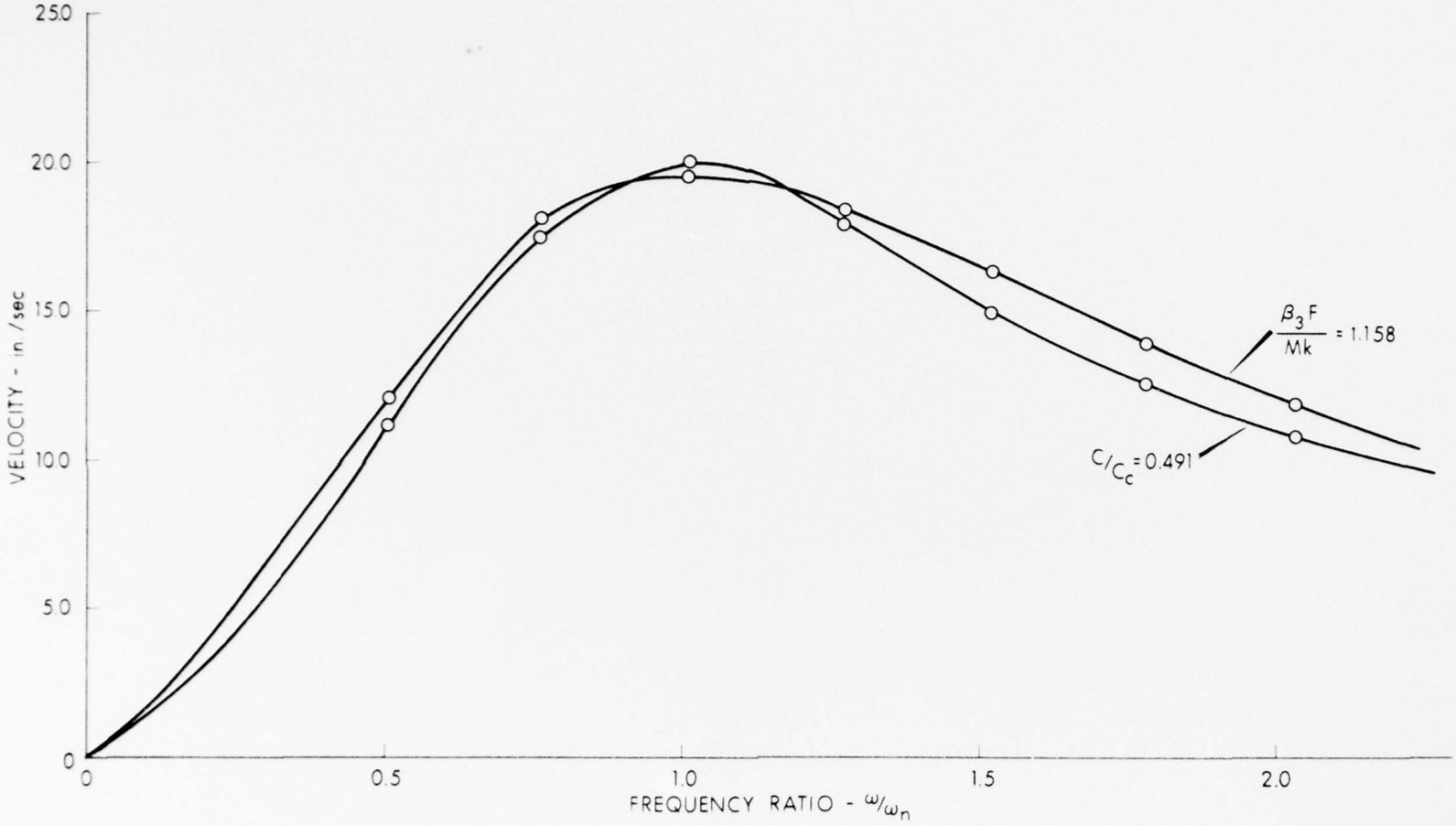

FIGURE 44
COMPARISON OF VELOCITIES OF VELOCITY-SQUARED AND VISCOUS DAMPING FOR EQUAL ENERGY DISSIPATED AT RESONANCE

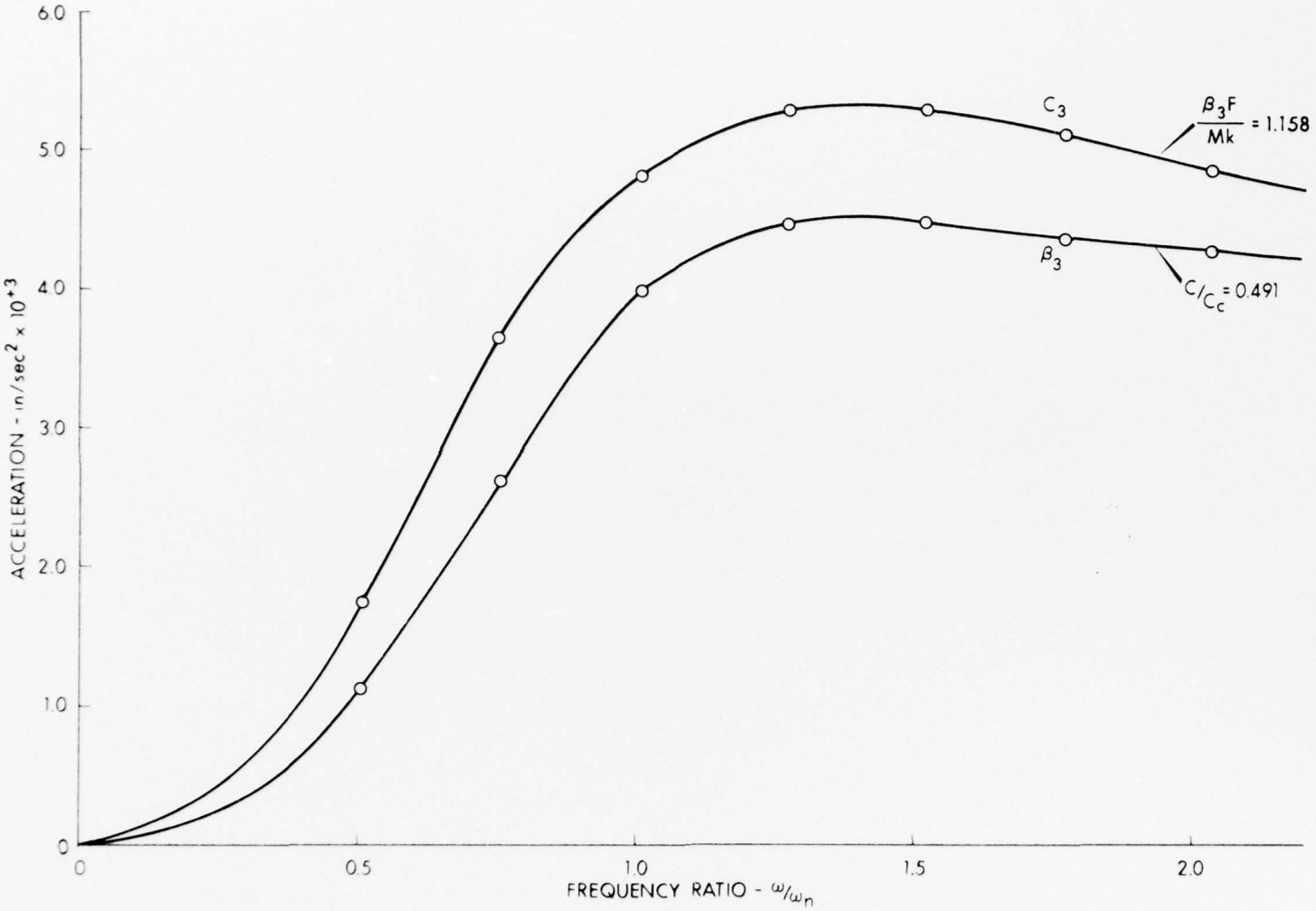

FIGURE 45
COMPARISON OF ACCELERATIONS OF VELOCITY-SQUARED AND VISCOUS DAMPING FOR EQUAL ENERGY DISSIPATED AT RESONANCE

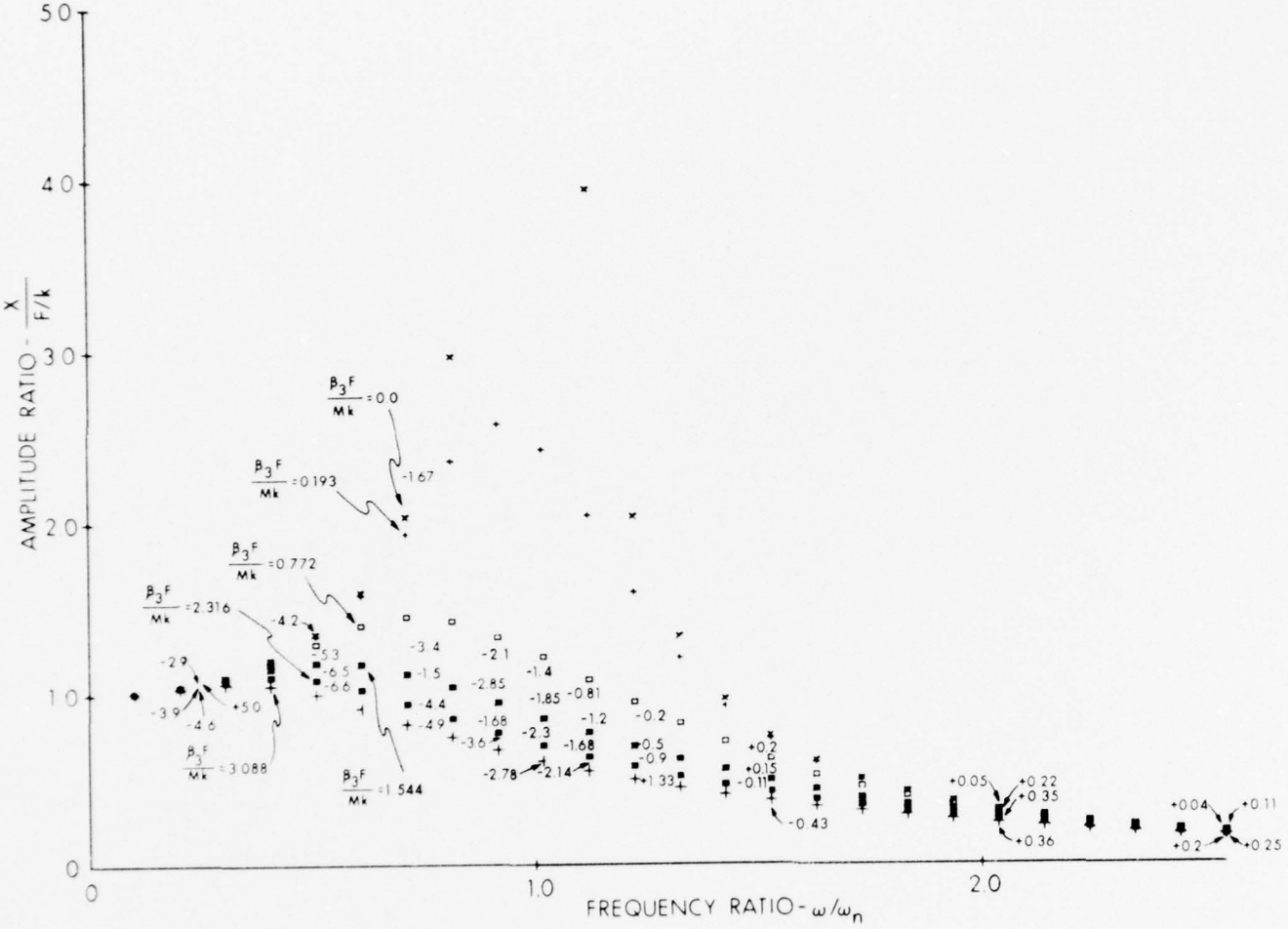

FIGURE 46
REPRESENTATIVE ERRORS FOR RESONANCE CURVES OF LINEARIZED METHOD
WITH VELOCITY-SQUARED DAMPING, FOR VARIOUS VALUES OF THE DAMPING RATIOS

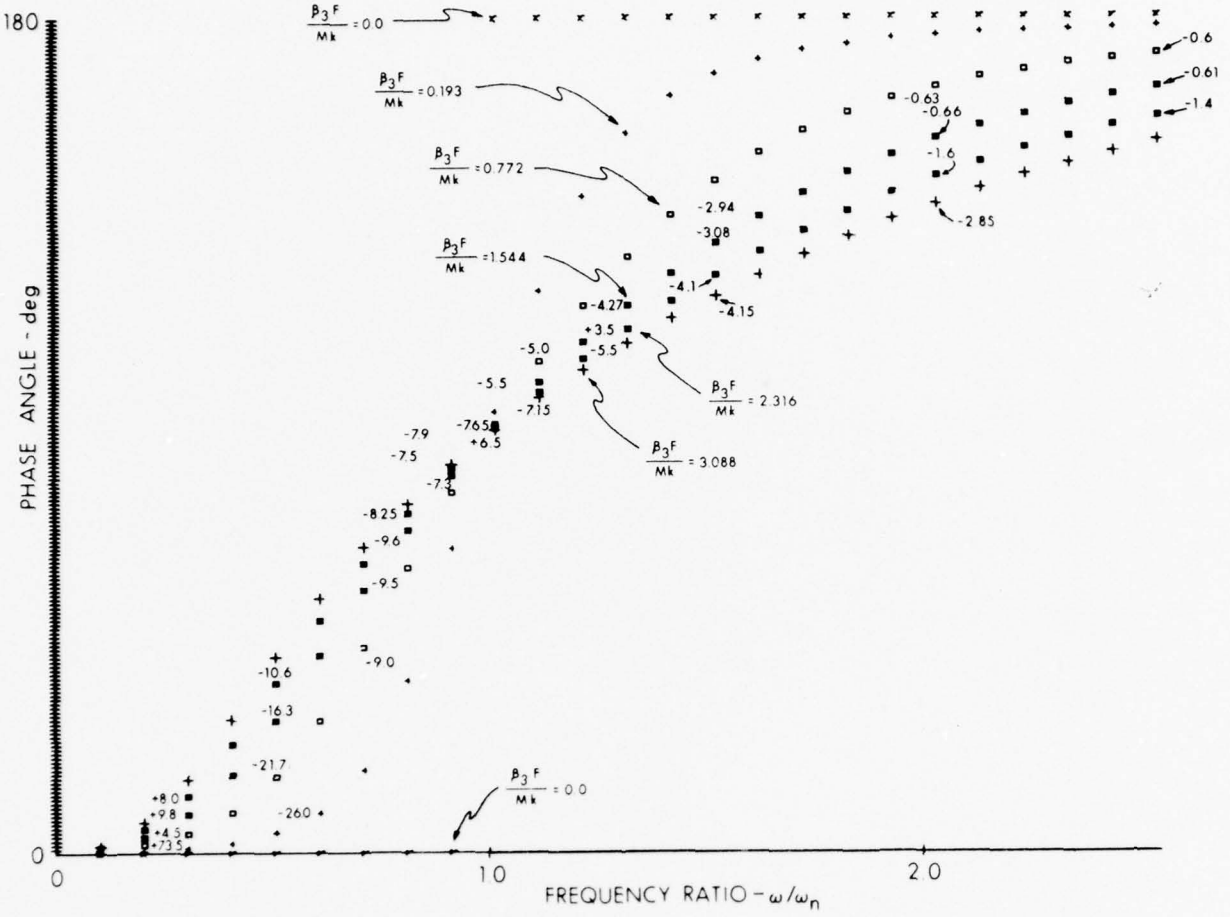

FIGURE 47
REPRESENTATIVE ERRORS FOR PHASE ANGLE CURVES OF LINEARIZED METHOD
WITH VELOCITY-SQUARED DAMPING, FOR VARIOUS VALUES OF THE DAMPING RATIOS

C. Dimensional Analysis

Demonstration of the Independence of the Dimensionless Ratios

The dimensionless ratios given in Table 5 can be shown to be linearly independent by matrix theory; however, the independence is demonstrated to guarantee that no mathematical errors have occurred. The independence of the ratios is demonstrated by solving the differential equations for various values of the parameters. By changing one parameter at a time the prediction of the response is confirmed.

The effect of changing the damping coefficient is evident by studying the response diagrams. As with the viscous case, ω_n remains unchanged, and the damped natural frequencies vary somewhat, depending upon the type of damping. Figure 41 shows the variation of the velocity-squared and viscous-damped natural frequencies. The displacement-squared and Coulomb-damped maximum frequency is given in Table 2. In all cases the damping ratio varies directly as the change in the damping coefficient.

The effect of changing the forcing amplitude, mass, and spring constant is demonstrated by holding all of the variables constant except the one being considered. The independence of each of the variables is verified in this manner. The effect of changing the above variables for viscous damping is well known; however, the results are repeated so that a comparison with the other cases can be made.

Viscous Damping

1. Effect of Changing the Forcing Function Amplitude

The magnification factor varies inversely as the change in the forcing function amplitude.

2. Effect of Changing Mass

The natural frequency and the damping ratio vary inversely as the square root of the mass change. The frequency ratio varies directly as the mass change.

3. Effect of Changing Stiffness

The magnification factor and natural frequency varies directly as the stiffness change. The damping and frequency ratios vary inversely as the square root of the stiffness change.

Velocity-Squared Damping

1. Effect of Changing the Forcing Function Amplitude

As in the case of viscous damping, the magnification factor varies inversely as the change in the forcing function amplitude; however, the proposed damping ratio varies directly as the change. The proof of the above statements is demonstrated by solving the equation of motion for F = 2.0 and F = 1.0 and comparing the results at several different frequencies. The results of these runs are shown in Tables 7 and 8. Table 7 shows the results of the run with F = 2.0 and β_3 = 0.001499089. All parameters, both steady-state and transient, are seen to be exactly equal to the results for F = 1.0 and β_3 = 0.002998178 shown in Table 8. It would be absolutely incorrect to plot the response diagram with the viscous critical ratio. Also, the conjecture of small damping is of little benefit since the variation of the magnification ratio is so large. The results show that the response is independent of frequency; therefore, time is not changed.

2. Effect of Changing the Stiffness

The magnification factor varies directly as the change of the stiffness. The frequency ratio varies inversely as the square root of

TABLE 7

VELOCITY-SQUARED DAMPING RESPONSE

WITH F=2.0, β_3=0.001499089, AND ω=5.0

THE DAMPING ENERGY PER CYCLE	Z PHASE =
4.086539058248E-01	2.837961-292
9.570771515835E-01	4.401158E 00
9.476862788899E-01	5.364568E 00

THE TOTAL TRANSIENT DAMPING ENERGY = 2.313417E 00

MAX DISP	AT TIME	MAX DISP	AT TIME	PHASE
2.27165107E 00	2.94000000E-01	2.27165107E 00	2.94000000E-01	1.47000000E 00
2.17622046E 00	1.57800000E 00	2.17622046E 00	1.57800000E 00	2.06370007E 00
2.17524407E 00	2.83200000E 00	2.17524407E 00	2.83200000E 00	1.30823724E 00

MAX VEL	AT TIME
1.370104399335E 01	1.379999999976E-01
-1.125473823195E 01	6.659999999101E-01
-1.056915394816E 01	1.937999998627E 00

MAX ACCEL	AT TIME
1.596996190056E 02	6.600000000210E-02
-6.898114462150E 01	1.583999998984E 00
-6.872092276812E 01	2.843999997713E 00

MAX DISPLACEMENT = 2.271651066898E 00 AT TIME = 3.125999997428E 00

MAX VELOCITY = 1.370104399335E 01 AT TIME = 2.969999997586E 00

MAX ACCELERATION = 1.596996190056E 02 AT TIME = 2.897999997658E 00

TABLE 8

VELOCITY-SQUARED DAMPING RESPONSE

WITH F=1.0, β_3=0.002998179, AND ω=5.0

THE DAMPING ENERGY PER CYCLE	Z PHASE =
1.021634945995E-01	2.714657-292
2.392693594215E-01	4.401158E 00
2.369216452236E-01	5.364568E 00

THE TOTAL TRANSIENT DAMPING ENERGY = 5.783545E-01

MAX DISP	AT TIME	MAX DISP	AT TIME	PHASE
1.13582552E 00	2.94000000E-01	1.13582552E 00	2.94000000E-01	1.47000000E 00
1.08811024E 00	1.57800000E 00	1.08811024E 00	1.57800000E 00	2.06370007E 00
1.08762204E 00	2.83200000E 00	1.08762204E 00	2.83200000E 00	1.30823724E 00

MAX VEL	AT TIME
6.8505215211 77E 00	1.379999999976E-01
-5.627368730260E 00	6.659999999101E-01
-5.284576901933E 00	1.937999998627E 00

MAX ACCEL	AT TIME
7.984980576090E 01	6.600000000210E-02
-3.449057512742E 01	1.583999998984E 00
-3.436046473682E 01	2.843999997713E 00

MAX DISPLACEMENT = 1.135825516365E 00 AT TIME = 3.125999997428E 00

MAX VELOCITY = 6.8505215211 77E 00 AT TIME = 2.969999997586E 00

MAX ACCELERATION = 7.984980576090E 01 AT TIME = 2.897999997658E 00

the change. The damping ratio varies inversely as the stiffness change. The proof of the above statements is demonstrated by solving the equation with $k = \frac{1}{2}$, $\beta_3 = 0.002998179$, and a forcing frequency of 7.071068 radians/second (Table 9). This permits the result to be compared with the solution for $\beta_3 = 0.005996358$, $k = 1.0$, and a frequency of 10 radians/second (Table 10). The following changes are noted:

a. The displacement varies inversely as Δk, i.e., 1

b. The velocity varies inversely as the square root of the change, i.e., $\sqrt{2}$

c. The accelerations are equal

d. The energy varies inversely as the change, i.e., 2

e. The phase angles at the positive peaks are equal

f. The time varies inversely as the square root of the change, i.e., $\sqrt{2}$.

These changes show that the correct expressions for the response ratios were used.

3. Effect of Changing Mass

The damping ratio varies inversely as the mass changes and the frequency ratio varies inversely as the square root of the mass change. The effect of doubling the mass for a forcing frequency of 7.071068 radians/second and $\beta_3 = 0.002998179$ is shown in Table 11. The corresponding data for a forcing frequency of 10.0 radians/second and $\beta_3 = 0.001499089$ is shown is Table 12. A comparison of these two figures show

a. The displacements are equal

b. The velocity varies inversely as the square root of the change, i.e., $\frac{1}{\sqrt{2}}$.

TABLE 9

VELOCITY-SQUARED DAMPING RESPONSE

WITH k=1/2, β_3=0.002998179, AND ω=7.071068

THE DAMPING ENERGY PER CYCLE	Z PHASE =
6.129588748561E-01	2.837961-292
4.218520360766E 00	3.622920E 01

THE TOTAL TRANSIENT DAMPING ENERGY = 4.831479E 00

MAX DISP	AT TIME	MAX DISP	AT TIME	PHASE
2.28340212E 00	3.26000000E-01	2.28340212E 00	3.26000000E-01	2.30516807E 00
2.29790562E 00	1.21400000E 00	2.29790562E 00	1.21400000E 00	4.18427952E 01

MAX VEL	AT TIME
-1.445684287784E 01	5.060000000638E-01
1.445009736781E 01	9.479999985313E-01

MAX ACCEL	AT TIME
-1.750517391338E 02	3.480000000622E-01
1.753078702983E 02	7.899999990943E-01

MAX DISPLACEMENT = 2.297911688976E 00 AT TIME = 1.658000000869E 00

MAX VELOCITY = 1.445684287784E 01 AT TIME = 1.720000001107E 00

MAX ACCELERATION = 1.753078702983E 02 AT TIME = 1.678000000946E 00

TABLE 10

VELOCITY-SQUARED DAMPING RESPONSE

WITH k=1, β_2=0.005996357, AND ω=10.0

THE DAMPING ENERGY PER CYCLE	Z PHASE =
3.0647802979222E-01	2.714657-292
2.1092579107506E 00	3.534088E 01

THE TOTAL TRANSIENT DAMPING ENERGY = 2.415736E 00

MAX DISP	AT TIME	MAX DISP	AT TIME	PHASE
1.1417060326E 00	2.3100000000E-01	1.1417060326E 00	2.3100000000E-01	2.3100000000E 00
1.1489467548E 00	8.5799999993E-01	1.1489467548E 00	8.5799999993E-01	4.1597787879E 01

MAX VEL	AT TIME
-1.0222606595206E 01	3.5699999993088E-01
1.0217622191126E 01	6.7199999961306E-01

MAX ACCEL	AT TIME
-1.7505638496666E 02	2.4600000003126E-01
-1.7526561263956E 02	8.7299999939286E-01

MAX DISPLACEMENT = 1.1489467486976E 00 AT TIME = 1.4849999987936E 00

MAX VELOCITY = 1.0222606595206E 01 AT TIME = 1.2149999990656E 00

MAX ACCELERATION = 1.7526561263956E 02 AT TIME = 1.4999999987186E 00

TABLE 11

VELOCITY-SQUARED DAMPING RESPONSE

WITH W=2.0, β_5=0.002998179, AND ω=7.071068

THE DAMPING ENERGY PER CYCLE	Z PHASE =
1.935485794966E-01	2.837961-292
1.168908778403E 00	1.030009E 01
9.287875850685E-01	1.168706E 01

THE TOTAL TRANSIENT DAMPING ENERGY = 2.291245E 00

MAX DISP	AT TIME	MAX DISP	AT TIME	PHASE
1.44092257E 00	3.06000000E-01	1.44092257E 00	3.06000000E-01	2.16374672E 00
1.3769523*E 00	6.95999999E-01	1.33182122E 00	1.15400000E 00	1.75342550E 01
1.3445825*E 00	1.59400000E 00	1.34117587E 00	2.04000000E 00	1.64903656E 01

MAX VEL	AT TIME
-1.149316488911E 01	4.520000000834E-01
-1.108384318068E 01	4.860000000917E-01
-9.200638269307E 00	2.227999999712E 00

MAX ACCEL	AT TIME
-1.262864653749E 02	3.280000000610E-01
7.980772990035E 01	7.159999993397E-01
7.974867694080E 01	1.624000000738E 00

MAX DISPLACEMENT = 1.440922573121E 00 AT TIME = 2.345999998448E 00

MAX VELOCITY = 1.149316488911E 01 AT TIME = 2.491999996884E 00

MAX ACCELERATION = 1.262864653749E 02 AT TIME = 2.367999998212E 00

TABLE 12

VELOCITY-SQUARED DAMPING RESPONSE

WITH W=1.0, β_3=0.001499089, AND ω=10.0

THE DAMPING ENERGY PER CYCLE	Z PHASE =
1.935470916709E-01	2.714657-292
1.168908045685E 00	9.557778E 00
9.287867069244E-01	1.052119E 01

THE TOTAL TRANSIENT DAMPING ENERGY = 2.291242E 00

MAX DISP	AT TIME	MAX DISP	AT TIME	PHASE
1.44093584E 00	2.16000000E-01	1.44093584E 00	2.16000000E-01	2.16000000E 00
1.3769584*E 00	4.92000000E-01	1.33182134E 00	8.15999999E-01	1.75335605E 01
1.3446061*E 00	1.12800000E 00	1.34113551E 00	1.44300000E 00	1.67780977E 01

MAX VEL	AT TIME
-1.625332586234E 01	3.209999999672E-01
-1.561187902873E 01	3.449999999430E-01
-1.301170499355E 01	1.574999998702E 00

MAX ACCEL	AT TIME
-2.525434128765E 02	2.310000000289E-01
1.596175879677E 02	5.069999997737E-01
1.594711325160E 02	1.148999999132E 00

MAX DISPLACEMENT = 1.440935837047E 00 AT TIME = 1.658999998617E 00

MAX VELOCITY = 1.625332586234E 01 AT TIME = 1.763999998511E 00

MAX ACCELERATION = 2.525434128765E 02 AT TIME = 1.673999998602E 00

c. The acceleration varies inversely as the change, i.e., $\frac{1}{2}$

d. The energy per cycle is equal

e. The positive phase angles are equal

f. The time varies directly as the square root of the change, i.e., $\sqrt{2}$.

D. Adams-Moulton Numerical Analysis

The dimensionless numerical steady-state response curves given in Chapter IV were plotted from the data gathered by the Adams-Moulton method. The same equations, coefficients, and forcing function were used in these solutions as were used in the linearized solutions. The curves are plotted using the dimensionless ratios given in Table 3.

Since the concept of the dimensional analysis, as introduced, is not generally used in the analysis of dynamic systems, it is necessary to give a few results which will serve for elucidating the theoretical considerations given in Chapter IV. The results are limited in number because of the computer time involved; however, these data are sufficiently accurate to demonstrate the proposed procedure.

The curves are generated by assigning various fixed values to the damping ratio and varying the frequency from 5 to 50 radians/second. The value of the damping ratios cover the range above critical, i.e., the point where the amplitude decreases continuously as the input frequency is increased.

As in the viscous case, all curves show a predominate resonance peak; however, the Coulomb and displacement-squared cases indicate resonances in addition to the predominant peak. The additional peaks are most noticeable in the phase angle response curves and are seen to be

dependent on the damping. In general, for small values of damping and low frequency, the output amplitude is substantially the same as the input. At the higher frequencies the output oscillations decrease asymptotically toward zero.

E. Time-Histories of Motion

Unlike the input motion, the output motion is a distorted sinusoidal function of time; however, both functions have the same frequency for all damping cases. The degree of distortion varies from simple sinusoidal distortion to random distortion. The sinusoidal distortion has amplitude, frequency, and phase components, depending on the type and degree of damping. In general, velocity-squared damping for small values of the damping constant is frequency-distorted.

The random distortion is due to the discontinuities in the damping function. These discontinuities are of such magnitude that it is virtually impossible to attach any mathematical description to the most predominant disturbance.

Although one is intuitively aware of the above statements, it does not seem impossible to trace a distortion as the damping constant becomes increasingly larger so that a final identification of the characteristic would be possible. Also, the success of such an analysis would depend on the size of the incremental steps in the experimental procedure. Although several attempts were made to take small increments from a known condition, the variations in amplitude, phase, and frequency just before and after the discontinuity would not permit a meaningful analysis. In the general case the amplitude, phase, and frequency vary over a cycle of motion; therefore, the time of occurrence of the discontinuity is such that a

completely different set of initial conditions occur. Also, it is impossible to ascertain the length of the transients induced after the discontinuity.

The time-history curves for velocity-squared damping, Figs. 22 through 24, have the same general shape. The shape of the curve was estimated to have the same general characteristics as the response diagram, i.e., for leading and lagging phase between the input forcing function and the resulting output, the variation in shape over a cycle of motion would exhibit a definite frequency characteristic. A representative cycle of motion was chosen, and the frequency for a quarter cycle was calculated by measuring the length of time from a zero crossing to a peak, and vice versa. The phase angle vector diagram is shown in Fig. 48. The phase angles are shown for the first quarter cycle. Intuitively the motion should vary as the forcing function; therefore, a sine wave with the calculated frequency was assumed. Table 14 gives the results of this investigation for the first quarter cycle of motion from zero to the peak amplitude. Table 15 gives the result for the fit to the second quarter cycle from the peak to the zero crossing. All of the calculations for the assumed motion were performed on the desk calculator. The values of the numerical motion are from the digital solution. The close correlation of the values indicate the correctness of the assumptions for the steady-state displacement, i.e., the motion could be represented by

$$x = 0.424875 \sin(30.0t - 1.3096)$$

in the interval from zero to $\frac{\pi}{2}$, and $x = 0.424875 \sin(30.0t + 1.41593)$ in the interval from $\frac{\pi}{2}$ to π. The change in the sign of the damping force is most evident at the peaks of the wave forms, as indicated in Fig. 24.

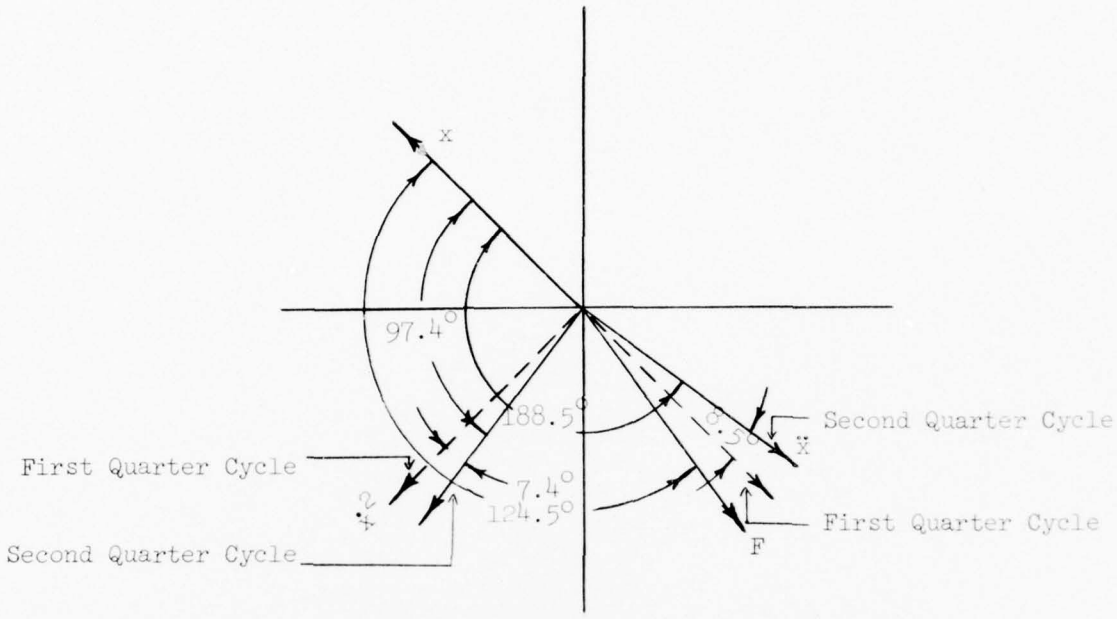

FIGURE 48

PHASE ANGLE VECTOR DIAGRAM FOR VELOCITY-SQUARED DAMPING WITH $\beta_3 = 0.006$ AND $\omega = 30.0$

The values shown on the above phase angle vector diagram and in Tables 14 and 15 were calculated from the numerical solution. The phase angles were calculated by the same procedure as is used in the numerical program. The angles shown in the figure are for the first quarter cycle of the steady-state motion. The changes in velocity and acceleration angles were determined by multiplying the difference between the time of occurrence of the zero value of the derivative of the corresponding quantity by the forcing frequency.

The angular frequency of the sine wave that is assumed to match the displacement for the first and second quarter of the cycle is calculated by determining the period of an assumed sine wave. The period is determined by taking the difference in the time of occurrence of the zero and peak amplitudes. The value of ω is determined by $\omega = \frac{2\pi}{T}$, where T = time change, seconds. The values given in the tables were determined by using a four-place sine table.

TABLE 13

THE AMPLITUDE TIME VALUES OF DISPLACEMENT FOR THE FIRST QUARTER CYCLE OF MOTION FOR A SINE WAVE OF 30.0 RADIANS/SECOND, AND A PEAK AMPLITUDE OF 0.424875 INCHES

ωt	X sin ωt Calculated Values
0.075	0.0318
0.150	0.063
0.225	0.094
0.300	0.1256
0.375	0.1556
0.450	0.1848
0.525	0.2130
0.600	0.2399
0.675	0.2655
0.750	0.2896
0.825	0.3121
0.900	0.3328
0.975	0.3517
1.05	0.3686
1.125	0.3834
1.200	0.3960
1.275	0.4064
1.35	0.4146
1.425	0.4204
1.500	0.4238
1.575	0.4249

TABLE 14

THE AMPLITUDE TIME VALUES OF DISPLACEMENT FOR THE FIRST QUARTER CYCLE OF MOTION ASSUMING A SINE WAVE OF 28.690343872 RADIANS/ SECOND, AND A PEAK AMPLITUDE OF 0.424875 INCHES

Time, t	ωt	X sin ωt Calculated Values	X sin ωt Numerical Solution
0.0025	0.07173	0.030	0.030
0.0050	0.14345	0.0607	0.0607
0.0075	0.21518	0.090	0.090
0.0100	0.28690	0.120	0.120
0.0125	0.35863	0.149	0.149
0.0150	0.43036	0.177	0.176
0.0175	0.50208	0.204	0.203
0.0200	0.57381	0.231	0.231
0.0225	0.64553	0.255	0.255
0.0250	0.71726	0.279	0.279
0.0275	0.78898	0.301	0.301
0.0300	0.86071	0.322	0.321
0.0325	0.93244	0.341	0.340
0.0350	1.00416	0.358	0.357
0.0375	1.07589	0.373	0.372
0.0400	1.14761	0.387	0.386
0.0425	1.21934	0.398	0.398
0.0450	1.29107	0.408	0.408
0.0475	1.36279	0.415	0.415
0.0500	1.43452	0.421	0.421
0.0525	1.50624	0.424	0.425

TABLE 15

THE AMPLITUDE TIME VALUES OF DISPLACEMENT FOR THE SECOND QUARTER CYCLE OF MOTION ASSUMING A SINE WAVE OF 31.415927 RADIANS/SECOND AND A PEAK AMPLITUDE OF 0.424875 INCHES

Time, t	ωt	X sin ωt Calculated Values	X sin ωt Numerical Solution
0.0550	1.72788	0.420	0.420
0.0575	1.80642	0.413	0.414
0.0600	1.88496	0.404	0.405
0.0625	1.96350	0.392	0.395
0.0650	2.04204	0.379	0.381
0.0675	2.12058	0.363	0.364
0.0700	2.19912	0.344	0.345
0.0725	2.27766	0.323	0.324
0.0750	2.35619	0.300	0.301
0.0775	2.43470	0.276	0.276
0.0800	2.51327	0.249	0.250
0.0825	2.59181	0.222	0.222
0.0850	2.67035	0.193	0.194
0.0875	2.74890	0.163	0.162
0.0900	2.82743	0.131	0.133
0.0925	2.96597	0.099	0.100
0.0950	2.98451	0.066	0.066
0.0975	3.06305	0.033	0.032
0.1000	3.14159	0.0002	0.0002

The velocity peak is sharper than the viscous case. The acceleration curve has a spike-shaped peak which would be expected for the skewed velocity.

The above analysis indicates practically no incremental phase variations within the quarter cycles considered; therefore, the differentiated displacement should generally represent the velocity and acceleration. This is obviously incorrect. The curves and the data show that additional terms in the solution are required. The difficulties of representing arbitrarily small variations in the displacement were mentioned in the statement of the problem.

These variations become larger as the forcing function magnitude is increased. The deviations become so large that the motion becomes unstable for all damping cases, since the response is a function of the forcing magnitude. The unstable character of the response may occur in the displacement, velocity, acceleration, or in the higher derivatives. The time-histories for Coulomb and displacement-squared damping show the effects on the stability of the motion. Obviously a similar response exists for "jerk" in the velocity-squared case. It should be noted that the distorted velocity and acceleration have the same period as the displacement.

Motion curves that are typical of each response curve are given in the previous chapter. Both the steady-state and transient motions are correct for the corresponding damping case and can be used for the design or analysis of any system described by the equations of motion. The data analysis performed by the computer program permits the printout of the pertinent transient information and these data were recorded for each point on the response diagrams. The information is not presented because of the volume of the material.

CHAPTER VI

CONCLUSIONS

Linearization techniques have been applied to the characteristic damping functions to allow the prediction of the steady-state response of the systems. The amplitude, velocity, acceleration and phase angle diagrams are compared with an accurate solution. The errors for these assumptions are given in Chapter V. The magnitude of the errors indicate that any value of the damping greater than zero is significant and cannot be called "small."

The error in determining a damping coefficient by linearized assumptions varies over a considerable range. For a fixed frequency, the error approaches zero; however, the large variations in the wave form as a function of input forcing function magnitude makes it impossible to give a general value of the error.

The dimensionless ratios given allow one to read at a glance from the resonance curves, the effects of the resonant frequencies, the displacement, velocity, and acceleration, and the degree of the damping; moreover, the motion wave forms can be specified directly. Plotting the response with arbitrary dimensional quantities, as is frequently done in the literature, turns out to be less surveyable.

A difficulty encountered in the interpretation of dynamic results is the vagueness of the effects of the linearized assumptions. The accuracy of these linearized assumptions is established for the Ritz two-term and equivalent energy methods by direct comparison with the numerical solution. Various limits of the accuracy have been established so that the design problem at hand may be treated with the desired accuracy.

The dimensional analysis of the problem is the most important aspect of the investigation. Sufficient familiarity with the dimensionless ratios has been established to allow a simple and convenient presentation of the results. Simplicity is attained by looking for the independent dimensionless ratios that are convenient for the presentation of universal design curves. The value of presenting the data in terms of the viscous critical damping ratio, δ, is definitely incorrect. The method presented can be established before determining the solution. This method of establishing valid conclusions from a general dimensional analysis provides one of the most significant contributions.

The principle advantage of studying the wave forms for the various damping cases is the determination of the predominant frequency content in the response. This will permit the determination of harmonics not necessarily in the environment. With the frequency range established, experimental test instrumentation can be selected with the proper response characteristics. For example, the proper choice of accelerometer, filter, amplifier, and recorder response could not be made for a damped system without some knowledge of the frequencies involved. Also, a knowledge of the wave form is invaluable for the design and analysis of equipment.

The steady-state and transient response characteristics of these systems with other forcing functions would be of tremendous value to the design engineer. A complete collection of such data exists for viscous-damped systems;[4] however, virtually nothing is tabulated concerning the response of the nonlinear systems given in this thesis. Since the forcing function is completely described by the magnitude and shape of the cycle, the dimensionless ratios can be applied directly to these systems. Also,

future work might include investigations of combined damping cases. The author has run several combined damping cases. The range of the damping coefficient can be predicted by the Ritz procedure for all cases. In general, the response does not contain as many discontinuities as the basic types of damping presented. It should be noted that a general study of this type would be almost impossible because of the number of combinations of damping coefficients and functions. The numerical program in the appendix can be used for a general study.

APPENDIX

COMPUTER PROGRAM FOR RITZ TWO-TERM APPROXIMATION

```
      INTEGER W,B
      REAL IRAD,ITEMP
      DIMENSION OMGA(50),BETA(5,10),WP(50),B2P(10),X(7,10,50),B4P(10),
     1THETA(7,10,50),OMGP(25),T(200),THET(25),XPL(25),XPJ(25),THETJ(25)
      READ 1,W,B
    1 FORMAT(2I5)
      DO 2 I=1,W
    2 OMGA(I)=I
      DO 3 I=1,5
      READ 4,(BETA(I,J),J=1,B)
    4 FORMAT (10F8.7)
      PRINT 113
    3 PRINT 5,(I,J,BETA(I,J),J=1,B)
    5 FORMAT (50X,6H BETA(,I2,1H,,I2,4H) = F10.7)
      INX2=0
      INX3=0
      INX4=0
      RO=19.6468827
      PI=3.1415926536
      P9=64./(9.*PI*PI)
      E3=2.6666666666
      AK = W/RO
      RAD=180./PI
      DO 111 I=1,B
  111 B2P(I)=16.*(BETA(2,I)/PI)**2
      DO 112 J=1,W
  112 WP(J)=1.-(OMGA(J)/RO)**2
      DO 6 I=1,B
      PRINT 113
  113 FORMAT(1H1)
      IF(I.EQ.1)300,301
  300 PRINT 302
  302 FORMAT (112H         SINCE B1, B2, AND B3 ARE ALL EQUAL TO ZERO, TH
     1E VALUES LISTED FOR X1, X2, X3,---X7 ARE BOTH (+) AND (-).,/ )
  301 PRINT 114,I
  114 FORMAT (4H  B=,I2, 8X,2HX1,14X,2HX2,14X,2HX3,14X,2HX4,14X,
     12HX5,14X,2HX6,14X,2HX7)
      DO 6 J=1,W
      B1W=(BETA(1,I)*OMGA(J))**2
      B3W=(BETA(3,I)*OMGA(J)**2)**2
```

```
      IF (B3W.EQ.0)500,501
  500 X(1,I,J)=1/WP(J)
      X(2,I,J)=1/WP(J)
      X(3,I,J)=1/WP(J)
      X(4,I,J)=1/WP(J)
      X(5,I,J)=1/WP(J)
      X(6,I,J)=1/WP(J)
      X(7,I,J)=1/WP(J)
      DO 28 N=1,7
      IF (X(N,1,J))28,21,21
   28 X(N,1,J)=-X(N,1,J)
   21 CONTINUE
      GO TO 20
  501 IF(1-B2P(I))600,8,8
  600 X(1,I,J)=99.999999
    8 X(1,I,J)=SQRTF(1.-B2P(I))/WP(J)
      X(2,I,J)=1./SQRTF(WP(J)**2+B1W)
      X(3,I,J)=SQRTF((SQRTF(WP(J)**4+4*P9*B3W)-WP(J)**2)/(2*P9*B3W))
      B4P(I)=4*(BETA(4,I)/PI)**2
  190 X(4,I,J)=1/SQRTF(WP(J)**2+B4P(I))
      X(5,I,J)=SQRTF((SQRTF(WP(J)**4+(64.*(BETA(5,I)**2))/(9.*PI*PI))-WP
     1(J)**2)/((32.*(BETA(5,I))**2)/(9.*PI*PI)))
      IF(1-B2P(I))9,10,10
    9 X(6,I,J)=99.99999
      GO TO 11
   10 X(6,I,J)=SQRTF((1-B2P(I))/(WP(J)**2+B1W))
   11 IF ((WP(J)**2+B1W)**2-(4*P9*B3W*(B2P(I)-1)))181,181,14
  181 X(7,I,J)=99.99999
      GO TO 20
   14 IF (SQRTF((WP(J)**2+B1W)**2-(4*P9*B3W*(B2P(I)-1)))-
     1(WP(J)**2+B1W))181, 13,13
   13 X(7,I,J)=SQRTF((SQRTF(((WP(J)**2+B1W)**2)-(4*P9*B3W
     1*(B2P(I)-1)))-(WP(J)**2+B1W))/(2*P9*B3W))
      DO 25 N=1,7
      IF(X(N,I,J))26,25,25
   26 X(N,I,J)=-X(N,I,J)
   25 CONTINUE
   20 PRINT 15,J,X(1,I,J),X(2,I,J),X(3,I,J),X(4,I,J),X(5,I,J),X(6,I,J),
     1X(7,I,J)
   15 FORMAT(4H  J=,I2,7(2X,E14.7))
      BP=(4.*BETA(2,I))/(PI*X(1,I,J))
      BW=BETA(1,I)*OMGA(J)
      BWX=(E3*BETA(3,I)*OMGA(J)**2*X(3,I,J))/PI
```

```
      BPX=(2*BETA(4,I)/PI)/WP(J)
      THETA(1,I,J)=ATANF(BP/WP(J))*RAD
      THETA(2,I,J)=ATANF(BW/WP(J))*RAD
      THETA(3,I,J)=ATANF(BWX/WP(J))*RAD
      THETA(4,I,J)=ATANF(BPX)*RAD
      THETA(5,I,J)=ATANF(((4.*BETA(5,I)*X(5,I,J))/(3.*PI))/WP(J))*RAD
      THETA(6,I,J)=ATANF((BW+BP)/WP(J))*RAD
      THETA(7,I,J)=ATANF((BW+BP+BWX)/WP(J))*RAD
      DO 18 K=1,7
      IF(THETA(K,I,J))17,18,18
   17 THETA(K,I,J)=180.+THETA(K,I,J)
   18 CONTINUE
      IF(I.EQ.1) 400,502
  400 DO 401 K=1,7
      IF(J.GE.20) 401,502
  401 THETA(K,I,J)=180
  502 PRINT 19,THETA(1,I,J),THETA(2,I,J),THETA(3,I,J),THETA(4,I,J),
     1THETA(5,I,J),THETA(6,I,J),THETA(7,I,J)
   19 FORMAT(7H THETA=,2X,F13.8,6(3X,F13.8))
    6 CONTINUE
   41 PRINT 42
   42 FORMAT (1H1
      PRINT 43
   43 FORMAT (4X,8HEQUATION,9X,4HBETA,12X,1HX,12X,5HTHETA,11X,4HOMGA,
     110X,5HERROR)
      IRAD=PI/180.
      DO 7 N=1,5
      DO 7 I=1,10
      DO 7 J=10,40,10
      RE=0
      RAF1=0
      T(1)=0
      DMAX=0.0
      VMAX=0.0
      AMAX=0.0
      IF (J.EQ.1)12,16
   12 ITEMP=.00314159
      GO TO 39
   16 IF (J.EQ.2)22,23
   22 ITEMP=.00157079
      GO TO 39
   23 IF (J.EQ.3)24,27
   24 ITEMP=.00104719
```

```
      GO TO 39
   27 ITE P=.00078539
   39 CONTINUE
      THETA(N,I,J)=THETA(N,I,J)*1RAD
      DO 40 K=1,200
      T(K)=ITEMP*K
      XGN = X(N,I,J)*SINF(OMGA(J)*T(K)-THETA(N,I,J))
      XGN1= X(N,I,J)*OMGA(J)*COSF(OMGA(J)*T(K)-THETA(N,I,J))
      XGN2 = -X(N,I,J)*OMGA(J)**2*SINF(OMGA(J)*T(K)-THETA(N,I,J))
      IF(N.EQ.1)31,32
   31 RAF1=XGN2/386.0+BETA(2,I)*XGN1/ABSF(XGN1)+XGN-SINF(OMGA(J)*T(K))
      GO TO 4011
   32 IF(N.EQ.2)33,34
   33 RAF1=XGN2/386.0+BETA(1,I)*XGN1+XGN-SINF(OMGA(J)*T(K))
      GO TO 4011
   34 IF (N.EQ.3)35,36
   35 RAF1=XGN2/386.0+BETA(3,I)*XGN1*ABSF(XGN1)+XGN-SINF(OMGA(J)*T(K))
      GO TO 4011
   36 IF (N.EQ.4)38,37
   38 RAF1=XGN2/386.0+BETA(4,I)*ABSF(XGN)*XGN1/ABSF(XGN1)+XGN-SINF(OMGA(
     1J)*T(K))
      GO TO 4011
   37 RAF1=XGN2/386.0+BETA(5,I)*XGN*XGN*XGN1/ABSF(XGN1)+XGN-SINF(OMGA(J)
     1*T(K))
 4011 RE=RE+RAF1*RAF1
      DMAX=AMV(DMAX,XGN,INX4,K)
      VMAX=AMV(VMAX,XGN1,INX3,K)
      AMAX=AMV(AMAX,XGN2,INX2,K)
   40 CONTINUE
      RE=SQRTF(RE 200)
      PRINT 50,N,I,X(N,I,J),THETA(N,I,J),J,RE
   50 FORMAT (6X,2H(X,I1,1H),12X,I2,7X,E10.5,6X,E8.5,13X,I2,8X,E10.5)
      PRINT 202,DMAX,VMAX,AMAX
  202 FORMAT (5X,3(E14.7,5X))
    7 CONTINUE
      END
```

```
      FUNCTION AMV(A1, A2, IN1, IN2)
      ABA2 = ABSF(A2)
      IF (A1-ABA2) 1, 2, 2
    1 AMV = ABA2
      IN1 = IN2
      RETURN
    2 AMV = A1
      END
```

```
      COMMON Y(12),M0,NN,XV(10),OMEGA,PRP,XRP,MORE,KT
      EQUIVALENCE (M1,NN),(MODE,M2),(KKA,M3),(A2,E1MAX),(A3,E1MIN),
     1            (A4,E2MAX),(A5,E2MIN),(A6,FACT)
      TYPE DREAL(4) YU
      MORE=-1
      READ 31,ID $ READ 31,IO $ PRINT 31,ID $ PRINT 41,IO
   31 FORMAT (20A4)
   41 FORMAT(//21H INPUT-OUTPUT FORMATS/1X,20A4)
      READ 25,ALPHA,OMEGA
      READ 20,M1,M2,M3,M4,M5,A1,A2,A3,A4,A5,A6
      READ IO(1),(Y(I),I=1,M1)
   20 FORMAT(5I5/F10.5,4E15.5,F10.5)
   25 FORMAT(3F15.5)
      READ 25,(A(I),D(I),B(I),I=1,M5)
      DO 902 LOW=1,5
      XUX(1)=0.005996357 $ XUX(2)=0.004316272 $ XUX(3)=0.002998179
  902 XUX(4)=0.001499089 $ XUX(5)=0.0000299818179
      DO 901 LOP=1,5 $ XRP=XUX(LOP)
      DO 900 LONGLOP=1,10 $ ALPHA=0.0 $ OMEGA=26.0 $ M0=1
      IF (PRP-5.0) 680,681,681
  680 PRP=5.0 $ A1=.006 $ A4=.008 $ A5=.004 $ A6=.002 $ GO TO 699
  681 IF (PRP-10.) 682,683,683
  682 PRP=10.0 $ A1=.003 $ A4=.004 $ A5=.002 $ A6=.001 $ GO TO 699
  683 IF (PRP-15.) 684,685,685
  684 PRP=15. $ A1=.002 $ A4=.0028 $ A5=.0012 $ A6=.0008 $ GO TO 699
  685 IF (PRP-18.) 686,687,687
  686 PRP=18. $ A1=.0016 $ A4=.0023 $ A5=.0009 $ A6=.0007 $ GO TO 699
  687 IF (PRP-20.)688,689,689
  688 PRP=20. $ A1=.0015 $ A4=.0021 $ A5=.0009 $ A6=.0006 $ GO TO 699
  689 IF (PRP-22.)690,691,691
  690 PRP=22. $ A1=.0013 $ A4=.0018 $ A5=.0008 $ A6=.0005 $ GO TO 699
  691 IF (PRP-25.)692,693,693
  692 PRP=25. $ A1=.0012 $ A4=.0016 $ A5=.0008 $ A6=.0004 $ GO TO 699
  693 IF (PRP-30.)694,695,695
  694 PRP=30. $ A1=.0009 $ A4=.0012 $ A5=.0006 $ A6=.0003 $ GO TO 699
```

```
  695 IF (PRP-40.)696,697,697
  696 PRP=40. $ A1=.0007 $ A4=.0009 $ A5=.0005 $ A6=.0002 $ GO TO 699
  697 IF (PRP-50.)698,699,699
  698 PRP=50. $ A1=.0006 $ A4=.0008 $ A5=.0004 $ A6=.0002
  699 CONTINUE
      BET(1)=.5 $ BET(2)=.5 $ BET(3)=1. $ BET(4)=0.0 $ LL=1 $ KM=1
      PRINT 223
  223 FORMAT(1H1)
      Y(1)=0.0 $ Y(2)=0.0
      PRINT 26,ALPHA,OMEGA
   26 FORMAT(/9H ALPHA = E14.7,10X,9H OMEGA = E14.7/)
      Y(M1+1)=ALPHA $ LT=2 $ IF(M5) 120,120,119
  119 LT=1
  120 PRINT 21  $ PRINT 22,M1,M2,M3,M4,M5 $ PRINT 23
   21 FORMAT(///37H   M1       M2       M3       M4       M5 )
   22 FORMAT(5(I5,3X))
   23 FORMAT(///76H   A1           A2              A3              A4
     1        A5           A6  )
      PRINT 24,A1,A2,A3,A4,A5,A6 $ PRINT 27 $ PRINT IO(6),(Y(I),I=1,M1)
   24 FORMAT(F10.5,4E15.5,F10.5////)
   27 FORMAT(16H STARTING VALUES)
      PRINT 223
C  ****  SET CONSTANTS  ****
      GO TO (7,88,88),M2
    7 MM=4 $ J1=4 $ GO TO 9
   88 MM=1 $ J1=1
    9 EPM=2.0*ABSF(OMEGA-ALPHA) $ E3=EPM $ TOT=1./2.+2.**(-32.)
      N2=NN+2 $ Y(N2)=A1      $ NP1=NN+1 $ R= 19.0/270.0 $ XV(MM)=Y(NP1)
      IF(E1MIN) 2,2,1
    2 E1MIN=E1MAX/55.0
    1 IF(FACT) 4,4,3
    4 FACT=1.0/2.0
    3 CALL DERFUN $ DO 320 I=1,NN $ NJK=I+N2 $ FV(MM,I)=Y(NJK)
  320 YU(MM,I)=Y(I) $ N3=N2+NN+1 $ N4=N3+1 $ GO TO (501,502),LT
  501 E3=ABSF(A(1)-B(1)) $ IF(D(1)) 505,504,505
  504 E3=ABSF(Y(N2)/2.0)
  505 ABM=E3
      PRINT 400,KM,A(KM),D(KM),B(KM) $ GO TO 1001
  400 FORMAT(30X,18H PRINTING INTERVAL13//10H START AT E14.6,5X,
     1 17H INCREMENTING BY E14.6,5X,15H AND FINISH AT E14.6//)
  502 PRINT 37
   37 FORMAT( 40X,28H PRINTING AT EACH MESH POINT)
C  ****  RUNGE-KUTTA METHOD  ****
```

```
 1001 DO 1034 K=1,4 $ DO 1350 I=1,NN
      DELY(K,I) = Y(N2)*FV(MM,I) $ Z=YU(MM,I)
 1350 Y(I) = Z+BET(K)*DELY(K,I) $ Y(NP1)=BET(K)*Y(N2)+XV(MM)
      CALL DERFUN $ DO 1100 I=1,NN
      NJK=I+N2
 1100 FV(MM,I)=Y(NJK)
 1034 CONTINUE $ DO 1039 I=1,NN
         DEL = (DELY(1,I)+2.0*DELY(2,I)+2.0*DELY(3,I)+DELY(4,I))/6.0
      YU(MM+1,I)=YU(MM,I)+DEL
 1039 CONTINUE $ MM=MM+1 $ XV(MM)=XV(MM-1)+Y(N2) $ DO 1400 I=1,NN
 1400 Y(I)=YU(MM,I) $ Y(NP1)=XV(MM) $ CALL DERFUN
      GO TO  (42,100,100),MODE
  100 DO 150 I=1,NN
      NJK=I+N2
  150 FV(MM,I)=Y(NJK)
      GO TO (1001,1001,1001,2000,2000),MM
C  ****  ADAMS-MOULTON METHOD  ****
 2000 DO 2048 I=1,NN
      DEL=Y(N2)*(55.0*FV(4,I)-59.0*FV(3,I)+37.0*FV(2,I)-9.0*FV(1,I))/24.
      Y(I)=YU(4,I)+DEL
 2048 DELY(1,I)=Y(I) $ Y(NP1)=XV(4)+Y(N2)  $ CALL DERFUN
      XV(5)=Y(NP1)     $ DO 2051 I=1,NN
      NJK=I+N2
      DEL=Y(N2)*(9.0*Y(NJK) +19.0*FV(4,I)-5.0*FV(3,I)+FV(2,I))/24.0
      YU(5,I)=YU(4,I)+DEL
 2051 Y(I)=YU(5,I) $ CALL DERFUN
      GO TO (42,42,3000),MODE
C  ****  ERROR ANALYSIS  ****
 3000 SSE=0.0 $ DO 3033 I=1,NN
      EPSIL=R*ABSF(Y(I)-DELY(I,I)) $ GO TO (3301,3307),KKA
 3301 IF(Y(I)) 3650,3307,3650
 3650 EPSIL=EPSIL/ABSF(Y(I))
 3307 IF(SSE-EPSIL) 3032,3033,3033
 3032 SSE=EPSIL
 3033 CONTINUE $ IF(E1MAX-SSE) 3034,3034,3035
 3034 IF(ABSF(Y(N2))-E2MIN) 42,42,4340
 3035 IF(SSE-E1MIN) 3036,42,42
 3036 IF(E2MAX-ABSF(Y(N2))) 42,42,5360
 4340 LL=1 $ MM=1 $ GO TO (4560,4660),M4
 4560 PRINT 800,SSE,Y(NP1),Y(N2)
      Y(N2)=Y(N2)*FACT $ PRINT 820,XV(1),Y(N2) $ GO TO 1001
  800 FORMAT(/18H MAXIMUM ERROR OF E17.10,4H AT E15.6,19H WITH STEP SIZE
     1 OF E15.8/)
```

```
  820 FORMAT(/27H ERROR TOO LARGE. BEGIN AT E15.6,19H WITH STEP SIZE OF
     1 E15.8/)
 4660 Y(N2)=Y(N2)*FACT $ GO TO 1001
 5360 GO TO (42,5361),LL
 5361 XV(2)=XV(3) $ XV(3)=XV(5)
      DO 5363 I=1,NN $ FV(2,I)=FV(3,I) $ NJK=I+N2 $ FV(3,I)=Y(NJK)
      YU(2,I)=YU(3,I)
 5363 YU(3,I) = YU(5,I) $ LL=2 $ MM=3 $ GO TO (5270,5370),M4
 5270 PRINT 800,SSE,Y(NP1),Y(N2)
      Y(N2)=2.0*Y(N2) $ PRINT 840,Y(N2) $ GO TO 1001
  840 FORMAT(/32H ERROR TOO SMALL. NEW STEP SIZE E15.8/)
 5370 Y(N2)=2.0*Y(N2) $ GO TO 1001
C  ****  EXIT ROUTINE  ****
   42 DO 322 I=1,NN
      NJK=I+N2
  322 FV(5,I)=Y(NJK) $ GO TO (701,602),LT
  142 DO 12 K=1,3 $ XV(K)=XV(K+1) $ DO 12 I=1,NN $ FV(K,I)=FV(K+1,I)
   12 YU(K,I)=YU(K+1,I) $ LL=2 $ MM=4 $ XV(4)=XV(5)
      DO 52 I=1,NN $ FV(4,I)=FV(5,I)
   52 YU(4,I)=YU(5,I) $ GO TO (1001,2000,2000),MODE
C  **** PRINTOUT WITH SPECIFICATIONS  ****
  701 TZ=ABSF(Y(N2))*ZOT
      GO TO (700,750,750),MODE
  700 KT=4 $ GO TO 430
  750 KT=1
  430 SPACE=A(KM)-XV(KT) $ Z=ABSF(SPACE)
      IF(Z-TZ) 437,437,436
  437 IF(SPACE) 413,403,413
  403 DO 404 I=1,NN
  404 Y(I)=YU(KT,I) $ GO TO 443
  436 KT=KT+1 $ GO TO (430,430,430,430,430,790),KT
  413 DO 438 I=1,NN
      NJK=I+N2
  438 Y(NJK)=FV(KT,I)
      DO 439 K=1,4 $ DO 440 I=1,NN
      NJK=I+N2 $ DELY(K,I)=SPACE*Y(NJK) $ Z=YU(KT,I)
  440 Y(I)=Z+BET(K)*DELY(K,I) $ Y(NP1)=BET(K)*SPACE+XV(KT)
  439 CALL DERFUN $ DO 442 I=1,NN
  442 Y(I)=YU(KT,I)+(DELY(1,I)+2.0*DELY(2,I)+2.0*DELY(3,I)+DELY(4,I))/6.
  443 PRINT 416,A(KM) $ PRINT 417 $ PRINT IO(6),(Y(I),I=1,NN)
  416 FORMAT(/24H INDEPENDENT VARIABLE = E15.6)
  417 FORMAT(20H DEPENDENT VARIABLES)
      IF(D(KM)) 715,746,715
```

```
  715 A(KM)=A(KM)+D(KM) $ E=ABSF(A(KM)-B(KM))
      IF(E-ABM) 744,746,746
  744 ABM=E $ GO TO 430
  746 KM=KM+1 $ IF(KM-M5) 702,702,648
  702 PRINT 223
      PRINT 400,KM,A(KM),D(KM),B(KM) $ E3=ABSF(A(KM)-B(KM))
      IF(D(KM)) 714,713,714
  713 E3=ABSF(Y(N2)/2.0)
  714 ABM=E3
      GO TO (700,750,750),MODE
  790 E=ABSF(XV(J1)-OMEGA)  $ IF(E-EPM) 706,648,648
  706 EPM=E $ GO TO 142
C  ****  PRINTOUT AT EACH MESH POINT  ****
  602 E=ABSF(OMEGA-XV(J1)) $ IF(E-EPM) 672,672,648
  672 EPM=E $ GO TO (600,650,650),MODE
  600 KT=4 $ GO TO 630
  650 KT=1
  630 E=ABSF(OMEGA-XV(KT)) $ IF(E-E3) 647,645,645
  647 E3=E $ DO 666 I=1,NN
  666 Y(I)=YU(KT,I)
      CALL APRINT(KT)
  645 KT=KT+1 $ GO TO (630,630,630,630,630,142),KT
  648 PRINT 223
  900 CONTINUE
  901 CONTINUE
      END
```

```
      SUBROUTINE APRINT(LIQ)
      DIMENSION DMD(22),DMT(22),VMV(22),VMT(22),AMA(22),AMT(22),
     1TX(500),DX(500),VX(500),AX(500),PDISP(22),BZ(42),T(900),
     2D(900),V(900),A(900),QTA(22),XMS(5,5,12),TST(12)
      COMMON Y(12),MO,NN,XV(10),OMEGA,PRP,XRP,MORE,KT
  219 FORMAT(1H2)
  220 FORMAT(13H DELTA TIME = E12.6, 5X, 13HFINAL TIME = E12.6, //, 16X,
     14HTIME,12X,12HDISPLACEMENT,12X,8HVELOCITY,12X,12HACCELERATION,/)
      IF (MORE) 93,93,94
   93 IN=1 $ IT=1 $ MORE=2
   94 IF (MO)203,303,303
```

```
303 TIM = 0.0E-20
    TMAX=DMAX=VMAX=AMAX=AEP=PDISP(1)=PEP=BZ(1)=0.0
    J1=J2=J3=J4=J5=J6=J7=J8=J9=J10=J11=1
    INX1=INX2=INX3=INX4=INX5=INX6=INX7=0
    MQ=0 $ MO=-1 $ SPACE=Y(4) $ PRINT 219 $ PRINT 220,SPACE,OMEGA
203 SPACE=Y(4)
    TX(J2)=XV(LIQ) $ DX(J2)=Y(1) $ VX(J2)=Y(2) $ AX(J2)=Y(6)
    CALL AMV(DMAX,DX(J2),INX1,J2) $ ZV1=TX(INX1)
    CALL AMV(VMAX,VX(J2),INX2,J2) $ ZV2=TX(INX2)
    CALL AMV(AMAX,AX(J2),INX3,J2) $ ZV3=TX(INX3)
    IF (J2-493) 51,51,52
 52 OMEGA=XV(LIQ)
    TIM = OMEGA $ GO TO 12
 51 CONTINUE
    IF (DX(J2)) 1,13,13
  1 IF (DX(J2-1)) 13,13,4
  4 IF (J3-1) 5,5,8
  5 JM=1 $ JR2=J2-1 $ PDISP(J3)=0.0 $ GO TO 782
  8 PDISP(J3)=0.0 $ JM=KX5+1 $ JR2=J2-1
782 DO 20 KR4=JM,JR2
    IF (DX(KR4)) 20,20,423
423 CALL AMV(PDISP(J3),DX(KR4),INX4,KR4) $ JMT=INX4 $ BZ(J4)=TX(INX4)
 20 DID=VIV=AIA=0.0 $ DO 420 KR1=JM,J2
420 CALL AMV(DID,DX(KR1),INX5,KR1) $ DMD(J6)=DX(INX5)
    DMT(J7)=TX(INX5) $ DO 421 KR2=JM,J2
421 CALL AMV(VIV,VX(KR2),INX6,KR2) $ VMV(J8)=VX(INX6)
    VMT(J9)=TX(INX6) $ DO 422 KR3=JM,J2
422 CALL AMV(AIA,AX(KR3),INX7,KR3) $ AMA(J10)=AX(INX7)
    AMT(J11)=TX(INX7)
    IF (JMT-2) 14,14,18
 18 WTV=(ABSF(VX(1)*VX(1)*VX(1))/2.0)*SPACE
    KMX=JMT-2
    WVT=0.0E-20
    DO 567 KX8=2,KMX
    TWV=ABSF(VX(KX8)*VX(KX8)*VX(KX8))*SPACE
567 WVT=WVT+TWV
    KX9=JMT
    XVT=(ABSF(VX(KX9)*VX(KX9)*VX(KX9))/2.0)*SPACE
    QTA(J5)=(WVT+XVT+WTV)*XRP
 14 IF (J3-2) 63,63,17
 17 IF (ABSF((PDISP(J3)-PDISP(J3-1))/PDISP(J3))-0.005) 10,10,63
100 IF (ABSF(((BZ(J4)-BZ(J4-1))-(BZ(J4-1)-BZ(J4-2)))/(BZ(J4)-BZ(J4-1))
   1)-0.005) 12,12,63
```

```
 12 CEP=BZ(J4)-BZ(J4-1)
    TAOL=0.0 $ IE=J2-1 $ DO 819 J2=1,IE
    ORE=(AX(J2)/386.0+XRP*VX(J2)*ABSF(VX(J2))+DX(J2)-
    1SINF(TX(J2)*PRP))**2
819 TAOL=TAOL+RE $ PRINT 839,TAOL
839 FORMAT (/10X,18H SUM OF SQUARES = E12.6/)
    PRINT 550
550 FORMAT (1H1)
    PRINT 720
720 FORMAT (//48X,25H VELOCITY SQUARED DAMPING//)
    CPA = SQRTF(386.0)
    DPA = 6.28318530727/PRP $ AQT=PRP/CPA $ PRINT 771,CPA
771 FORMAT(10X,21H NATURAL FREQUENCY = E12.6/)
    PRINT 770,PRP
770 FORMAT (10X,35H EXCITATION FREQUENCY IN RADIANS = E12.6/)
    PRINT 772,AQT
772 FORMAT (10X,44H RATIO OF EXCITATION TO NATURAL FREQUENCY = E12.6)
    PRINT 773,DPA
773 FORMAT (/10X,28H FORCING FREQUENCY PERIOD = E12.6/)
    PRINT 721
721 FORMAT (//49X,23H STEADY STATE RESPONSE //)
    PRINT 705,CEP
705 FORMAT (10X,40H ACTUAL LENGTH OF STEADY STATE PERIOD = E12.6/)
    YPQ = SQRTF((3.0*3.1415926536)/(8.0*XRP*PRP*PRP))
    PRINT 774,YPQ
774 FORMAT (10X,54H THE STEADY STATE DISPLACEMENT BY THE ENERGY METHOD
   1 = E12.6/)
    PRINT 711, DMD(J6)
711 FORMAT (10X,40H THE ACTUAL STEADY STATE DISPLACEMENT = E12.6/)
    QDA=1.0-((YPQ-DMD(J6))/YPQ)
    PRINT 741,QDA
741 FORMAT (/10X,22HSINE OF PHASE ANGLE = E12.6/)
    PIN=QTA(J5)/(3.1415926536*DMD(J6))
    PRINT 743,PIN
743 FORMAT (/10X,33H SINE OF PHASE ANGLE BY ENERGY = E12.6/)
    DEA=(8.0*XRP*PRP*PRP*DMD(J6)*DMD(J6)*DMD(J6))/3.0
    PRINT 777,DEA
777 FORMAT (10X,53H DAMPING ENERGY PER CYCLE WITH ACTUAL DISPLACEMENT
   1= E12.6/)
    DISP = ABSF(DMD(J6)/DMAX)
    PRINT 778,DISP
778 FORMAT (/10X,60H RATIO OF STEADY STATE TO MAXIMIUM TRANSIENT DISPL
   1ACEMENT = E12.6/)
```

```
      VISP = ABSF(VMV(J8)/VMAX)
      PRINT 779,VISP
  779 FORMAT (/10X,50H RATIO OF STEADY STATE VEL TO MAX TRANSIENT VEL =
     1E12.6/)
      AISP = ABSF(AMA(J10)/AMAX)
      PRINT 780,AISP
  780 FORMAT (/10X,54H RATIO OF STEADY STATE ACCEL TO MAX TRANSIENT ACCE
     1L = E12.6/)
      PRINT 781,DMD(J6)
  781 FORMAT (10X,38H MAXIMIUM STEADY STATE DISPLACEMENT = E12.6/)
      VDC=(8.0*DMD(J6)*PRP*XRP)/(3.0*3.14159265 6)
      PRINT 775,VDC
  775 FORMAT (10X,46H THE EQUIVALENT VISCOUS DAMPING COEFFICIENT = E12.6
     1/)
      CDV=(8.0*XRP*PRP*YPQ)/(3.0*3.14159265 6)
      PRINT 790,CDV
  790 FORMAT (/10X,34H EQUIV VIS COEF WITH CALC DISPL = E20.12/)
      CDEC=(8.0*XRP*PRP*PRP*YPQ*YPQ*YPQ)/3.0
      PRINT 776,CDEC
  776 FORMAT (10X,53H THE DAMPING ENERGY PER CYCLE BY THE ENERGY METHOD
     1= E12.6/)
      PRINT 706,QTA(J5)
  706 FORMAT (10X,35H ACTUAL DAMPING ENERGY PER CYCLE = E12.6/)
      ADQ=PRP*PRP*DMD(J6)*XRP
      PRINT 740,ADQ
  740 FORMAT (/10X,24H DAMPING FACTOR EQUAL = E12.6/)
      PRINT 550
      PRINT 725
  725 FORMAT (//5X,23H THE TRANSIENT RESPONSE//)
      PRINT 495
  495 FORMAT (2X,30H THE DAMPING ENERGY PER CYCLE /)
      KV1=J5-1
      DO 490 KV2=1,KV1
  490 PRINT 724,QTA(KV2)
  724 FORMAT (5X,E20.12)
      DEC = 0.0
      KVE=J5-1
      DO 549 KVI=1,KVE
  549 DEC=DEC+QTA(KVI)
      PRINT 726,DEC
  726 FORMAT (/10X,38H THE TOTAL TRANSIENT DAMPING ENERGY = E12.6/)
      PRINT 716
  716 FORMAT (//5X,9H MAX DISP,5X,8H AT TIME/)
```

```
      KQ1 = J6-1
      DO 491 KQZ=1,KQ1
  491 PRINT 717,DMD(KQZ),DMT(KQZ)
  717 FORMAT (5X,E20.12,5X,E20.12)
      PRINT 718
  718 FORMAT (//5X,8H MAX VEL,5X,9H AT TIME /)
      KQ2=J8-1
      DO 492 KQ3=1,KQ2
  492 PRINT 719,VMV(KQ3),VMT(KQ3)
  719 FORMAT (5X,E20.12,5X,E20.12)
      PRINT 722
  722 FORMAT (//5X,10H MAX ACCEL,5X,9H AT TIME /)
      KQ8=J10-1
      DO 493 KQ4=1,KQ8
  493 PRINT 723,AMA(KQ4),AMT(KQ4)
  723 FORMAT (5X,E20.12,5X,E20.12)
      PRINT 702, DMAX,ZV1
  702 FORMAT (/2X,19H MAX DISPLACEMENT =E20.12,2X,11H AT TIME = E20.12)
      PRINT 703, VMAX,ZV2
  703 FORMAT (/2X,15H MAX VELOCITY =E20.12,2X,11H AT TIME = E20.12/)
      PRINT 708,AMAX,ZV3
  708 FORMAT (/2X,19H MAX ACCELERATION =E20.12,2X,11H AT TIME = E20.12/)
      DO 9 KNI=1, J3 $ PDISP(KNI)=BZ(KNI)=0.0
    9 CONTINUE $ OMEGA=TX(J2) $ TIM=OMEGA
      J4=J5=J6=J7=J8=J9=J10=J11=1 $ MQ=1
      TST(IT)=AQT
      IF (IT-10) 95,90,95
   90 IN=IN+1 $ IT=1
   95 CALL PLOT (3.0,-12.0,-3) $ CALL PLOT (0.0,1.5,-3)
      J1=J1-1 $ AELTA=T(J1) $ CALL LARGEST(AELTA) $ AETA=AELTA/8.0
      CALL AXIS (0.0,0.0,4HTIME,-4,7.5,90.0,0.0,AETA,0.1,0.5,2)

      CALL LARGEST (DMAX) $ YMAX=DMAX $ DELTA=YMAX/3.0
      CALL AXIS (+3.0,0.0,4HDIS.,4,5.5,180.0,-YMAX,DELTA,0.1,0.5,2)

      T(J1+1)=0.0 $ T(J1+2)=AETA $ D(J1+1)=-YMAX $ D(J1+2)=DELTA
      CALL LINE(+D,T,J1,1,-1,MQ,0.04,0,0.0)
      CALL PLOT (9.0,0.0,-3) $ MQ=MQ+1
      CALL AXIS (0.0,0.0,4HTIME,-4,7.5,90.0,0.0,AETA,0.1,0.5,2)
      CALL PLOT (0.0,0.0,-3)
      CALL LARGEST (VMAX) $ YMAX=VMAX $ DELTA=YMAX/3.0
      CALL AXIS (+3.0,0.0,4HVEL.,4,5.5,180.0,-YMAX,DELTA,0.1,0.5,2)
      CALL PLOT (0.0,0.0,-3) $ V(J1+1)=-YMAX $ V(J1+2)=DELTA
```

```
      CALL LINE(-V,T,J1,1,-1,MQ,0.04,0,0.0)
      CALL PLOT (9.0,0.0,-3) $ MQ=MQ+1
      CALL AXIS (0.0,0.0,4HTIME,-4,7.5,90.0,0.0,AETA,0.1,0.5,2)

      CALL LARGEST (AMAX) $ YMAX=AMAX $ DELTA=YMAX/3.0
      CALL AXIS (+3.0,0.0,4HACC.,4,5.5,180.0,-YMAX,DELTA,0.1,0.5,2)
      CALL PLOT (0.0,0.0,-3) $ A(J1+1)=-YMAX $ A(J1+2)=DELTA
      CALL LINE(+A,T,J1,1,-1,MQ,0.04,0,0.0)
      CALL PLOT (9.0,0.0,-3) $ MQ=MQ+1
      XMS(1,IN,IT)=DMD(J6-1) $ XMS(2,IN,IT) =VMV(J8-1)
      XMS(3,IN,IT)=AMA(J10-1)
      B1A=((PRP*DMD(J6-1))/(2.0*3.1415926536))-(3.14159265364.0)
      I2A=B1A
      XMS(4,IN,IT)=((B1A-I2A)*360)
      IF (IN-5) 91,92,92
   92 CALL PLOT(0.0,1.0,-3)
      CALL AXIS(0.0,0.0,4HANG.,4,5.5,90.0,0.0,30.0,0.1,0.5,2)
      CALL PLOT(0.0,0.0,-3) $ MQ=1
      CALL AXIS(0.0,0.0,4HW/WN,-4,7.0,0.0,0.0,0.333,0.1,0.75,2)
      CALL PLOT(0.0,0.0,-3)
      TST(IT+1)=0.0 $ TST(IT+2)=.333 $ DO 49 III=1,5 $ XMS(4,III,11)=0.0
   49 XMS(4,III,12)=30.0
      CALL LINE(TST(IT),XMS(4,1,IT),IT,1,-1,MQ,0.04,0,0.0)
      CALL PLOT(0.0,0.0,-3) $ MQ=MQ+1
      CALL LINE(TST(IT),XMS(4,2,IT),IT,1,-1,MQ,0.04,0,0.0)
      CALL PLOT(0.0,0.0,-3) $ MQ=MQ+1
      CALL LINE(TST(IT),XMS(4,3,IT),IT,1,-1,MQ,0.04,0,0.0)
      CALL PLOT(0.0,0.0,-3) $ MQ=MQ+1
      CALL LINE(TST(IT),XMS(4,4,IT),IT,1,-1,MQ,0.04,0,0.0)
      CALL PLOT(0.0,0.0,-3) $ MQ=MQ+1
      CALL LINE(TST(IT),XMS(4,5,IT),IT,1,-1,MQ,0.04,0,0.0)
      CALL PLOT (12.0,-1.0,-3) $ MQ=1
      CALL AXIS (0.0,0.0,4HXSS ,4,7.5,90.0,0.0,0.5,0.1,0.5,2)
      CALL PLOT (0.0,0.0,-3)
      CALL AXIS(0.0,0.0,4HW/WN,-4,5.5,0.0,0.0,0.5,0.1,0.5,2)
      TST(IT+1)=0.0 $ TST(IT+2)=0.5
      DO 48 III=1,5 $  XMS(1,III,11)=0.0 $ XMS(1,III,12)=0.5
      XMS(2,III,11)=0.0 $ XMS(2,III,12)=10.0 $ XMS(3,III,11)=0.0
   48 XMS(3,III,12)=20.0
      CALL PLOT (0.0,0.0,-3)
      CALL LINE (TST(IT),XMS(1,1,IT),IT,1,-1,MQ,0.04,0,0.0)
      CALL PLOT (0.0,0.0,-3) $ MQ=MQ+1
      CALL LINE (TST(IT),XMS(1,2,IT),IT,1,-1,MQ,0.04,0,0.0)
```

```
      CALL PLOT (0.0,0.0,-3) $ MQ=MQ+1
      CALL LINE (TST(IT),XMS(1,3,IT),IT,1,-1,MQ,0.04,0,0.0)
      CALL PLOT (0.0,0.0,-3) $ MQ=MQ+1
      CALL LINE (TST(IT),XMS(1,4,IT),IT,1,-1,MQ,0.04,0,0.0)
      CALL PLOT (0.0,0.0,-3) $ MQ=MQ+1
      CALL LINE (TST(IT),XMS(1,5,IT),IT,1,-1,MQ,0.04,0,0.0)
      CALL PLOT(12.0,0.0,-3) $ MQ=1
      CALL AXIS(0.0,0.0,4HVSS ,4,7.5,90.0,0.0,10.0,0.1,0.5,2)
      CALL PLOT (0.0,0.0,-3)
      CALL AXIS(0.0,0.0,4HW/WN,-4,5.5,0.0,0.0,0.5,0.1,0.5,2)
      CALL PLOT (0.0,0.0,-3)
      CALL LINE (TST(IT),XMS(2,1,IT),IT,1,-1,MQ,0.04,0,0.0)
      CALL PLOT (0.0,0.0,-3) $ MQ=MQ+1
      CALL LINE (TST(IT),XMS(2,2,IT),IT,1,-1,MQ,0.04,0,0.0)
      CALL PLOT (0.0,0.0,-3) $ MQ=MQ+1
      CALL LINE (TST(IT),XMS(2,3,IT),IT,1,-1,MQ,0.04,0,0.0)
      CALL PLOT (0.0,0.0,-3) $ MQ=MQ+1
      CALL LINE (TST(IT),XMS(2,4,IT),IT,1,-1,MQ,0.04,0,0.0)
      CALL PLOT (0.0,0.0,-3) $ MQ=MQ+1
      CALL LINE (TST(IT),XMS(2,5,IT),IT,1,-1,MQ,0.04,0,0.0)
      CALL PLOT(12.0,0.0,-3) $ MQ=1
      CALL AXIS(0.0,0.0,4HASS ,4,7.5,90.0,0.0,20.0,0.1,0.5,2)
      CALL PLOT (0.0,0.0,-3)
      CALL AXIS(0.0,0.0,4HW/WN,-4,5.5,0.0,0.0,0.5,0.1,0.5,2)
      CALL PLOT (0.0,0.0,-3)
      CALL LINE (TST(IT),XMS(3,1,IT),IT,1,-1,MQ,0.04,0,0.0)
      CALL PLOT (0.0,0.0,-3) $ MQ=MQ+1
      CALL LINE (TST(IT),XMS(3,2,IT),IT,1,-1,MQ,0.04,0,0.0)
      CALL PLOT (0.0,0.0,-3) $ MQ=MQ+1
      CALL LINE (TST(IT),XMS(3,3,IT),IT,1,-1,MQ,0.04,0,0.0)
      CALL PLOT (0.0,0.0,-3) $ MQ=MQ+1
      CALL LINE (TST(IT),XMS(3,4,IT),IT,1,-1,MQ,0.04,0,0.0)
      CALL PLOT (0.0,0.0,-3) $ MQ=MQ+1
      CALL LINE (TST(IT),XMS(3,5,IT),IT,1,-1,MQ,0.04,0,0.0)
      CALL PLOT (9.0,0.0,-3) $ MQ=1
   91 IT=IT+1 $ KT=5 $ RETURN
   63 KX3=JMT $ KX5=J2-JMT+1 $ DO 547 KX4=1,KX5
      TX(KX4)=TX(KX3) $ DX(KX4)=DX(KX3) $ VX(KX4)=VX(KX3)
      AX(KX4)=AX(KX3)
  547 KX3=KX3+1
      J2=KX5 $ J3=J3+1 $ J4=J4+1 $ J5=J5+1 $ J6=J6+1 $ J7=J7+1 $ J8=J8+1
      J9=J9+1 $ J10=J10+1 $ J11=J11+1
   13 CONTINUE $ J2=J2+1 $ IF (TIM-XV(LIQ)) 6,6,30
```

```
  6 T(J1)=XV(LIQ) $ D(J1)=Y(1) $ V(J1)=Y(2) $ A(J1)=Y(6) $ J1=J1+1
    TIM = TIM + (SPACE*10.0)
 30 CONTINUE
    IF (ABSF(XV(LIQ))-ABSF(OMEGA))306,307,307
307 GO TO 12
306 RETURN
    END
```

```
    SUBROUTINE DERFUN
    COMMON Y(12),M0,NN,XV(10),OMEGA,PRP,XRP,MORE,KT
    Y(5)=Y(2)
    Y(6)=386.0*SINF(Y(3)*PRP)-386.0*XRP*Y(2)*ABSF(Y(2))-386.0*Y(1)
    END
```

```
    SUBROUTINE AMV(A1,A2,IN1,IN2)
    ABA2 = ABSF(A2)
    IF (A1-ABA2) 1, 2, 2
  1 A1=ABA2
    IN1 = IN2
  2 RETURN
    END
```

```
    SUBROUTINE LARGEST(YMAX)
    IF (YMAX-1000.0) 5,5,500
  5 IF (YMAX-100.0)17,17,100
 17 IF (YMAX-10.0)21,21,10
 21 IF (YMAX-1.0)14,14,1
 14 IF (YMAX-0.1)22,22,24
```

```
   22 IF (YMAX-0.01)26,26,27
   26 YMAX = 0.01
      RETURN
   27 SSMA = 0.02
      BO 28 JN=1, 9
      IF (YMAX-SSMA)31,31,28
   31 YMAX = SSMA
      RETURN
   28 SSMA = SSMA + 0.01
   24 SMAS = 0.2
      DO 18 N=1, 9
      IF (YMAX-SMAS) 25,18,18
   25 YMAX = SMAS
      RETURN
   18 SMAS = SMAS + 0.1
    1 UNIT = 2.0
      DO 4 J=1, 9
      IF (YMAX-UNIT)6,6,4
    6 YMAX = UNIT
      RETURN
    4 UNIT = UNIT + 1.0
   10 TENS = 20.0
      DO 30 K=1, 9
      IF(YMAX-TENS)20,20,30
   20 YMAX = TENS
      RETURN
   30 TENS = TENS + 10.0
  100 HUND = 200.0
      DO 400 L=1, 9
      IF (YMAX-HUND)200,200,400
  200 YMAX = HUND
      RETURN
  400 HUND = HUND + 100.0
  500 THOS = 2000.0
      DO 800 M=1, 9
      IF (YMAX-THOS)600,600,800
  600 YMAX = THOS
      RETURN
  800 THOS = THOS + 1000.0
      END
```

REFERENCES

1. Bogoliubov, N. N. and Y. A. Mitropolsky, Asymptotic Methods in the Theory of Non-Linear Oscillations, Hindustan Publishing Corp. (India) Delhi-6, 1961, Chapter 1.

2. Cunningham, W. J., Introduction to Nonlinear Analysis, McGraw-Hill Book Co., New York, N. Y., 1958, pp. 121-170.

3. Den Hartog, J. P., Mechanical Vibrations, McGraw-Hill Book Co., New York, N. Y., 1947, pp. 435-439.

4. Harris, C. M. and C. E. Crede, Shock and Vibration Handbook, McGraw-Hill Book Co., New York, N. Y., 1961, Vol. 2.

5. Hildebrand, F. B., Introduction to Numerical Analysis, McGraw-Hill Book Co., New York, N. Y., 1956, p. 199.

6. Hoerner, S. F., Fluid-Dynamic Drag, published by the author, 1965.

7. Jacobsen, L. S. and R. S. Ayre, Engineering Vibrations, McGraw-Hill Book Co., New York, N. Y., 1958, p. 229.

8. Minorsky, N., Nonlinear Oscillations, D. Van Nostrand Co., Princeton, N. J., 1962, pp. 211-231.

9. Murphy, Glenn, Similitude in Engineering, The Ronald Press Co., New York, p. 36.

10. Partin, J. R., Jr., Numerical Techniques for Applying Averaging Methods to Nonlinear Ordinary Differential Equations, a dissertation, The University of Texas, 1965.

11. Randall, Robert H., An Introduction to Acoustics, Addison-Wesley Press, Inc., Cambridge, Mass., 1951, p. 109.

12. Stoker, J. J., Nonlinear Vibrations, Interscience Publishers, Inc., New York, N. Y., 1950.

13. Thomson, W. T., Mechanical Vibrations, Prentice-Hall, Inc., New York, N. Y., 1953, p. 58.

14. Timoshenko, Stephen, Strength of Materials, Part II, Advanced Theory and Problems, D. Van Nostrand Co., Princeton, N. J., 1957, Chapter X.

15. Truxal, John G., Control Engineers Handbook, McGraw-Hill Book Co., New York, N. Y., 1958, pp. 13-49 to 13-55.

16. Wieland, H. E., Analysis of the Dynamic Flexural Response of Beams Using the Concept of Mechanical Impedance, a thesis, The University of Texas, 1966.

2 January 1967

DISTRIBUTION LIST FOR DRL-A-272,
A Technical Report under Contract NObsr-93125 (U)

Copy No.	
1	Commander, Naval Ship Systems Command Department of the Navy Washington, D. C. 20360 Attn: Glenn C. Moore, Ships 1622D
2	Commander, Naval Ship Systems Command Department of the Navy Washington, D. C. 20360 Attn: Carey D. Smith, Ships 1622
3	Commander, Naval Ship Systems Command Department of the Navy Washington, D. C. 20360 Attn: D. L. Baird, Ships 1633F
4 - 6	Office of Naval Research Department of the Navy Washington, D. C. 20360 Attn: Commander F. L. Crump, Jr., USN Code 463
7	Commanding Officer and Director David Taylor Model Basin Department of the Navy Washington, D. C. 20007
8	Commander, Naval Air Systems Command Department of the Navy Room 1531-A, Munitions Building Washington, D. C. 20360 Attn: AIR-53305
9	Commander U. S. Naval Ordnance Laboratory White Oak Silver Spring, Maryland 20910
10	U. S. Naval Research Laboratory Office of Naval Research Anacostia Washington, D. C. 20390 Attn: Mr. Sam Hanish, Code 2739

2 January 1967

DISTRIBUTION LIST FOR DRL-A-272 (CONT'D)
A Technical Report under Contract NObsr-93125 (U)

Copy No.	
11	Commander U. S. Navy Electronics Laboratory San Diego, California 92152
12	Commander U. S. Navy Underwater Sound Laboratory Fort Trumbull New London, Connecticut 06321
13	Headquarters, Naval Material Command Department of the Navy Washington, D. C. 20360 Attn: Mr. D. F. Ream, NAVMAT 0326
14	Stanford Research Institute Menlo Park, California 94025 Attn: Dr. Vincent Salmon
15	Acoustics Division, DRL/UT
16 - 20	J. F. Byers, DRL/UT
21	G. E. Ellis, DRL/UT
22	D. E. Evertson, DRL/UT
23	M. V. Mechler, DRL/UT
24	D. R. Sanders, DRL/UT
25 - 26	Library, DRL/UT
27 - 30	DRL Reserve, Mech. Engr. Files, DRL/UT

END

DATE
FILMED

4-77